# NOVEL ROLES FOR THE *DROSOPHILA MELANOGASTER* ORTHOLOG OF SMARCAL1 IN DNA DAMAGE REPAIR

Julie Korda Holsclaw

A dissertation submitted to the faculty at the University of North Carolina at Chapel Hill in partial fulfillment of the requirements for the degree of Doctor of Philosophy in the Curriculum in Genetics and Molecular Biology in the School of Medicine.

Chapel Hill
2017

Approved by:

Jeff Sekelsky

Jean Cook

Robert Duronio

Dale Ramsden

David Kaufman

©2017
Julie Korda Holsclaw
ALL RIGHTS RESERVED

# ABSTRACT

Julie Korda Holsclaw: Novel roles for the *Drosophila melanogaster* ortholog of SMARCAL1 in DNA damage repair
(Under the direction of Jeff Sekelsky)

Schimke immuno-osseous dysplasia (SIOD) is a monogenic, autosomal recessive disorder with highly variable penetrance and expressivity caused by biallelic mutations in the gene *SMARCAL1*. SMARCAL1 and its orthologs have been implicated in multiple repair pathways including replication-associated DNA damage repair and stability, gene expression in response to environmental stress, and non-homologous end joining. Early studies of SMARCAL1 suggest a role in double strand break (DSB) repair but have not been thoroughly tested.

DSBs pose a serious threat to genomic integrity. If unrepaired, they can lead to chromosome fragmentation and cell death. If repaired incorrectly, they can cause mutations and chromosome rearrangements. DSBs are repaired using end-joining or homology-directed repair strategies, with the predominant form of homology-directed repair being synthesis-dependent strand annealing (SDSA). SDSA is the first defense against genomic rearrangements and information loss during DSB repair, making it a vital component of cell health and an attractive target for chemotherapeutic development. SDSA has also been proposed to be the primary mechanism for integration of large insertions during genome editing with CRISPR/Cas9. Despite the central role for SDSA in genome stability, little is known about the defining step: annealing. I hypothesized that annealing during SDSA is performed by SMARCAL1, which can anneal RPA-coated single DNA strands during

replication-associated DNA damage repair. I utilized unique genetic tools in *Drosophila melanogaster* to test whether the fly ortholog of SMARCAL1, Marcal1, mediates annealing during SDSA. Repair that requires annealing is significantly reduced in *Marcal1* null mutants in both a synthesis-dependent and synthesis-independent (single-strand annealing) assays. Elimination of the ATP binding activity of Marcal1 also reduced annealing-dependent repair, suggesting that the annealing activity requires translocation along DNA. Unlike the null mutant, however, the ATP binding-defect mutant showed reduced end-joining, shedding light on the interaction between SDSA and end-joining pathways. Lastly, I found that *Marcal1* genetically interacts with *Blm* in SDSA and replication-associated repair. Blm prevents replication fork damage that is often repaired via Marcal1-mediated pathways. These data contribute to our understanding of DNA damage repair mechanisms and regulation.

To Dee and Tom Korda, for opportunity, curiosity, grit, and fearlessness.

To Rowan, for laughter, love, and the bravery to be who you are.

To Tain for resilience, kindness, and always trying to do the right thing.

And to Matt, for being the steadfast star around which I orbit.

You make all things possible.

# ACKNOWLEDGEMENTS

I owe a huge debt of gratitude to my advisor, Jeff Sekelsky, for his trust, his enthusiasm, and his respect for my ideas throughout my studies. Thanks for always having time for me, no matter how often or unpredictably I leaned on your doorframe. It has been an honor to be a member of your lab.

Many thanks to my committee: Robert Duronio, Jean Cook, Dale Ramsden, and David Kaufman. Thank you all for good ideas, solid advice, and valued criticism both inside and outside of meetings.

I would also like to thank my undergraduate advisor Tom Wolkow for convincing me that I could thrive in graduate school, for guiding me toward UNC, and for endless support along the way. You were right, grad school was one of the best times of my life.

I especially want to thank my labmates: Dr. Lydia Morris, Dr. Nicole Crown, Dr. Noelle-Erin Romero, Dr. Stephanie Bellendir, Dr. Kathryn Kohl, Dr. Gregorz Zapotoczny, (almost) Dr. Danielle Rognstad, (future) Dr. Talia Hatkevich, (future) Dr. Morgan Brady, (future) Dr. Kale Hartmann, and (future) Dr. Juan Carvajal Garcia. Thanks for writing edits, insightful comments, and rigorous criticism—you have been so much more than co-workers and I treasure your brilliant minds and open hearts.

A special thanks to Susan Cheek for being amazing in every way: genetics resource, workplace mediator, shoulder to cry on, and unabashed lover of yacht rock. You have brightened every day in the fly room; everyone should have a Susan.

TABLE OF CONTENTS

LIST OF FIGURES

LIST OF TABLES

# LIST OF ABBREVIATIONS

| | |
|---|---|
| alt-EJ | Alternative end joining |
| BIR | Break induced replication |
| bp | Base pair |
| BSyn | Bloom syndrome |
| cNHEJ | Canonical non-homologous end joining |
| CO | Crossover |
| CPL | Cisplatin |
| CPT | Camptothecin |
| dHJ | Double Holliday junction |
| D-loop | Dissociation loop |
| DSB | Double strand break |
| dsDNA | Double-stranded DNA |
| EJ | End joining |
| ETS | Etoposide |
| HCHO | Formaldehyde |
| HDR | Homology-directed repair |
| HJ | Holliday junction |
| HN2 | Nitrogen mustard |
| HU | Hydroxyurea |

| | |
|---|---|
| IR | Ionizing radiation |
| Kb | Kilobase |
| LTR | Long terminal repeat |
| MEF | Mouse embryonic fibroblast |
| MMEJ | Microhomology-mediated end joining |
| MMS | Methyl methanesulfonate |
| NCO | Non-crossover |
| NDJ | Nondisjunction |
| nt | Nucleotide |
| SDSA | Synthesis-dependent strand annealing |
| SIOD | Schimke immuno-osseous dysplasia |
| SNP | Single nucleotide polymorphism |
| SSA | Single strand annealing |
| ssDNA | Single-stranded DNA |
| TMEJ | Polymerase theta mediated end joining |

# CHAPTER 1: HOMOLOGY-DIRECTED REPAIR OF DOUBLE-STRAND BREAKS[1]

DNA double-strand breaks (DSBs) are stochastic and detrimental in somatic cells. They can arise from exogenous exposures such as chemical mutagens in the environment, ionizing radiation, and UV light (reviewed in Ciccia and Elledge 2010; Sage and Shikazono 2016). They can also occur as a byproduct of endogenous cellular processes including oxidative stress during cellular metabolism, replication problems, or repair of other DNA lesions that are converted into DSBs during replication or for processing (reviewed in Pfeiffer *et al.* 2000). Altogether, DSBs are a common occurrence in mitotic cells, with a predicted frequency of ~50 endogenous DSBs per cell cycle in human cells—an amount equivalent to 1500 rads of ionizing radiation (Vilenchik and Knudson 2003).

Proper repair of DSBs in somatic cells is paramount to the health of the cell and the organism as a whole. Unrepaired DSBs can lead to chromosome fragmentation and apoptosis; however, repair can also generate products that affect viability such as insertions, deletions, and gross rearrangements (Tsai and Lieber 2010). Recombinational repair of mitotic DSBs can be detrimental, causing loss of heterozygosity and chromosome rearrangements that affect viability. Here I discuss the major pathways for DSB repair in mitotic cells, focusing on synthesis-dependent strand annealing (SDSA), a form of homology-directed repair (HDR), and the relationship between SDSA and end-joining (EJ).

[1] This chapter is adapted from previously published work in the book *Genome Stability*. The original citation is as follows:
Korda Holsclaw J, Hatkevich T, Sekelsky J. "Meiotic and Mitotic Recombination: First in Flies." In Kovalchuk, I and Kovalchuk, O (Eds), 2016 *Genome Stability*. Cambridge: Elsevier Inc. *Academic Press*.

## *Drosophila* as a model system: Why flies?

*Drosophila melanogaster* has many benefits for genetic study of DSB repair, including simple husbandry; established genetic tools; a relatively small, well-annotated genome; and fast generation time. In addition to these basic necessities, *Drosophila* is the only multicellular eukaryotic system with genetic tools to study SDSA, and HDR is favored over other repair strategies (elaborated on below) increasing my ability to recover HDR events. Furthermore, meiotic recombination occurs only in female flies; male flies have an alternate system for the proper segregation of their chromosomes that does not rely on crossing over of homologous chromosomes (Hawley 2002), allowing the recovery of mitotic repair events in subsequent generations for analysis. Most importantly, the only other model system with SDSA tools, yeast, lacks a known *SMARCAL1* ortholog (as discussed in Chapter 2), the primary gene investigated in these studies.

## Homology-directed repair

In *Drosophila*, as in other eukaryotes, mitotic DSB repair strategies can be separated into two major categories: processes that require a template (HDR) and processes that do not (EJ). HDR necessitates access to an undamaged copy of DNA—either a sister chromatid or a homologous chromosome. It can have multiple outcomes including both non-crossover (NCO) and crossover (CO) products, but mitotic regulation in *Drosophila* favors NCO formation (Andersen *et al.* 2011; Kuo *et al.* 2014; Sarbajna *et al.* 2014; LaFave *et al.* 2014). The understanding of HDR has been driven primarily by studies of meiotic recombination (particularly in yeast) and somatic HDR has been proposed to utilize the same intermediate, the double Holliday junction (dHJ) (reviewed in Jasin and Rothstein 2013).

HDR strategies share a common set of steps (central model in Figure 1.1) that begin with resection of the 5' ends of the break to yield 3' single-stranded DNA tails that are

protected by the single-strand binding protein RPA. Brca2 facilitates exchange of RPA for Rad51, creating a filament competent to search for and invade a homologous duplex template, typically the sister chromatid or homologous chromosome (Jensen *et al.* 2010; Reuter *et al.* 2014). The invading strand anneals to the template strand, displacing its complement and generating a structure called a D-loop (Figure 1.1, step 2). Synthesis off the template extends the invading strand.

It is at this point that the HDR strategies diverge. In SDSA (central model in Figure 1.1), the D-loop is disassembled and a complementarity test between the nascent strand and the opposing end of the break is performed. If complementarity is found, the two ends anneal. Trimming of non-complementary overhangs, filling of gaps, and ligation restore a duplex DNA molecule (Gloor *et al.* 1991; Nassif and Engels 1993; Pâques *et al.* 1998). An alternative form of HDR (orange box in Figure 1.1) occurs when the opposing end of the break anneals to the D-loop in a process called 2$^{nd}$-end capture. Continued synthesis from both ends and subsequent ligation produces a dHJ, which must be further processed to give duplex products. This model of repair has been called a variety of names throughout the literature, but for clarity, I will refer to it as the dHJ model in this work.

EJ, on the other hand, involves direct ligation of the broken ends, often after end-processing that can result in small insertions or deletions (Figure 1.1, blue box). *Drosophila* actively uses at least three variations of EJ depending on the context of the break: canonical non-homologous end joining (cNHEJ); microhomology mediated end joining (MMEJ), which is referred to as polymerase theta-mediated end joining (TMEJ) in metazoans and in this work; and alternative (cryptic) end joining (alt-EJ). cNHEJ is utilized as an early response prior to the first steps leading to HDR and is mediated by the Ku70/80 heterodimer and Lig4 (see Initial strategy choice); whereas TMEJ is utilized later in repair, after resection (see Special circumstances) and is dependent on polymerase theta (POLQ) (mus308 in

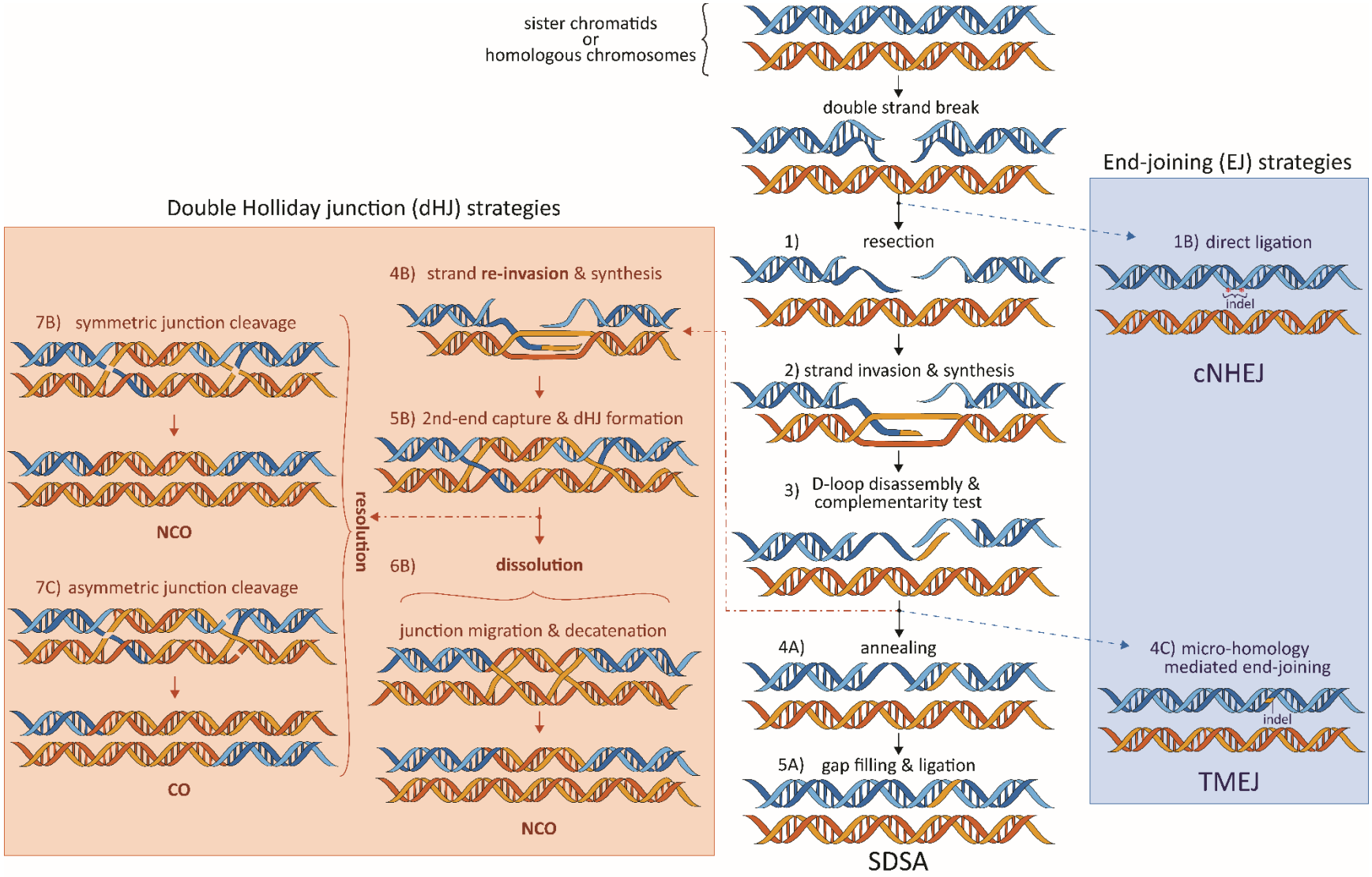


**Figure 1.1 Strand model of DSB repair strategies.**

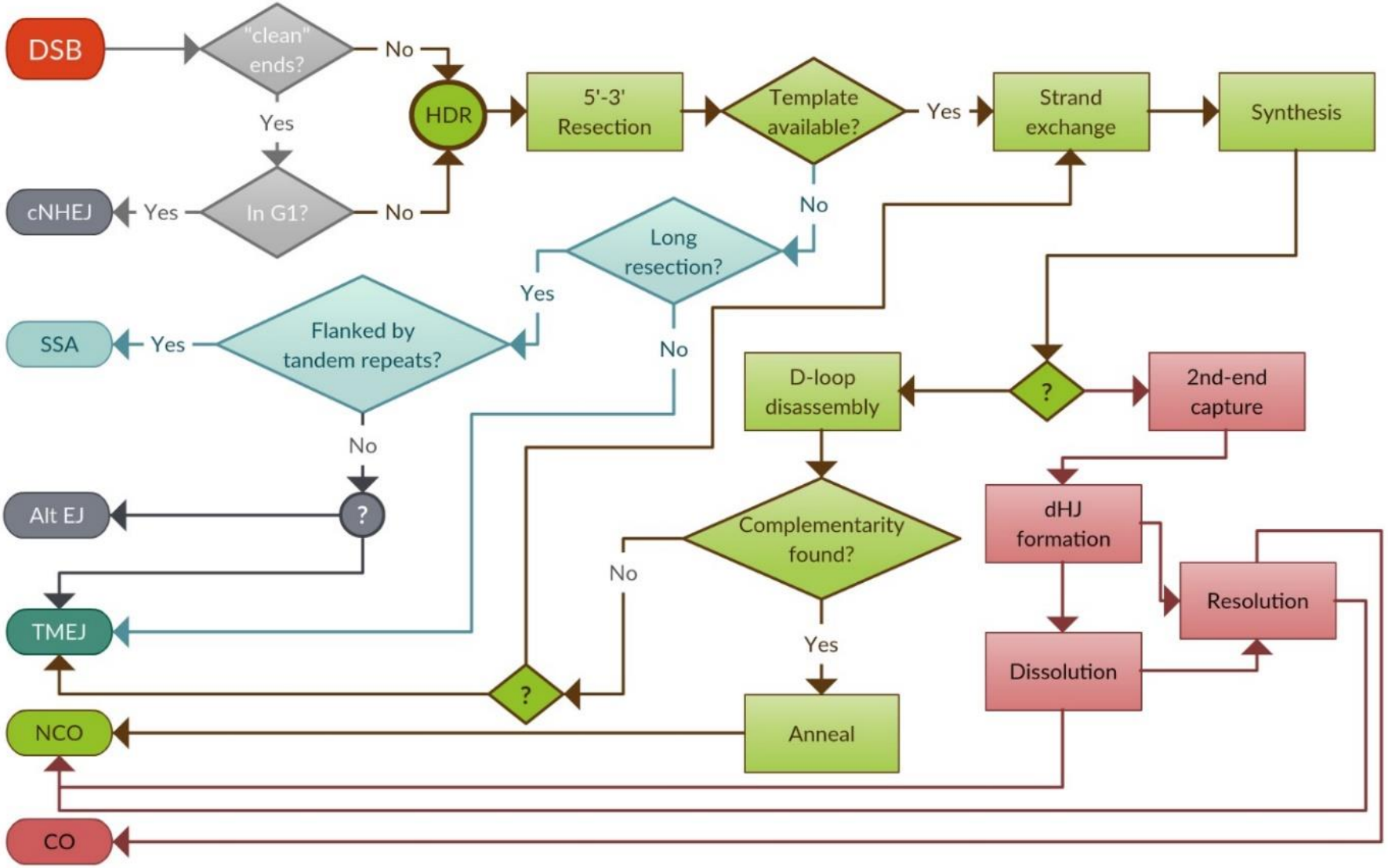


**Figure 1.2 Diagram of DSB repair strategy processes and choices.**

**Figure 1.1 Strand model of DSB repair strategies.** A DSB occurs in the blue DNA molecule. 1) 5' resection marks the first step of HDR and results in 3' ssDNA tails; alternatively, direct ligation may occur via cNHEJ (1B). 2) Rad51-coated ssDNA tails invade a template duplex, displacing one strand to creating a D-loop, and prime synthesis. 3) The D-loop is disassembled and a complementarity test between the opposing ends of the break occurs. 4A) SDSA is defined by annealing between complementary sequences, followed by 5A) trimming and/or gap filling and ligation to restore an intact duplex DNA molecule. 4B) If complementarity is not found, the strand can re-invade the template for further synthesis or 4C) utilize micro-homologies to end join via TMEJ, which is associated with indels around the break site (or incomplete filling of a gap). If the DSB occurs between two direct repeats, complementary sequences may be exposed during resection, and annealing can occur without synthesis. This process (not depicted, but see Special circumstances section) is called single-strand annealing (SSA). 5B) Re-invasion can lead to annealing of the opposing end to the D-loop ($2^{nd}$-end capture); this can also occur during the first round of invasion if the D-loop is not disassembled. Ligation generates a dHJ intermediate that can be processed via 6B) dissolution or 7B-C) resolution. Dissolution involves migration of the junctions toward each other and decatenation via topoisomerase activity resulting in a non-crossover (NCO) product. Resolution requires endonucleolytic activity and can result in a crossover (CO) product, which can be detrimental.

**Figure 1.2 Diagram of DSB repair strategy processes and choices.** A flow chart representation of decision points and processes that contribute to DSB repair outcomes in model systems based on the literature and the work presented here. Ovals represent start/end points; Diamonds are decision points; rectangles are processes. End joining events are in gray; single strand annealing in light blue; synthesis dependent strand annealing in green; double Holliday junction model in pink.

*Drosophila*) (Mimitou and Symington 2009a; Williams *et al.* 2014; Rodgers and McVey 2016; Wyatt *et al.* 2016). Alt-EJ is less understood and represents a category of EJ that is both Lig4 and mus308 independent. EJ strategies employ a range of mechanisms, including direct ligation of the ends (cNHEJ) and annealing of micro-homologies (TMEJ) (Yu and McVey 2010; Garcia *et al.* 2011).

Traditionally, the processes leading to repair of a break via HDR have been thought of as a series of irrevocable choices often leading to the formation of dHJ intermediates, as shown in Figure 1.1. Discoveries in the past 25 years, however, have shown that DSB repair is a much more flexible and dynamic process than previously proposed (Figure 1.2), starting with the early response at the break.

***Initial strategy choice***

Extensive work in yeast and mammalian cells has established the MRN complex (Mre11-Rad50-Nbs in *Drosophila*) as the DSB sensor for mitotic cells. The MRN complex activates the DNA damage response protein kinase ATM (*Drosophila* tefu), which then phosphorylates many downstream factors to initiate repair, one of which is the histone variant H2AX (*Drosophila* H2AV) (reviewed in Mimitou and Symington 2009; Daley *et al.* 2015). The γH2AV signal peaks within five minutes of gamma irradiation in flies and provides a scaffold to recruit additional proteins to amplify the repair signal (Madigan *et al.* 2002).

In yeast and mammalian cells, initial strategy choice is cell cycle-dependent. In G0-G1, phosphorylated 53BP1 binds the broken ends of a DSB to block 5'-3' resection of the ends, preventing HDR. During S-G2, when the genome has been replicated and a sister chromatid is available as a template, BRCA1 is phosphorylated by ATM leading to degradation of 53BP1, freeing the ends for resection (reviewed in Mimitou and Symington 2009; Daley *et al.* 2015). Thus, it appears that the choice between HDR and cNHEJ is decided by whether or not resection occurs.

Additionally, the role of 53BP1 suggests the default repair mechanism for DSBs is HDR, and cNHEJ occurs only if the ends are protected from resection. Equal recruitment of early repair factors for both strategies, regardless of cell cycle phase, has been observed in response to laser microbeam irradiation in human cells (Kim *et al.* 2005). These data suggest a dynamic repair response that is regulated at the break by cell cycle dependent activating factors as opposed to cell cycle dependent expression of genes.

It is less clear how initial strategy choice is made in *Drosophila*. While the core components of the early response are conserved, flies lack both 53BP1 and BRCA1 raising the question of how ends are protected or whether they are protected at all from resection

during G0-G1. Equally confounding is how cNHEJ is carried out. DNA-PKcs is a kinase that interacts with the Ku70/80 heterodimer at the break to both tether the ends and activate downstream factors via phosphorylation (reviewed in Waters *et al.* 2014; Williams *et al.* 2014). *Drosophila* has no known ortholog of this key regulatory factor, however, *Lig4* mutant flies have elevated lethality when exposed to ionizing radiation and this phenotype is synergistic with mutations in *Rad54*, a gene involved in HDR, suggesting cNHEJ is functional and utilized in wild-type flies (Gorski *et al.* 2003). Flies also lack key end-processing factors such as Artemis, Polλ, and Polμ and, while there is evidence of end-processing in Lig4 proficient flies (Bozas *et al.* 2009), it remains unclear how such processing is accomplished.

According to limited studies, strategy choice is somewhat age-dependent, with HDR strongly favored in older flies (>2 weeks) while EJ is utilized more in young flies (<2 weeks) (Preston *et al.* 2006a). There are a few caveats worth noting in this study: 1) the dominant repair pathway was single-strand annealing (SSA) (described in Special circumstances), a pathway strongly favored by the 157-bp repeats flanking the cut site in the reporter construct; 2) age-dependent pathway choice has only been studied in the male germline and these studies may reveal cell-type specific pathway choice (mature sperm-EJ vs. stem cells-HDR) rather than a true age correlation; 3) These studies report final repair events seen in the progeny of males, which could result from a variety of processes and decision points (Figure 1.1). Incongruously, tumorigenesis in epithelial cells of older flies correlates with errors in HDR, but not EJ, suggesting adverse effects on fitness with utilization of HDR as flies age (Dekanty *et al.* 2015).

Strategy choice does not seem to be affected by the chromatin environment of the break in *Drosophila*. It has been proposed that heterochromatin is naturally more resistant to DSBs due to compaction and when breaks occur, EJ is the preferred repair pathway to

avoid illegitimate recombination due to the highly repetitive nature of heterochromatic DNA. Chiolo *et al.* showed that neither of these hypotheses is supported in *Drosophila*: heterochromatin is as susceptible to DSB formation via ionizing radiation as euchromatin, and HDR is the dominant pathway for repair. *Drosophila* heterochromatin forms a distinct region within the nucleus and using high-resolution microscopy, Chiolo and colleagues were able to show γH2AV within the heterochromatin domain in response to $\gamma$ radiation. It was further shown that resection occurred within the heterochromatin domain but the remaining steps of HDR were suspended until the break physically moved to the outer periphery of the heterochromatin and was stripped of the heterochromatin marker HP1a, presumably to reduce compaction and enable repair factors access to the lesion (Chiolo *et al.* 2011). These studies did not test HDR factors downstream of resection and it remains unclear if heterochromatic DSBs are repaired via SSA or SDSA (or the dHJ model). These data do indicate that EJ and HDR have a dynamic and contextual relationship and that flies may utilize repair strategies that rely on resection at a much higher frequency than other metazoans.

***Resection***

The most extensive studies of resection have been performed in *S. cerevisiae*, however, studies in human and murine cells have provided important insights as well. Once successfully bound to the ends of the break, the human MRN complex promotes 5'-3' resection via an interaction with CtIP (*D.melanogaster* CG5872 is a putative ortholog) (Sartori *et al.* 2007). In yeast, this initial resection is limited in length to ~200 nt (reviewed in Symington and Gautier 2011) after which long resection is facilitated by EXO1 or DNA2-WRN/DNA2-BLM (Nimonkar *et al.* 2011; Sturzenegger *et al.* 2014; Myler *et al.* 2016). The 3' ssDNA tails become coated with the single strand binding protein RPA, which has been shown to inhibit EXO1-mediated resection (Myler *et al.* 2016).

While initial resection represents the first pro-HDR decision, the shift from short resection to long resection creates a potential decision point between HDR and TMEJ. Mus308 utilizes microhomologies between two ssDNA ends to facilitate end-joining (described in more detail in Special circumstances), however, the efficiency of that process with human POLQ is limited by how proximal the microhomology is to the ssDNA termini (personal communication J. Carvajal Garcia). It is possible that two-step resection in mammals creates continued opportunity for EJ once cNHEJ is excluded, though this hypothesis currently lacks experimental evidence. My observations in *Drosophila* suggest that TMEJ is rarely utilized prior to strand exchange (Chapter 3).

***Strand exchange***

Once sufficiently resected, human BRCA2 facilitates the exchange of RAD51 for RPA on the 3' ssDNA tails (Jensen *et al.* 2010; Jensen 2013; Bakr *et al.* 2016; Chalermrujinanant *et al.* 2016), creating a nucleoprotein filament competent for homology searching and strand exchange. The RAD51 nucleoprotein filament is stabilized by RAD51 paralogs, which vary in number and degree of similarity to RAD51 depending on the organism studied (reviewed in Karpenshif and Bernstein 2012; Amunugama *et al.* 2013). The stabilized filament searches the dsDNA template strand for homology using multiple contact points along the filament (Forget and Kowalczykowski 2012).

In *Drosophila*, there appears to be a preference for the sister chromatid as a template, even when an intrachromosomal template is available (Do *et al.* 2013). Do *et al*. further showed that increasing the polymorphisms between two copies of the same gene reduced the use of the diverged gene as a template, suggesting that preference of the sister over the homolog may be a byproduct of homology search mechanisms. SNP sequencing is the primary method for determining which template is used; therefore, it is possible that the homolog is utilized with the same efficiency as the sister when the break occurs in a region

of strong conservation provided the homologs are in close proximity within the architecture of the nucleus. This type of repair event would be indistinguishable from repair off the sister chromatid. *Drosophila* homologs are paired throughout the cell cycle in somatic cells (Henikoff 1997), which provides ample opportunity for homolog templating and may help to explain the strong preference for HDR in flies.

Work in yeast has shown that once Rad51 has facilitated pairing of a sufficient number of nucleotides with the template to make dissociation kinetically unfavorable (Qi *et al.* 2015), Rad54 strips Rad51 from the invading strand, annealing it to the template strand in the process, and displacing its complement to form a structure called a displacement loop (D-loop) (Wright and Heyer 2014). Wright and Heyer's experiments highlight many important functions for Rad54. The first is to strip Rad51 from the invading strand to facilitate assembly of synthesis machinery. The second is to properly anneal the invading strand to the template, which is also necessary for synthesis to occur. Lastly, and arguably most importantly, this process forces annealing of the invading strand to a single template. Rad51 homology searches consist of multiple contacts along the nucleoprotein filament that can interact with multiple dsDNA strands. Rad54 requires a filament terminus for activity, thus ensuring that the 3' end of the invading strand is properly annealed to a single template strand. These studies also found that Rad54 activity is halted by dsDNA, which suggests that the entire resected tail is annealed to the template prior to synthesis initiation.

***Special circumstances***

Resection almost invariably leads to template strand invasion, though there are notable exceptions as elaborated below.

**Polymerase theta mediated end joining**

Recent studies have uncovered a type of EJ that is reliant on microhomologies near the termini of the resected ends and is mediated by POLQ/mus308. It has also been referred to as microhomology mediated end joining (MMEJ) as well as alt-EJ, though the latter is a generalized category that encompasses any EJ that is mediated by cryptic factors. In MEF cells, microhomologies of 4 nt that are ≤ 25 nt from the termini are strongly favored (Wyatt *et al.* 2016) suggesting TMEJ is preferred when resection is short or aborted (as suggested in Resection). *In vivo* evidence from *Drosophila* support this interpretation as TMEJ is utilized predominantly after synthesis during gap repair in wild type flies (Chan *et al.* 2010) and SSA is highly favored in assays without an available template or with tandem homologies of greater lengths than those favored by mus308 (Rong and Golic 2003; Preston *et al.* 2006a; Mukherjee *et al.* 2009). These data argue that long resection is a poor substrate for TMEJ and long resection is often employed early at the break. Altogether, these data suggest TMEJ is utilized most often as an exit strategy for attempted HDR and not as a primary repair means directly after resection in *Drosophila*.

**Single strand annealing**

SSA has been proposed to occur when resected ends are complementary to each other such as when a DSB is generated between tandem repeats (reviewed in Bhargava *et al.* 2016). SSA appears to occur readily in yeast cells, which lack key factors necessary for TMEJ, most notably a POLQ ortholog. Rad52 mediates SSA in both yeast and human cells, whereas other organisms like *Drosophila* completely lack a Rad52 ortholog. Rad52 also has an expanded role in yeast compared to other organisms: it both anneals during SSA and loads Rad51 onto resected tails (New *et al.* 1998), whereas Brca2 is the Rad51 loader in other organisms (Thomas *et al.* 2013; Jensen 2013). This makes yeast Rad52 uniquely situated to utilize SSA over HDR whenever homologies are present, unlike other systems

that require removal of Rad51 or inhibition of Rad51 loading as well as recruitment of an annealase after resection.

SSA has been observed in other organisms as well, though predominantly in artificial situations where long resection has occurred and a template is unavailable (Pâques *et al.* 1998; Rong and Golic 2003; Storici *et al.* 2006). Preston *et al*. observed high incidence of SSA in *Drosophila* when there was 157 bp of homology between the two break termini, even in the presence of a repair template (Preston *et al.* 2006a), suggesting that SSA is efficiently utilized in flies. It is unclear how SSA is regulated or how the choice between SSA, TMEJ, and strand exchange is made. Difficulties in sequencing largely repetitive regions make it difficult to test the extent of SSA utilization across the genome and deleterious repair of a break within direct repeats can arise from multiple repair strategies, including TMEJ, SDSA, and the dHJ model.

***Synthesis***

Determining the primary synthesis machinery for HDR is difficult due to multiple functions of polymerases within the nucleus. Translesion polymerases have been implicated in DSB repair, specifically REV1 and polymerase zeta (Polζ) (Kane *et al.* 2012; Sharma *et al.* 2012). Replicative polymerase delta (Polδ) as well as the Pol32 subunit have also been implicated in HDR, though cautious interpretation should be used for these studies as any mutation in *Polδ* or *Pol32* impacts replication dynamics (reviewed in Prindle and Loeb 2012). Kane *et al.* proposed that translesion polymerases are recruited early but lack processivity or stable association with DNA (Kane *et al.* 2012). In this model, Polδ can be swapped for the translesion polymerases to facilitate longer synthesis. For a more detailed review of polymerase roles in HDR, I point the reader to this recent review (McVey *et al.* 2016)

Synthesis length appears to be highly variable *in vivo*. In yeast, break induced replication (BIR) can result in synthesis from the break to the end of the chromosome,

though this process has yet to be observed in other systems (Saini *et al.* 2013). In contrast, HDR-induced synthesis for as few as 5 bp has been observed in *Drosophila* (Adams *et al.* 2003). While it is tempting to assume length varies with experimental system, it is more likely that synthesis is a highly tractable process with upper and lower limits and observed variation in synthesis length is at least partially the product of differences in experimental design.

### *Dissociation loops*

#### Structure

Little is known about the structure of D-loops *in vivo*, specifically the structure of D-loops as synthesis progresses beyond 100 nt. There are two main models for HDR D-loop progression: the migrating bubble and the ever-extending bubble (Figure 1.3). In the migrating bubble model, nascent DNA is extruded as synthesis progresses, as observed in yeast BIR (Saini *et al.* 2013). The extruded DNA is presumably coated in RPA which is known to interact with many repair factors, including the annealase SMARCAL1 (Ciccia *et al.* 2009; Yusufzai *et al.* 2009; Bhat *et al.* 2014; Xie *et al.* 2014). In contrast, D-loops could form ever-extending bubbles which are structurally similar to replication bubbles without lagging strand synthesis or bi-directionality. In this model the nascent strand is protected through base pairing with the template while the displaced strand is protected by RPA. The ever-extending model is predicted to favor 2$^{nd}$-end capture by preventing complementarity tests of the nascent strand as well as encouraging RPA-mediated interactions between the D-loop and the opposing ssDNA tail via Rad52 activity (McIlwraith and West 2008; Nimonkar *et al.* 2009).

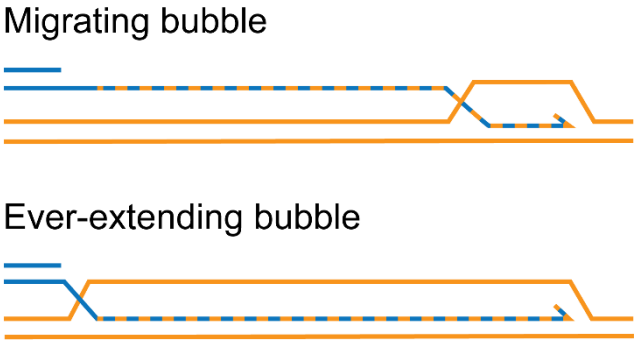


**Figure 1.3 Models of D-loop progression during synthesis.** Top: The migrating bubble model extrudes nascent DNA, which would aid complement-arity tests during synthesis.

Bottom: The ever-extending bubble model protects nascent DNA from complementarity tests until synthesis machinery is disassembled and leaves the displaced strand open to 2nd-end capture.

It is possible that both models are utilized depending on the desired outcome. Migrating bubbles would likely favor SDSA whereas ever-extending bubbles are more conducive to dHJ formation. It is also possible that the size of the break plays a role in D-loop structure. A gap that requires significant synthesis via a highly processive polymerase may generate a different type of D-loop than a clean break, which may use less processive polymerases.

Long-tract, conservative synthesis in BIR proceeds through a migrating bubble (Saini *et al.* 2013), which suggests that ever-extending bubbles are specific to semi-conservative replication during S-phase. Perhaps bubble structure is influenced by whether or not synthesis is semi-conservative (all HDR synthesis is conservative). Long synthesis necessitates the highly processive Polδ, which would be a substantial roadblock to D-loop dissociation since putative D-loop dissociating helicases have limited unwinding activity past ~800 bp (Brosh *et al.* 2000; Romero *et al.* 2016). Dissociation kinetics were not measured in these experiments, though it is possible that multiple molecules of D-loop dissociators could dismantle a long D-loop if their rate was faster than the polymerase rate of synthesis. So little is known about the structure of D-loops *in vivo*; it is a field of study with exciting possibilities for future research.

**Disassembly**

Many enzymes can disassemble D-loops *in vitro*, making it difficult to determine which are involved *in vivo*. Genetic evidence suggests the BTR complex, consisting of Blm helicase, Top3a, and RMI1/2 (*Drosophila* lack known orthologs of both RMI proteins) plays a

role in D-loop disassembly. McVey *et al.* showed that *Blm* mutants were defective in D-loop disassembly (McVey *et al.* 2007), while Fasching *et al.* showed that the yeast ortholog of Blm, Sgs1, could only disassemble protein-free D-loops *in vitro* whereas Top3a was capable of disassembling protein-bound D-loops, which are more likely to be biologically significant (Fasching *et al.* 2015). These data suggest that the Blm-Top3a interaction is necessary for proper D-loop disassembly *in vivo.*

The helicase RTEL1 has been shown to both prevent protein-bound D-loop formation and disassemble pre-formed protein-bound D-loops *in vitro*, though corroboration *in vivo* has been hampered by embryonic lethality of RTEL1 null mutations in both mice and *Drosophila* (Ding *et al.* 2004; Barber *et al.* 2008; observations in our lab). Cell culture studies performed by Ding and Barber suggest RTEL1 inhibits HDR, though the mechanism remains unclear.

The yeast and *Drosophila* orthologs of FANCM helicase, Mph1 and Fancm respectively, are also capable of disassembling D-loops *in vitro* (Prakash *et al.* 2009; Romero *et al.* 2016). Both RTEL1 and FANCM achieve D-loops disassembly without disrupting the Rad51 nucleofilament, which suggests they act upstream of Rad54 and may be utilized to abort HDR prior to synthesis, which could promote TMEJ or SSA. Interestingly, *Fancm* mutants have slightly elevated mitotic CO and slightly reduced SDSA in *Drosophila*, supporting a role for Fancm in facilitating NCO outcomes of HDR (Kuo *et al.* 2014). More studies are necessary to clarify this role.

The mechanics of D-loop disassembly also remain unclear. Blm interacts with RPA which stimulates its helicase activity, particularly on partial duplexes with 256 bp of dsDNA and D-loops of ~800 bp (Brosh *et al.* 2000), which would be most efficient on the migrating bubble model of synthesis. In this scenario, Blm could interact with RPA bound to the displaced strand to facilitate unwinding from either end. Blm also has a preference for 5'-3'

directionality, which could promote migration of the bubble as well as facilitate removal of the invading strand (Bachrati *et al.* 2006). *Drosophila* Fancm has 3'-5' polarity but can only unwind D-loops of less than 20 bp *in vitro*, and it has been suggested that Fancm may recruit Blm to D-loops for dissociation (Romero *et al.* 2016).

As previously mentioned, translesion polymerases have been implicated in HDR and lack processivity. It is possible that Blm-Top3a track behind the synthesis machinery, reducing the size of the D-loop and extruding the nascent strand until the polymerase dissociates from the DNA, at which point the 3' end of the invading strand becomes unfettered and can be removed by Fancm to completely disassemble the D-loop. This hypothesis supports the stochastic synthesis lengths observed in repair assays.

***Complementarity tests and annealing***

Little is known about the mechanisms of repair after D-loop disassembly, how the ends interact to perform complementarity tests, or which factors are responsible for annealing the two ends. Studies in budding yeast have identified Rad52 as an important mediator of annealing during SSA (Ivanov *et al.* 1996; Storici *et al.* 2006; Jensen 2013), however mammalian *Rad52* mutations do not result in strong HDR defects (Rijkers *et al.* 1998). Human RAD52 has been found to be important for 2$^{nd}$-end capture through interactions with RPA and Rad51 (McIlwraith and West 2008; Nimonkar *et al.* 2009; Khade and Sugiyama 2016), which suggests that RAD52 functions in animals may be confined to steps of HDR where Rad51 is active, such as strand invasion, making it unlikely that RAD52 is the mediator of annealing during SDSA.

Recent studies in mammalian systems have uncovered a class of helicases with ATP-driven annealing activity called annealing helicases (Yuan *et al.* 2012). Members of this family can anneal two RPA-coated, complementary single DNA strands, making these enzymes ideal candidates for annealing during SDSA. The first member of this family to be

identified, SMARCAL1, is highly conserved throughout metazoans (as well as plants and some protists), though it is notably absent from yeast supporting an expanded role for Rad52 in that organism. SMARCAL1 and the *Drosophila* ortholog, Marcal1, have been shown to interact with RPA to facilitate annealing and increased the annealing rate of ssDNA oligos in solution as well as traditional annealing assays (described in more detail in Chapter 2) (Yusufzai *et al.* 2009; Kassavetis and Kadonaga 2014). Further support for a role of Marcal1 in annealing during SDSA is suggested by a previous study showing that mutations in *mei-41*, which encodes the *Drosophila* ortholog of ATR, significantly reduce annealing during both SDSA and SSA (LaRocque *et al.* 2007), suggesting that an ATR-activated protein, such as SMARCAL1/Marcal1, catalyzes annealing during DSB repair.

***The dHJ model***

Mitotic crossovers (CO), a product of dHJ processing, are observed in certain *Drosophila* genetic backgrounds, such as *Blm* and *Fancm* mutants, suggesting that the dHJ model is still a valid and utilized pathway for repair in flies (LaFave *et al.* 2014). dHJ formation occurs when the second resected end of a DSB anneals to the D-loop and begins synthesis. This process is thought to occur sequentially, with strand invasion occurring first to open the D-loop, followed by synthesis then annealing of the opposing ssDNA tail to the D-loop ($2^{nd}$ end capture). As synthesis continues on both strands, the nascent strands eventually meet the opposing sides and ligate to the remaining 5' ends to form a concatenated joint molecule—the dHJ. dHJs are toxic structures that prevent proper segregation during mitosis and block transcription (Sarbajna *et al.* 2014; Pipathsouk *et al.* 2016); it is imperative that the chromosomes are separated accurately, preferably without exchange of genetic information in the form of COs. There are two possible mechanisms for disentanglement: dissolution via migration and decatenation or resolution via endonucleolytic cleavage.

Migration and decatenation is carried out by the BTR complex in humans (BLM, TOPO3α, RMI1/2) and the STR complex in yeast (Sgs1, Top3α, Rmi1) (Plank *et al.* 2006; Wu *et al.* 2006). BLM helicase migrates the junctions toward each other and TOPO3α (a type I topoisomerase) decatenates the strands through nicking and religating one strand of the dsDNA. The RMI proteins are thought to provide stability to the complex as well as facilitate decatenation through coordination with TOPO3α. Mitotic COs are elevated in *Blm* mutant flies, suggesting that the function of the complex is conserved in *Drosophila* (LaFave *et al.* 2014). Interestingly, flies do not have orthologs to the RMI proteins; the C-terminal region of Top3α has a large insertion that may play a similar role but this hypothesis has not been tested (Chen *et al.* 2012).

The presence of mitotic COs in *Blm* mutants, rather than an increase in lethality, suggests unbiased resolution of dHJs (with equal probability of yielding CO or NCO) by structure-specific endonucleases called resolvases. Andersen *et al.* showed that *Blm* mutations are lethal when combined with mutations in the genes *mus81*, *mus312*, or *Gen* (MUS81, SLX4, GEN1, respectively in humans), all of which encode subunits of putative HJ resolvases (Andersen *et al.* 2011). The synthetic lethality of the double mutants could be partially rescued by mutating *spn-A*, (in the case of *mus81 Blm* double mutant, fully rescued) suggesting that the phenotype was strand invasion-dependent and therefore related to a toxic HDR product. The absence of mitotic COs in flies with wild-type *Blm*, combined with the viability of single endonuclease mutants, indicate that the primary pathway for disentangling dHJs is Blm-mediated dissolution with endonuclease cleavage serving as a back-up mechanism.

The evidence presented in this chapter indicate that DSB repair is a much more dynamic and tractable process than previously proposed. The dHJ model was thought to be the predominant form of DSB repair since it was first proposed (Szostak *et al.* 1983). However, advances in assay design led to the discovery of SDSA (Nassif and Engels 1993),

which is gaining traction as the primary form of HDR in mitotic cells. More recent studies identified TMEJ as another form of DSB repair utilized in mitotic cells (Chan *et al.* 2010; Yu and McVey 2010). Surprisingly, we still know relatively little about the defining step of SDSA, annealing, or how strategies downstream of resection and upstream of dHJ formation interact with each other. In this work, I explore the role of Marcal1, the *Drosophila* ortholog of the annealing helicase SMARCAL1, in SDSA. My studies open new avenues to explore, particularly in how annealing affects other decisions (such as TMEJ and dHJ formation) during HDR.

# CHAPTER 2: SMARCAL1: STRUCTURE, ACTIVITY, AND DISEASE STATES

Human SMARCAL1 (originally called HARP for HepA-Related Protein) and its orthologs have been implicated in multiple repair pathways including replication-associated DNA damage repair and stability, gene expression, and NHEJ. Here I summarize what is known about the activity of SMARCAL1 in cellular processes; the structure of the SMARCAL1 protein and its known interactions with other proteins; and how these attributes contribute to the severity and progression of Schimke immuno-osseous dysplasia (SIOD), the disease caused by biallelic mutations in *SMARCAL1*.

## Structure and conserved interactions

Human SMARCAL1 has a C-terminal SWI/SNF2 family helicase domain and two N-terminal HARP domains (Coleman *et al.* 2000; Yusufzai and Kadonaga 2008). *Drosophila* Marcal1 is 41% identical and 60% similar to human SMARCAL1 across the helicase domain (based on BLAST alignment of residues 154-679 of Marcal1 to residues 337-869 of SMARCAL1). Marcal1 has a single HARP domain versus the two in SMARCAL1 (Figure 2.1A); the presence of two HARP domains appears to be unique to chordates.

The distance between the helicase ATPase domain and the proximal HARP domain is critical for the annealing function of SMARCAL1 *in vitro* (Ghosal *et al.* 2011; Bétous *et al.* 2012), and that distance is conserved in Marcal1. *In vitro* studies comparing the activity of Marcal1 to SMARCAL1 showed that both proteins have robust annealing activity; Marcal1 annealed a variety of structures including splayed arms and Holliday junctions but was unable to regress a model replication fork (Kassavetis and Kadonaga 2014). The authors

also noted that oligo annealing during substrate preparation was accelerated in the presence of either SMARCAL1 or Marcal1, suggesting that two strands of ssDNA do not have to be in the same DNA molecule for efficient annealing activity catalyzed by SMARCAL1 orthologs. Based on these studies, it is possible that Marcal1 performs a subset of roles compared to SMARCAL1.

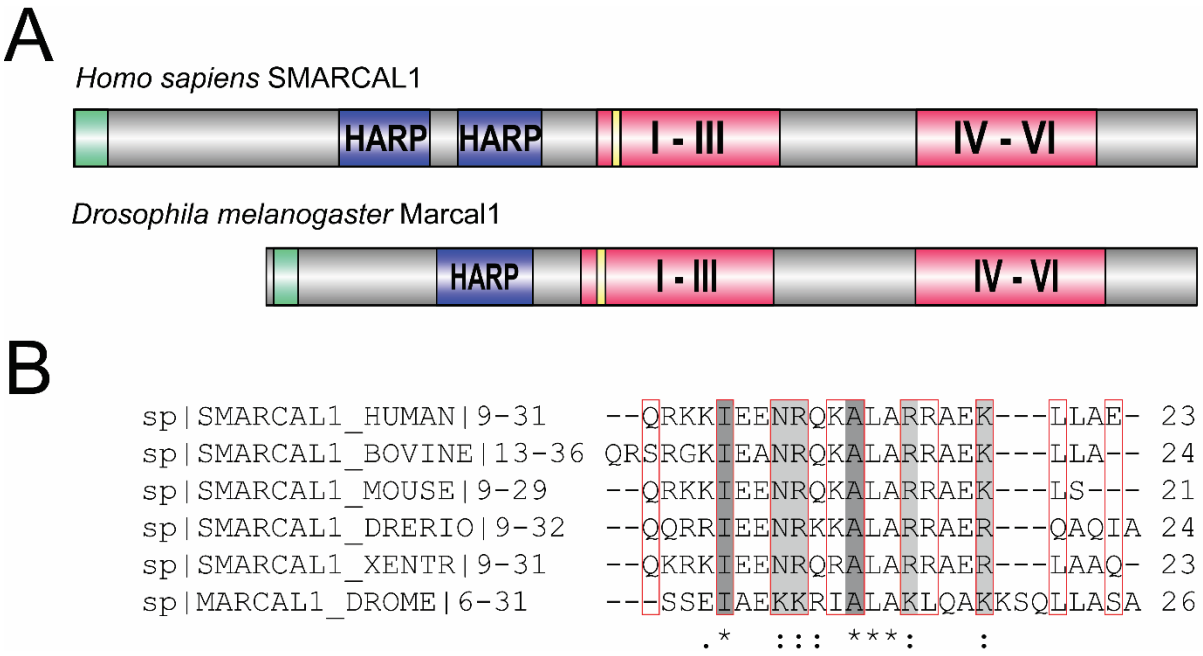


**Figure 2.1 SMARCAL1 domain conservation.** (A) Schematic of human SMARCAL1 (top) and Drosophila Marcal1 (bottom). Green: RPA interacting domains. Blue: family-specific HARP domains. Pink I-III: SWI/SNF2 family motifs I-III responsible for ATP binding (yellow bar) and ATP hydrolysis. Pink IV-VI: SWI/SNF2 family IV-VI helicase motifs. (B) Conservation of 9 key residues (red boxes) of the RPA-binding interface of SMARCAL1. Top to bottom: *Homo sapiens*, *Bos taurus*, *Mus musculus*, *Danio rerio*, *Xenopus tropicalis*, *Drosophila melanogaster*. Dark gray indicates full conservation of a key residue; asterisk (*) indicates full conservation of a residue not predicted to bind RPA. Light gray indicates high similarity of a key residue; colon (:) indicates high similarity of a residue not predicted to bind RPA. Amino acid positions are listed to the right of the sequences.

Human SMARCAL1 and *Drosophila* Marcal1 have been shown to interact with the single strand binding protein RPA, specifically the 32 kDa subunit RPA2 (also called RPA32, because of its size), and this interaction is required for its recruitment to DNA (Ciccia *et al.* 2009; Yusufzai *et al.* 2009; Bhat *et al.* 2014; Kassavetis and Kadonaga 2014). Structural

studies of the human SMARCAL1-RPA2 interface have identified 11 key residues in the N-terminus of SMARCAL1 that directly interact with RPA2 (Feldkamp *et al.* 2014) (Figure 1.4B, red boxes). These studies also found that SMARCAL1 bound RPA more tightly than RAD52. It was proposed that the increased affinity of RPA for SMARCAL1 may reveal an order of events at sites of DNA damage, with SMARCAL1 recruited prior to RAD52. An alternative possibility is that SMARCAL1 can outcompete RAD52 if both are recruited at the same time. It is, therefore, possible that the strong conservation of the nine core RPA-interacting residues in vertebrate SMARCAL1 orthologs is due to presence of RAD52 in these organisms. *Drosophila* lack a RAD52 ortholog and this could explain the reduced conservation of the RPA-interacting domain in flies.

Differential conservation of the RPA binding domain could also cause altered substrate specificity, however, the difference seen in branch migration activity between human and *Drosophila* orthologs is most likely due to the number of HARP domains and not RPA binding. SMARCAL1 recruitment, but not substrate specificity, is reliant on the presence of RPA, presumably to position SMARCAL1 at the proper ssDNA:dsDNA junction (parental-nascent vs. parental-parental, depending on whether the fork needs to be regressed or is already regressed) (Bétous *et al.* 2013b). In the absence of RPA, SMARCAL1 can bind any ssDNA:dsDNA junction with equal affinity and SMARCAL1 protein without the RPA-interacting domain (SMARCAL1Δ32) likewise shows no junction preference. Both SMARCAL1 and SMARCAL1Δ32 can regress model replication forks and model Holliday junctions, indicating that SMARCAL1 activity is independent of RPA interaction (Yusufzai and Kadonaga 2008; Bétous *et al.* 2013b). The HARP domains of SMARCAL1 appear to affect substrate specificity (Ghosal *et al.* 2011; Mason *et al.* 2014) and Mason *et al.* found single nucleotide changes within the HARP domain could influence

binding to different substrates. These observations suggest that Marcal1 may bind a reduced number of substrates compared to human SMARCAL1.

SMARCAL1 appears to be highly regulated. It is phosphorylated by ATM,ATR, and DNA-PK in response to DNA damage (Bansbach *et al.* 2009; Postow *et al.* 2009; Couch *et al.* 2013), though the most characterized is ATR-dependent phosphorylation. SMARCAL1 has multiple putative phosphorylation sites, three of which have been confirmed to affect SMARCAL1 activity (Couch *et al.* 2013; Carroll *et al.* 2014). S652 is phosphorylated in an ATR-dependent manner yet reduces ATPase activity, whereas S889 phosphorylation appears to stimulate ATPase activity. These data suggest phosphorylation serves to attenuate SMARCAL1 activity in response to stimuli.

## Activity

### *Replication*

The first *in vitro* studies of human SMARCAL1 showed that it was able to anneal a partially unwound, RPA-coated plasmid in an ATP-dependent manner, however, it failed to exhibit any unwinding activity expected of a canonical helicase (Yusufzai and Kadonaga 2008). These studies also showed that SMARCAL1 preferentially bound forked DNA structures. From this work, SMARCAL1 came to be known as an “annealing helicase” with the potential for replication-associated roles.

Functional assays in human cells support a role for SMARCAL1 during replication. Bansbach *et al*. showed that SMARCAL1 forms foci that co-localized with ATRIP in response to treatment with hydroxyurea (HU), a ribonucleotide reductase inhibitor, suggesting a role in fork stability during replication stalling (Bansbach *et al.* 2009). They further showed that increased loading of RPA as well as hyper-phosphorylation of RPA occurs in SMARCAL1 depleted cells, suggesting an accumulation of ssDNA during

replication and activation of S-phase checkpoints in the absence of SMARCAL1. Further studies by Bétous *et al.* showed that SMARCAL1 travels with the replisome during normal synthesis and prevents mus81-mediated DSBs during replication (Bétous *et al.* 2012).

*In vitro* studies of SMARCAL1 binding and activity support these findings. SMARCAL1 can bind almost any structure with a ssDNA-dsDNA junction including dsDNA with overhangs of both polarities (5' and 3'); forked structures with 2 strands (splayed arms), 3 strands (leading or lagging strand), or 4 strands (model replication fork); forked structures with variable and asymmetrical arm lengths; structures with ssDNA gaps; 3-way junctions; and 4-way junctions (resembling Holliday junctions) (Bétous *et al.* 2012). All structures stimulated ATPase activity, though ssDNA of at least 5 nt is needed to achieve full activity, implicating replication uncoupling as a key activator of SMARCAL1 activity. Later work established that SMARCAL1 preferentially regresses model replication forks with leading strand gaps (indicative of uncoupling) and migrates regressed forks (chicken foot structure, similar to a single Holliday junction) to restore a functional fork with a lagging strand gap (Bétous *et al.* 2013b). These studies highlight a critical role for SMARCAL1 in replication stability.

***Gene expression***

SMARCAL1 was first identified in a sequence similarity-based screen for SNF2 family chromatin remodelers (Coleman *et al.* 2000) and assumed to be a new type of SNF2 family chromatin remodeler with functions in transcription and nucleosome remodeling, though the authors noted that SMARCAL1 family proteins did not have domains characteristic of transcription roles such as bromodomains, chromodomains, or zinc fingers. Additionally, the SNF2 family DEAD box necessary for ATP hydrolysis is altered to DESH in SMARCAL1 family proteins, making SMARCAL1 and its orthologs structurally distinct from

other SNF2 family proteins. While these data suggest that SMARCAL1 may have a specialized role in the cell, gene expression studies remain an active area of research.

SMARCAL1 has been shown to co-precipitate with SPT16 which complexes with SSRP1 to form the FACT heterodimer (Bétous *et al.* 2013a). FACT has multiple roles within the cell, one of which is chaperoning H2A/H2B histones during transcription (Mandemaker *et al.* 2014). Studies in *Drosophila* showed that mutations in transcriptional components rescued a very mild wing vein phenotype seen in Marcal1 overexpression assays (Baradaran-Heravi *et al.* 2012a). While the authors argue that this phenotype is indicative of an interaction with transcription machinery, an alternate interpretation is that reducing transcription results in less ssDNA:dsDNA junctions that could be aberrantly bound by Marcal1 when it is overexpressed. Furthermore, SPT16 catalyzes the exchange of DNA-PK phosphorylated H2AX/H2B for H2A/H2B in response to DNA damage (Heo *et al.* 2008), confirming a role for SPT16 outside of transcription and suggesting the co-precipitation could be mediated by H2AX and not direct protein-protein interactions. The presence or absence of histones was not tested nor was a direct interaction between SMARCAL1 and SPT16 confirmed in the study.

Heat stress (39.5° C for 6.5 hrs) is lethal for *SMARCAL1*$^{del/del}$ mice and *Marcal1*$^{del}$ flies raised at 25-30°C showed reduced viability and hatch rates (Baradaran-Heravi *et al.* 2012a). The authors also found gene expression profiles to be different between wild-type and *Marcal1*$^{del}$ flies in response to heat shock. It is important to note that 25°C is a standard temperature for raising flies and I observed that heteroallelic *Marcal1* null flies had high fecundity under normal, control (25°C) conditions. I also did not observe increased lethality when performing heat shock (37°C for 1 hour on two subsequent days) necessary for promoter activation during the *P*{*wIw*} assay (Chapter 3). It is likely that the heat sensitivity observed by Baradaran-Heravi *et al*. is due to the genetic background of the homozygous

stock used rather than the effect of the *Marcal1*$^{del}$ mutation, which also casts doubt on the gene expression data observed in these experiments. The gene expression defects and heat stress phenotype observed in *SMARCAL1*$^{del/del}$ mice is much more pronounced than the *Drosophila* phenotype. This could be due to differences between the orthologs (see Structure and interactions) or it could be due to unassociated differences between the two organisms.

***DSB repair***

Early studies of SMARCAL1 suggest a role in DSB repair in addition to its replication-associated roles. SMARCAL1 depletion via RNAi resulted in activation of the DNA damage response and formation of γH2AX foci (a histone variant used as a marker of DNA damage, often DSBs) that co-localized with DSB repair factors such as Rad51 (Bansbach *et al.* 2009). Bansbach *et al*. also showed that endogenous SMARCAL1 formed foci during S/G2 in response to treatment with ionizing radiation (IR), consistent with a role in DSB repair.

SMARCAL1 is phosphorylated by ATR, ATM, and DNA-PK (Bansbach *et al.* 2009), suggesting a role in DNA damage repair in both replication-associated and replication-independent contexts. SMARCAL1 also precipitates with Ku 70/80, though, this could be due to pulldown of a common interacting protein such as RPA or H2AX (Ku70/80 also precipitates with γH2AX) (Heo *et al.* 2008; Bétous *et al.* 2013a). Studies in DT40 cells showed that SMARCAL1$^{-/-}$ cells were sensitive to camptothecin (CPT), a topoisomerase I inhibitor; etoposide (ETS), a topoisomerase II inhibitor; and ionizing radiation (IR) (Keka *et al.* 2015). Ku70$^{-/-}$ cells were more sensitive to ETS than SMARCAL1$^{-/-}$ and SMARCAL1$^{-/-}$ Ku$^{-/-}$ cells had a sensitivity phenotype identical to Ku$^{-/-}$ suggesting that Ku acts earlier in DSB repair than SMARCAL1. The same pattern was observed for Lig4$^{-/-}$ and DNA-PKcs$^{-/-}$ human cells, with NHEJ factors acting upstream of SMARCAL1 in DSB repair.

Interestingly, BRCA2$^{-/-}$ (a factor required for RAD51 loading during HDR) human cells were not sensitive to ETS, suggesting that SMARCAL1 has a role that is activated by topoisomerase II inhibition and is independent of HDR (Keka *et al.* 2015). Consistent with this observation are studies showing that SMARCAL1 and BRG1 positively influence each other's expression in response to doxorubicin treatment (Haokip *et al.* 2016). Doxorubicin is another topoisomerase II inhibitor that acts by intercalating DNA, whereas ETS forms a ternary complex with topoisomerase II and the nicked DNA, preventing religation. It is possible that topoisomerase II inhibition reflects a role in transcription, though a role in DSB repair independent of HDR cannot be excluded.

## Disease states

Biallelic mutations in *SMARCAL1* cause the rare genetic disease Schimke immuno-osseous dysplasia (SIOD). SIOD is a pleiotropic disease that affects the growth and development of the spine and the ends of long bones (spondyloepiphyseal dysplasia) (Hunter *et al.* 2010). Major characteristics of SIOD include: immune cell deficiency, specifically T-cell deficiency, and increased incidence of non-Hodgkin lymphoma (Basiratnia *et al.* 2011; Baradaran-Heravi *et al.* 2012b); focal segmental glomerulosclerosis of the kidney that ultimately leads to steroid-resistant nephropathy and end stage renal failure (Safder *et al.* 2014; Sarin *et al.* 2015); and vaso-occlusive processes including atherosclerosis and cerebral ischemia (Kilic *et al.* 2005; Deguchi *et al.* 2008; Morimoto *et al.* 2012).

SIOD has penetrance and expressivity, which can be a challenge for proper diagnosis. Onset of disease can occur prenatally through late childhood and patients can have a multitude of symptoms in addition to those listed above or a few (Lou *et al.* 2002). Lou *et al.* also found that age of onset and genotype does not always predict longevity,

though most patients with severe SIOD die in early childhood from renal failure, stroke, or infection.

Even though SIOD has been shown to be monogenic, nearly half of patients with clinical SIOD do not have identifiable mutations in coding regions of *SMARCAL1* (Hunter *et al.* 2010). Two separate studies have shown that intronic splice site mutations, which are not normally tested in genetic screens, can have variable effects on disease severity, suggesting that an individual's splicing factors may play a role in disease expression (Dekel *et al.* 2008; Carroll *et al.* 2015), however efforts to establish genotype-phenotype correlations have been largely inconclusive (Lücke *et al.* 2005; Yue *et al.* 2010; Simon *et al.* 2014). Siblings with the same mutations in *SMARCAL1* can have grossly different clinical features, suggesting that cryptic factors sensitize a patient with SMARCAL1 deficiency. Sensitization could be caused by endogenous processes like splicing or gene expression, genetic interactions with replication or DNA damage repair genes, or environmental exposures.

The unexplained variability in SIOD disease expression highlights the need for diverse molecular and genetic studies of SMARCAL1 and its orthologs. In this work I provide evidence of a novel role for Marcal1, the *Drosophila* ortholog of SMARCAL1, in DNA damage repair via SDSA. My work contributes to a growing list of SMARCAL1 functions, which can be variably affected by different mutations and may help to explain why SIOD patients have high allelic heterogeneity (Clewing *et al.* 2007) and a broad range of phenotypes.

# CHAPTER 3: ANNEALING OF COMPLEMENTARY SEQUENCES DURING DOUBLE STRAND BREAK REPAIR IS MEDIATED BY THE *DROSOPHILA* ORTHOLOG OF SMARCAL1[1]

## Introduction

Synthesis-dependent strand annealing (SDSA) is gaining acceptance as the predominant form of homology-directed repair (HDR) in mitotic cells due to its parsimony and a growing amount of circumstantial evidence, such as the rarity of mitotic crossovers in wild-type backgrounds (Andersen and Sekelsky 2010). Despite this growing support, there are few assays in existence with the capacity to determine whether non-crossover gene conversion events are generated through SDSA or the double Holliday junction (dHJ) pathway (Chapter 1). As such, little is known about the defining step of SDSA: annealing. Based on the evidence presented in Chapters 1 and 2, I hypothesize that SMARCAL1 plays a significant role in annealing during SDSA.

*Drosophila* is one of the few model systems with genetic tools available to assay SDSA, making it an ideal system to test whether SMARCAL1 plays a role in annealing during SDSA *in vivo*. I show here that *Drosophila Marcal1* mutants have elevated lethality when exposed to double strand break (DSB)-inducing agents, indicating Marcal1 has a role in HDR. I used well-characterized assays to demonstrate that annealing during both SDSA and SSA is severely reduced in *Marcal1* mutants. Abrogating Marcal1 ATP-binding reduces

[1] This work presented in this chapter was previously published in *Genetics*. The original citation is as follows:
Korda Holsclaw J and Sekelsky J. 2017 Annealing of complementary DNA sequences during double-strand break repair in *Drosophila* is mediated by the ortholog of SMARCAL1. *Genetics*. doi: 10.1534/genetics.117.200238 [Epub ahead of print]

end joining (EJ) as well as annealing, suggesting that Marcal1 activity is epistatic to polymerase theta mediated end joining (TMEJ). Altogether, these data uncover new information about HDR that further our understanding of DSB repair, which will aid in improving the efficiency of chemotherapeutics and laboratory technologies such as CRISPR/Cas9. These data also have the potential to direct studies of human SMARCAL1 that can aid in prognoses of patients with Schimke immuno-osseous dysplasia (SIOD), the disease caused by bi-allelic mutations in SMARCAL1.

## Results

### Marcal1 *mutants show elevated lethality when exposed to DSB-inducing agents*

I tested whether Marcal1 has a role in DSB repair by exposing mutant larvae to DNA damaging agents and measuring survival to adulthood relative to unexposed siblings. *Marcal1* mutant survival was not affected when exposed to methyl methanesulfonate (MMS), an alkylating agent (Lundin *et al.* 2005), or nitrogen mustard (HN2), which generates both mono-adducts and inter-strand crosslinks (Povirk and Shuker 1994) (Figure 2). Studies in mice have shown that *SMARCAL1* null mutations confer sensitivity to killing by hydroxyurea (HU) (Baradaran-Heravi *et al.* 2012b), a ribonucleotide reductase inhibitor thought to result in stalled replication forks (Hammond *et al.* 2003); however, *Marcal1* mutant larvae showed no decrease in survival when exposed to HU. HU treatment is most detrimental in cells sensitive to perturbations in replication which is consistent with published *in vitro* evidence that Marcal1 cannot regress a four-stranded model replication fork (Kassavetis and Kadonaga 2014) and suggests Marcal1 may not have a significant role in protecting stalled forks in flies.

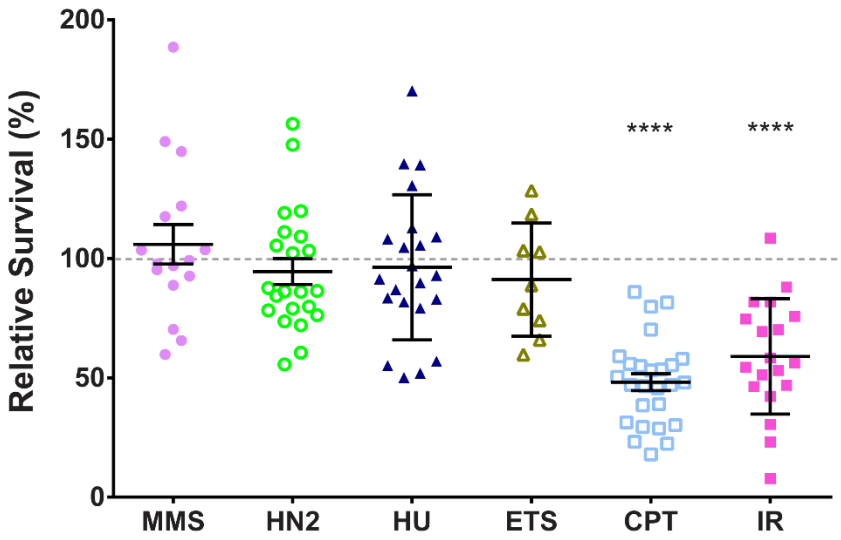


**Figure 3.1 *Marcal1* mutants are sensitive to killing by DSB-inducing agents.** Flies heterozygous for null mutations in *Marcal1* were mated in two broods of at least 10 vials, with each vial representing a biological replicate. Brood one was unexposed; brood two received a dose of MMS (methyl methanesulfonate), HN2 (nitrogen mustard), HU (hydroxyurea), ETS (etoposide), CPT (camptothecin), or IR (ionizing radiation) during larval feeding. Relative survival was calculated as the ratio of homozygous mutant to heterozygous control adults in treated vials, normalized to the same ratio in the corresponding unexposed vial. Dotted line represents 100% relative survival. ****, $P$ <0.0001 in paired *t*-tests between unexposed and exposed vials. Dosage, number of replicates, and total progeny counts are in Table 3.1.

I found a significant reduction in survival of *Marcal1* mutant larvae exposed to ionizing radiation (IR), an established DSB-inducing agent (Radford 1985). *Marcal1* mutant flies were also sensitive to killing by camptothecin (CPT), similar to both mouse and human cell studies (Baradaran-Heravi *et al.* 2012b). CPT prevents topoisomerase I from re-ligating DNA after it has nicked a strand and become covalently bound to the end (Pommier *et al.* 2010). CPT is thought to be most lethal during replication, where the nick can become a DSB. Previous studies have suggested that CPT lesions are repaired via HDR in *Drosophila* (Andersen *et al.* 2011) and in chicken DT40 cell lines (Maede *et al.* 2014). Interestingly, *Marcal1* mutant flies did not have elevated lethality when exposed to etoposide (ETS), a topoisomerase II poison that generates DSBs (Pommier *et al.* 2010).

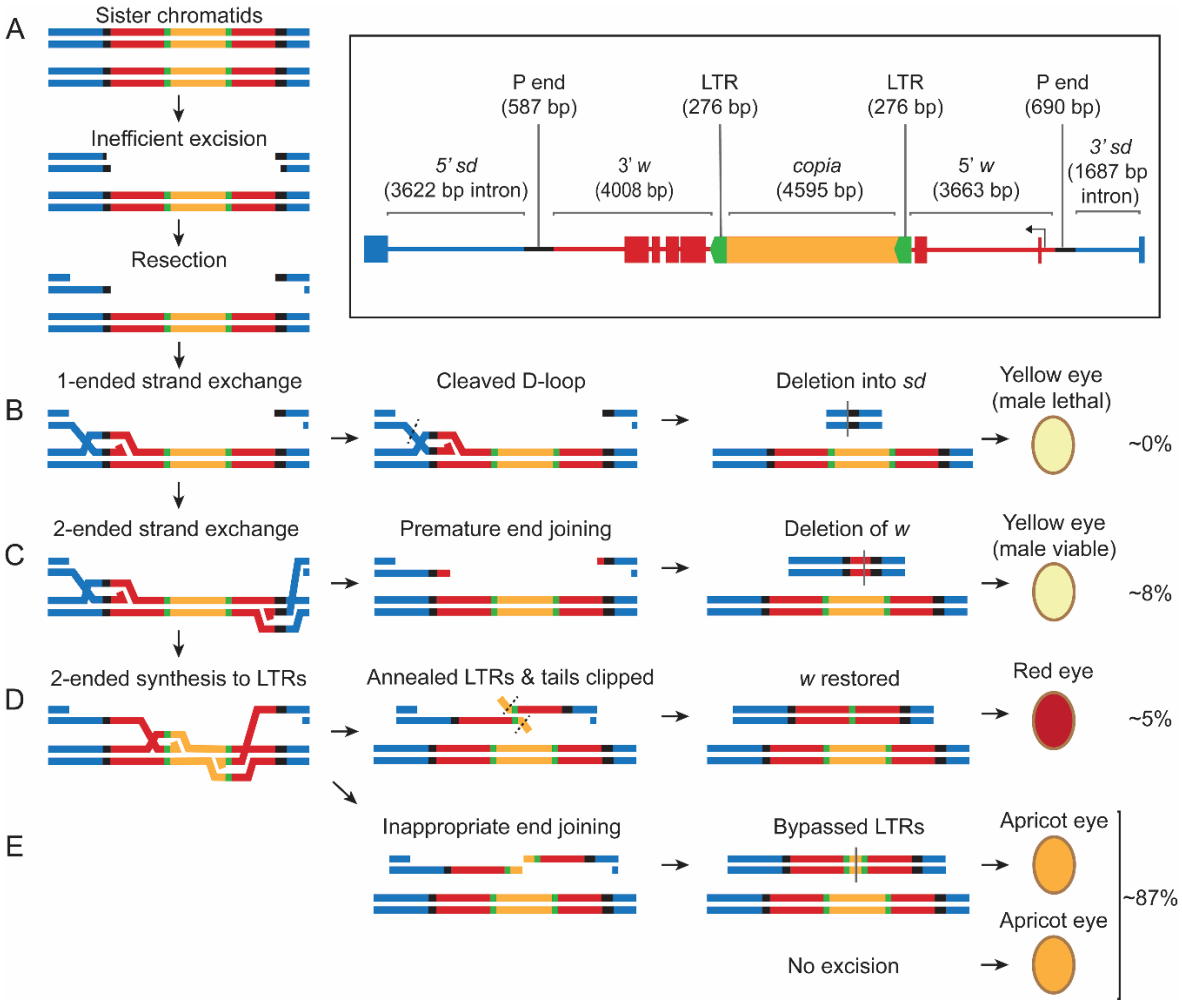


**Figure 3.2 The *P{w$^a$}* assay for SDSA.** *Inset*: The construct is a 14-kb P element inserted into the 2$^{nd}$ intron of the essential gene *scalloped* (*sd*) (blue) in reverse orientation (diagram is relative to genome coordinates on *X* chromosome). Black segments represent *P* element sequences needed for excision. Red segments are exons (boxes) and introns (lines) of a *white* (*w*) gene, the product of which loads eye pigments when functional. This copy of *w* is interrupted by a *copia* retrotransposon (orange central box) which is flanked by two 276-bp LTRs (green directional boxes), resulting in partial loss of w function and an apricot-eyed phenotype. (A) Line representations of the construct on two sister chromatids in the male germline. Exposure to inefficient P transposase results in excision of the construct from one sister, leaving 17-nt non-complementary overhangs on each side and the ends are resected. (B) One of the 3' ssDNA tails invades the intact sister to initiate synthesis. If D-loop dissociation is defective, the D-loop is cleaved, creating a deletion into a *sd* exon on one or both sides of the construct. When mated to a homozygous *P{w$^a$}* female, the progeny with flanking deletions will have a yellow eye (due to the full copy of the construct from the mother) but the event will be male-lethal in subsequent generations (~0% of progeny from wild-type males have this phenotype). (C) Premature end joining after two-ended strand exchange and some synthesis results in complete loss of *w* function; progeny will have yellow eyes and viable males in subsequent generations (~8% of progeny from wild-type males). (D) Synthesis of the LTRs followed by annealing, tail clipping and gap filling restores *w* function and progeny have a red eye (~5% of progeny from wild type males).

**Figure 3.2 (continued from previous page)** (E) Synthesis to the LTRs followed by inappropriate end joining in *copia* results in an apricot eye in the progeny and is indistinguishable from non-excision or full gene conversion events via dHJ intermediates (~87% of progeny from wild-type males). These progeny are scored but not counted as repair events.

A genetic screen of DT40 cells found that mutations in EJ genes conferred sensitivity to ETS and resistance to CPT whereas mutations in HR genes resulted in higher sensitivity to CPT than to ETS (Maede et al. 2014). It is possible that Marcal1 mutants are sensitive to ETS at higher doses than those tested here, however the data from CPT and IR treatments sufficiently support my hypothesis that *Marcal1* is involved in DSB repair

**Marcal1 *mutants have reduced annealing capacity during gap repair***

Because *Marcal1* mutants are sensitive to agents that cause DSBs, I tested the ability of these mutants to repair a double-stranded gap by SDSA. I used the well-characterized *P*{*w*$^{a}$} assay in the germline of male *Drosophila* (Figure 3.2) (Kurkulos *et al.* 1994; McVey *et al.* 2007). *P*{*w*$^{a}$} is a 14 kb *P* element that is a non-lethal insertion into the first intron of the essential gene *scalloped* (*sd*) on the *X* chromosome (Figure 3.2, inset).

The *P* element contains a *white* (*w*) gene, the product of which loads red pigment into the eye, interrupted by an intronic *copia* retrotransposon flanked by two 276-bp long terminal repeats (LTRs). The *copia* insertion alters *w* splicing and results in an apricot-colored eye in hemizygous males or homozygous females. When exposed to an inefficient source of *P* element transposase, the *P*{*w*$^{a}$} element is excised from one chromatid; the intact sister chromatid serves as an efficient template for HDR. Excision generates 17-nt non-complementary overhangs on both sides of the break, which are structurally similar to short resected ends and are poor substrates for end-joining via cNHEJ (Symington and Gautier 2011). Repair events from single males are recovered in female progeny by crossing to females homozygous for *P*{*w*$^{a}$}.

For SDSA to occur, both sides of the break must be extended (via synthesis) beyond the first region of complementarity, the *copia* LTRs, and these must be annealed correctly (Figure 3.2). The resultant product deletes *copia* except for a single LTR, resulting in restoration of *w* splicing, observable as red eyes in progeny inheriting this product. If EJ occurs either without synthesis or after incomplete synthesis, *w* function is lost, resulting in yellow-eyed progeny (due to the maternally-inherited complete *P*{$w^a$} copy). Complete restoration of *P*{$w^a$} could occur via a dHJ intermediate or through SDSA or EJ that synthesizes past the LTRs. These are not scored as repair events because they cannot be differentiated from a lack of excision; however, lack of excision is the most frequent class (>85% of progeny), whereas complete restoration is estimated to be <2% in wild-type males. SDSA and EJ events are quantified as a percentage of total scorable progeny (daughters that do not inherit the transposase source) from each male, including apricot-eyed progeny. I also measured the distribution of events per male.

I found that *Marcal1* mutants had significantly reduced SDSA (red-eyed progeny) compared to wild type both in percentage of total progeny scored (Figure 3.3A) and in number of males with observable SDSA events in the progeny (Figure 3.4). EJ (yellow-eyed progeny) was not significantly changed in *Marcal1* mutants (Figure 3.3B). SDSA could be reduced if *P* element excision is reduced or strand exchange is impaired. To test this, I performed the assay in a *Brca2* mutant. *Drosophila* Brca2 has a strand exchange function similar to that of human BRCA2 (Brough *et al.* 2008), so I expected strand exchange to be defective in *Brca2* mutants and for all repair to be the result of EJ events prior to strand invasion, which would be observable as yellow-eyed progeny. As expected, I observed no red-eyed progeny in *Brca2* single mutants and a compensatory increase in yellow-eyed progeny compared to wild type (Figure 3.3A-B).

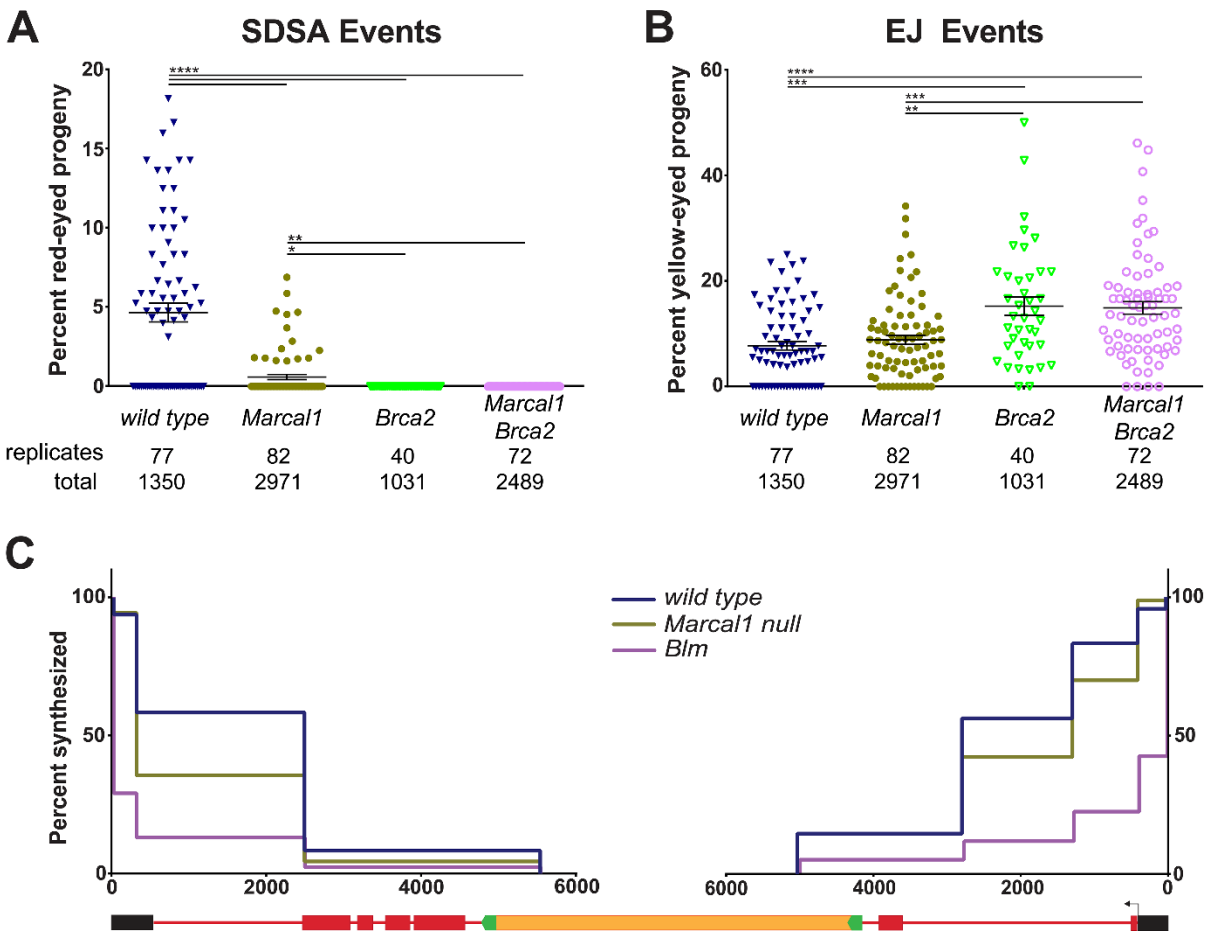


**Figure 3.3 *Marcal1* mutants have reduced SDSA capacity in the *P*{*w*$^a$} assay.** (A) SDSA events are measured as the percentage of scored progeny with red eyes. Mean and SEM are indicated. *Marcal1* null mutant, *Brca2* mutant, and *Marcal1 Brca2* double mutant frequencies were all significantly reduced compared to wild type. The numbers of single males (biological replicates) and total progeny scored are listed below the graph. (B) EJ events were measured as the percentage of scored progeny with yellow eyes. *Brca2* and *Marcal1 Brca2* mutants had significantly elevated EJ compared to wild type and *Marcal1* single mutants. *P*-values: ****, *P* <0.0001, **, *P* <0.002, *, *P* <0.05, based on parametric ANOVA. (C) Synthesis tracts in repair events recovered in yellow-eyed progeny were measured using a series of PCRs (Table 3.2). Each interval was measured independently and quantified as a percentage of total independent events analyzed. *X*-axis denotes distance (in nucleotides) from each end of the gap, on the same scale as the schematic of *P*{*w*$^a$} below. *Y*-axis is percent of events analyzed that had a positive PCR and therefore synthesized at least as far as the most internal primer. *Marcal1* (*n*= 90) was not significantly different from wild type (*n*=48) when corrected for multiple intervals (Materials and Methods). *Blm* (*n*=75) mutants were significantly different (*P* <0.0001) from both wild type and *Marcal1*.

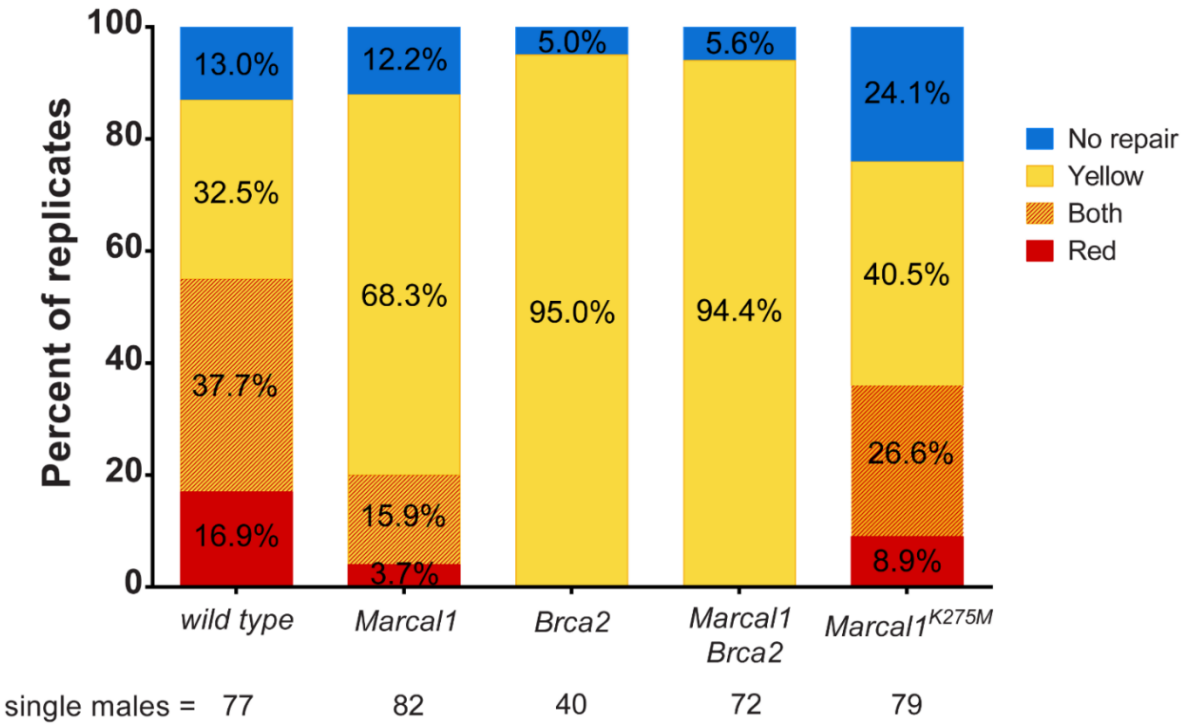


**Figure 3.4 Distribution of repair events per replicate (single male).** Each male (replicate) from the *P*{*w*$^{a}$} assay was categorized according to the distribution of repair events observed in his progeny and the data are displayed as a percentage of all males assayed in each genotype. Red indicates red-eyed progeny were observed; yellow indicates yellow-eyed progeny; both indicates red- and yellow-eyed progeny; and no repair indicates no red or yellow-eyed progeny were observed. Apricot-eyed progeny were observed in the progeny of every male.

If *Marcal1* mutations reduce *P* element excision or affect the pathway upstream of Brca2 function in DSB repair, I would expect *Marcal1 Brca2* double mutants to have reduced EJ compared to *Brca2* single mutants due to an overall reduction in observable repair products. However, I found *Marcal1 Brca2* double mutants to have a repair phenotype that was not significantly different from *Brca2* single mutants (Figure 3.3A-B). I therefore conclude that the decreased SDSA in *Marcal1* mutants results from a loss of function downstream of strand invasion.

While the *Marcal1* mutant phenotype could result from defective LTR annealing, it could also be due to compromised D-loop disassembly or reduced capacity to synthesize past the LTRs. In *Blm* mutants, which are believed to be defective in D-loop disassembly,

the synthesis length in repair products is significantly shorter than in wild-type males (McVey *et al.* 2007).

In addition, many repair events have deletions from the break site into the flanking *sd* gene; these are hypothesized to arise from nucleolytic cleavage of D-loops that cannot be disassembled (Adams *et al.* 2003; McVey *et al.* 2004a). I analyzed the aggregated amount of synthesis from each end of the break in all observed EJ events to determine the overall synthesis pattern within the population of EJ events (Figure 3.3C). Synthesis tracts in *Marcal1* mutants was similar in length to those of wild-type flies but significantly longer tracts in *Blm* mutants (Figure 3.3C). Repeated rounds of strand exchange, synthesis, and D-loop dissociation have been observed in previous assays of gap repair (McVey *et al.* 2004b) and my finding that aggregated synthesis tract lengths in *Marcal1* mutants is similar to wild type suggests that the length of synthesis per cycle, while likely having some stochastic component, is unchanged by loss of Marca1. Also, I did not observe any flanking deletions among EJ repair products from *Marcal1* mutants, whereas 48% of EJ repair in *Blm* mutant was associated with deletion. Altogether, these data suggest that the reduction in red-eyed progeny in *Marcal1* mutants is not due to defects in synthesis or inability to disassemble D-loops. These data support the hypothesis that *Marcal1* mutants have a defect in LTR annealing.

**Marcal1 *mediates annealing independent of synthesis***

SMARCAL1 annealing studies have been restricted to replication-associated roles and I observed reduced annealing in *Marcal1* mutants using the *P*{$w^a$} assay, which requires synthesis for annealing. I wanted to know if Marcal1 mediates annealing in contexts that do not require synthesis, so I used SSA assay called *P*{*wIw*} (Rong and Golic 2003).

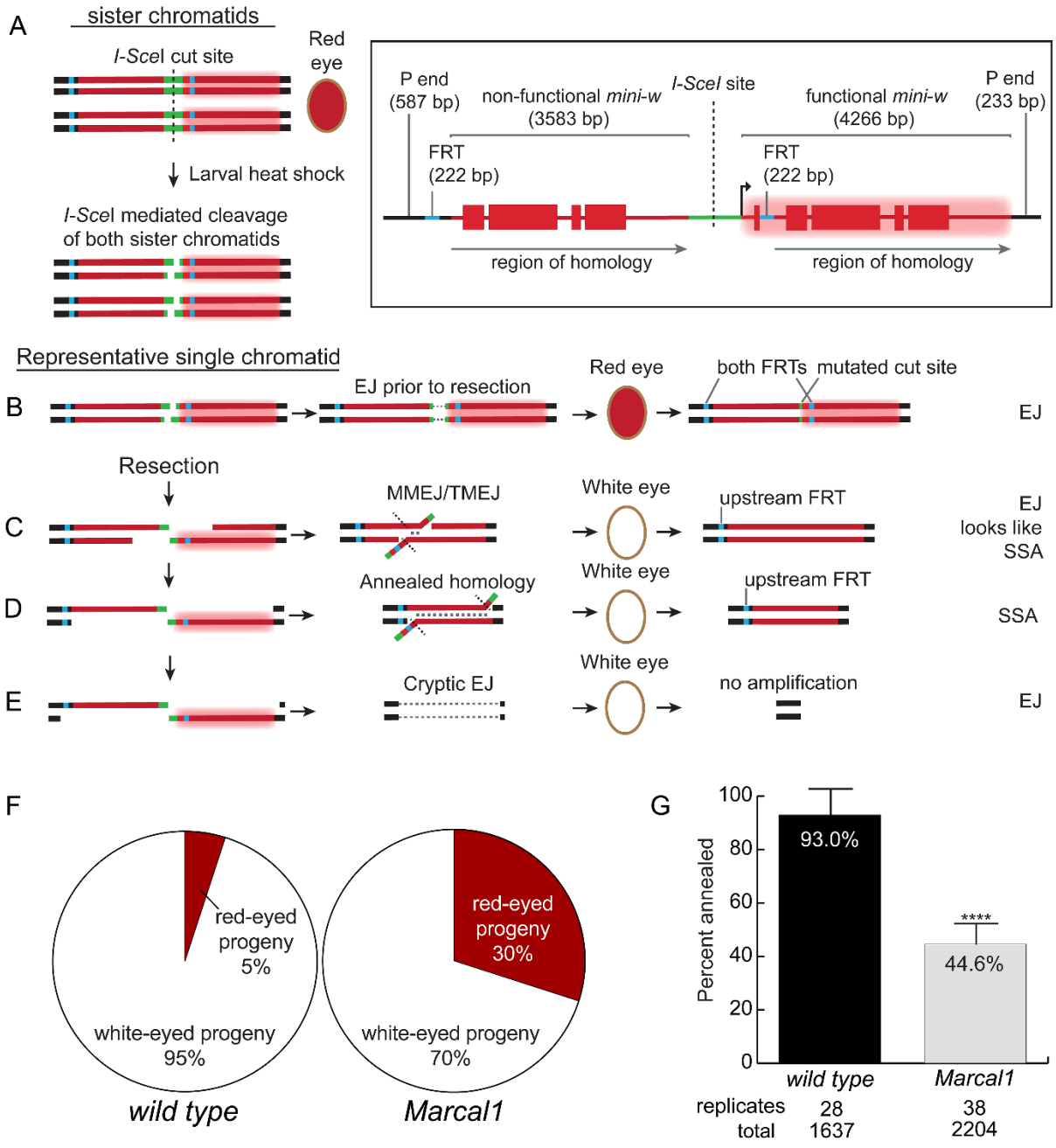


**Figure 3.5 *Marcal1* mutants have reduced annealing capacity in the *P{wIw}* assay.** *Inset*: The construct is on chromosome *3* and consists of two copies of the *mini-white* (*mini-w*) gene that are tandemly arrayed and separated by a linker containing an *I-Sce*I recognition site. The upstream copy is missing exon 1 and intron 1 rendering it non-functional, while the downstream copy is functional (represented by a red glow in the schematic), and produces a wild-type red eye in a *w* null background. The upstream *mini-w* has a 5' FRT site and the downstream copy has an FRT insertion in intron 1. PCR amplification of the FRT anchored in *mini-w* yields different size products for each gene which is used to identify the presence or absence of each copy. (A) The assay is performed in the male germline with *P{wIw}* heterozygous. *I-Sce*I is expressed via heat shock during larval development, resulting in DSBs with 4-nt overhangs on both sister chromatids.

**Figure 3.5 (continued from previous page)** (B) Mutational cNHEJ can occur at the cut site, yielding red-eyed progeny and the presence of both FRTs but a mutated *I-Sce*I cut site. (C) If resection is insufficient to expose complementary sequences, MMEJ/TMEJ can give white-eyed progeny with a deletion that includes the downstream FRT. These events cannot be differentiated from products of SSA unless the deletion is sufficiently large (>1000 bp); if no difference in size was observed, these events were classified as SSA. (D) Full resection of at least 3.6 kb reveals complementarity between the ssDNA ends that can be annealed. This results in white-eyed progeny with only the upstream FRT site; such events were categorized as SSA. (E) Excessive resection can result in deletion of the entire construct, resulting in white-eyed progeny with no amplification products. (F) Percentage of total progeny with white or red eyes for wild type and *Marcal1* mutants. P <0.0001 using $\chi^2$ test. (G) Percentage of repair products that involved annealing, after molecular analysis correction (Figure 3.6). *Marcal1* null mutants had significantly reduced annealing compared to wild type, *P* <0.0001. Error bars are SD. Biological replicates (single males) and total progeny scored are denoted below each genotype.

*P*{*wIw*} is a *P* element that has two *mini-white* (*mini-w*) genes in tandem (Figure 3.5, inset). The downstream copy (~4.3 kb) is functional, while the upstream copy (~3.6 kb) is non-functional due to a deletion of the promoter and first exon. The two are separated by a linker region containing an *I-Sce*I recognition site and can be differentiated by amplifying FRT sites present in the 5' region of each copy (Figure 3.5, inset). *I-Sce*I is expressed in the germlines of male larvae heterozygous for an insertion of *P*{*wIw*} on chromosome *3* and repair events are recovered in the progeny (Figure 3.5A). Previous studies have shown that *I-Sce*I cuts at >90% efficiency in this context, thus the most common outcome is cutting of both sister chromatids (Rong and Golic 2003). Since the homologous chromosome does not have a *P*{*wIw*} insertion, strand invasion is a rare event; however, full resection of both sides can reveal the 3.6 kb of complementarity between the upstream and downstream copies of *mini-w*. If these sequences are annealed, completion of SSA repair gives a product that retains only a non-functional copy of *mini-w*; progeny that inherit this repair event will have white eyes and the upstream FRT site (Figure 3.5D).

Red-eyed progeny can result from EJ with little or no resection or from an uncut construct; which will have both FRT sites and a mutated *I-Sce*I cut site (Figure 3.5A-B). White eyes can also result from EJ repair with deletion into the promoter of the downstream

*mini-w*, which will have both FRT sites (not depicted); however, EJ events with deletions that extend into the downstream FRT site can be indistinguishable from SSA events (Figure 3.5C).

I observed a significant difference in the distribution of eye color between wild type and *Marcal1* mutants (Figure 3.5F). Every *Marcal1* mutant male had progeny with both eye colors, whereas almost 40% of wild-type males did not produce any red-eyed progeny. I collected 10 (or all if less than 10) red-eyed progeny from each male for molecular analyses.

These analyses showed no difference in cutting efficiency of *I-Sce*I between *Marcal1* and wild type (Figure 3.6A), suggesting that the increase in red-eyed progeny in *Marcal1* mutants is not due to reduced induction of DSBs. Furthermore, the distribution of EJ events in red-eyed flies was strikingly similar between *Marcal1* and wild type, which suggests that the type of EJ utilized is not affected by Marcal1. This is consistent with a role for Marcal1 after resection since the type of EJ is dictated by the structure of the DNA ends.

I also collected 10 white-eyed progeny for analysis. 98% of the white-eyed males from wild-type flies were consistent with annealing by SSA (Figure 3.6B). In stark contrast, 34% of analyzed white-eyed progeny from *Marcal1* mutant males were confirmed as EJ. It is likely that this number is under-reported because the large regions of homology in the construct obscures identification of EJ events that are similar in size to the predicted annealed length. Altogether, these data show significantly reduced SSA annealing capacity in *Marcal1* null mutants (44.6%) compared to wild type (93.0%) (Figure 3.5G), indicating Marcal1 is important for annealing in both synthesis-dependent (SDSA) and synthesis-independent (SSA) repair strategies.

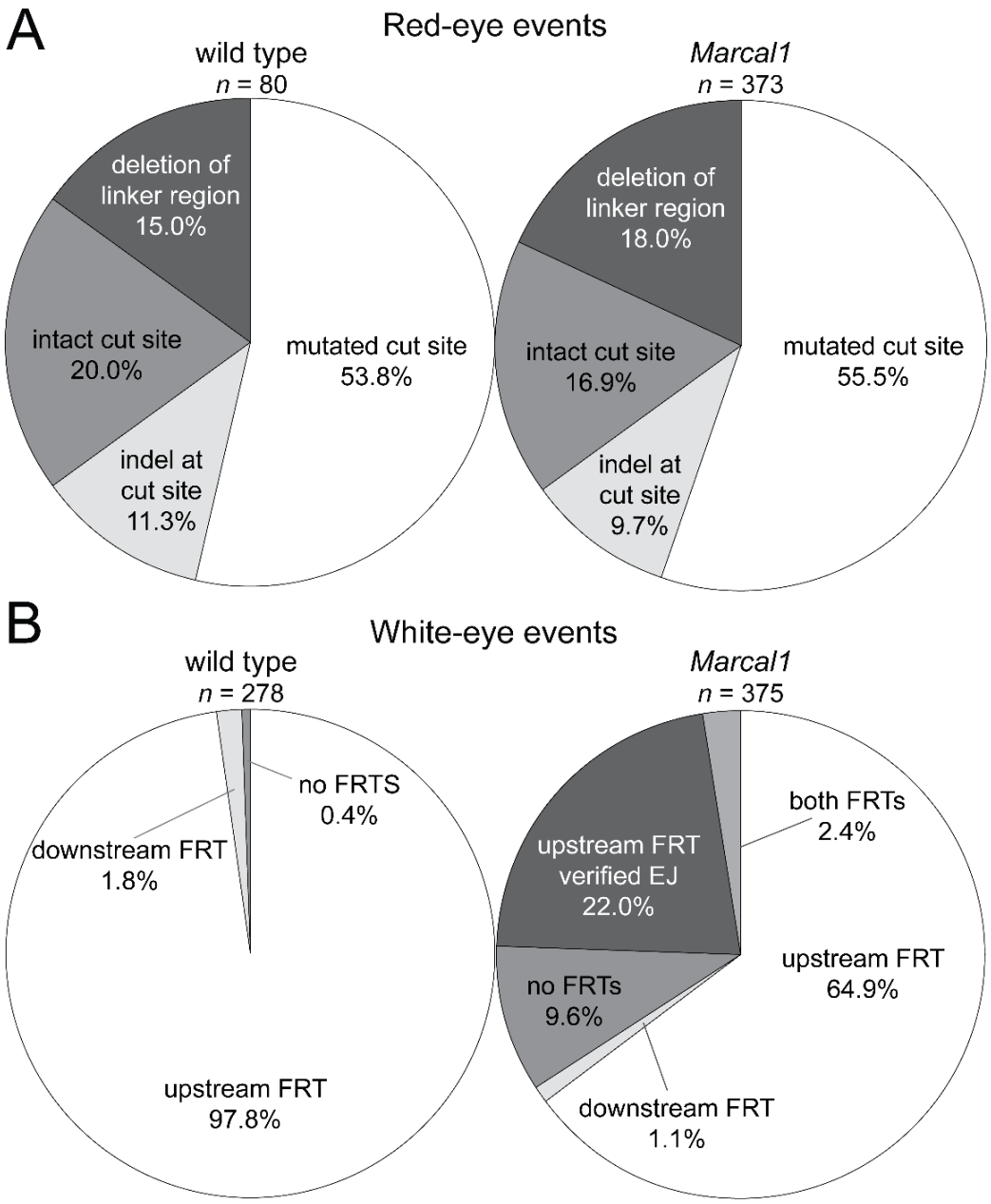


**Figure 3.6 Distribution of *P{wIw}* events in wild type and Marcal1 mutants after molecular analysis.** A) Distribution of molecularly analyzed events from collected red-eyed progeny as a percentage of total red analyzed events (listed below genotype). Mutated cut site: amplified band (primer set wIw_cut, Table 3.3) was not cut with *I-Sce*I; indel at cut site: band was smaller or larger than predicted; intact cut site: band was cut with *I-Sce*I; deletion of linker region: no amplification with primer set. B) Distribution of molecularly analyzed events from collected white-eyed progeny as a percentage of total white analyzed events (listed below genotype). Upstream FRT: only FRT associated with upstream *mini-w* amplified (primer set, Table 3.3) (categorized as annealed events); upstream FRT verified EJ: larger or smaller than predicted products from whole construct amplification (categorized as EJ events); downstream FRT: only downstream FRT amplified (verified to be in the upstream locus, removed from final data set); both FRTs: both amplified (categorized as EJ events); no FRTs: no amplification (categorized as EJ events).

***ATP-binding is required for Marcal1 activity during SDSA***

I next asked if Marcal1 translocation is required for annealing during SDSA. Helicases use the conserved Walker A and Walker B motifs to bind and hydrolyze ATP for translocation. SMARCAL1 can bind DNA in the absence of ATP (Yusufzai and Kadonaga 2008), so I abolished the ATP-binding site in the Walker A motif by mutating the conserved lysine to a methionine (K275M) in the endogenous *Marcal1* gene via CRISPR/Cas9. I then tested the ability of *Marcal1*$^{K275M}$ ATP-binding defective mutants to repair a gap using the *P*{*w*$^{a}$} assay.

*Marcal1*$^{K275M}$ mutants had a reduction in SDSA similar to that of *Marcal1* null mutants (Figure 3.7A), suggesting that translocation is required for its function during SDSA. Surprisingly, EJ events were significantly reduced compared to wild type and *Marcal1* null mutants (Figure 3.7B), revealing a genetic interaction between *Marcal1* and EJ pathways. I compared synthesis patterns in *Marcal1*$^{K275M}$ mutants to wild type and *Marcal1* null mutants. I found that *Marcal1*$^{K275M}$ mutants did not have significantly different synthesis length compared to either genotype (Figure 3.7C).

Lastly, I tested the ability of *Marcal1*$^{K275M}$ mutants and *Marcal1*$^{K275M}$ heterozygotes to anneal complementary sequences during SSA using the *P*{*wIw*} assay. White-eyed flies were significantly decreased in *Marcal1*$^{K275M}$ mutants (66.88%), compared to *Marcal1*$^{K275M}$ heterozygotes (95.59%) (Figure 3.7D). The white-eyed frequency in heterozygotes was not statistically different from wild type (wild type data from Figure 3.5B) and like wild type, 40% of *Marcal1*$^{K275M}$ heterozygous males had no red-eyed progeny (all *Marcal1*$^{K275M}$ homozygous males had red-eyed progeny). The percentage of red- and white-eyed progeny in *Marcal1*$^{K275M}$ mutants was not significantly different from *Marcal1* null mutants (null data from Figure 3.5B), suggesting that ATP-binding does not affect EJ in the absence of strand exchange, synthesis, and D-loop dissociation.

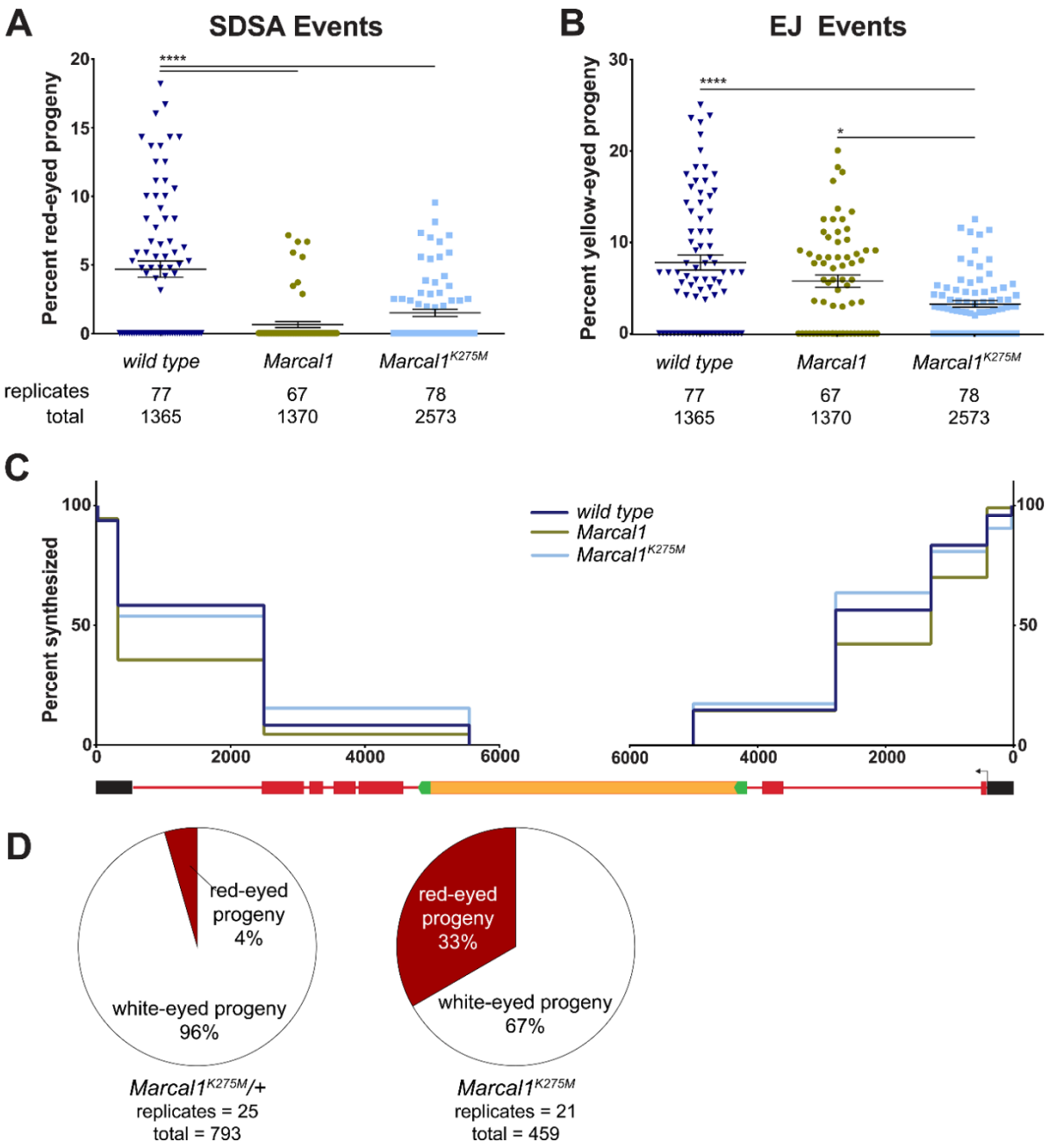


**Figure 3.7 *Marcal1*$^{K275M}$ mutants have reduced SDSA and EJ capacity**. SDSA (A) and EJ (B) events were measured in *Marcal1*$^{K275M}$ mutants as described in Figure 3.3. SDSA was similar between *Marcal1*$^{K275M}$ and *Marcal1* null, but EJ events were significantly reduced in *Marcal1*$^{K275M}$ compared to both wild type and *Marcal1* null mutants. (C) Synthesis tracts lengths, measured as described in Figure 3.3C. No significant differences were found between *Marcal1*$^{K275M}$ (*n*=52) and wild type (*n* = 48) or *Marcal1* null mutants (*n*=90). (D) *Marcal1*$^{K275M}$ heterozygotes and *Marcal1*$^{K275M}$ mutants were tested in the *P*{*wIw*} SSA assay as described in Figure 3.5. Heterozygotes had 96% white-eyed progeny, which is not statistically different from wild type (Figure 3.5F) based on a parametric ANOVA test. *Marcal1*$^{K275M}$ mutants had 67% white-eyed progeny, which was significantly reduced compared to heterozygotes but not significantly different from *Marcal1* null mutants (Figure 3.5F).

These data also show that ATP-binding is required for annealing during SSA, supporting our findings from *P*{*w*$^{a}$} and establishing a requirement for ATP hydrolysis in annealing activities of Marcal1.

## Discussion

Prior to the studies reported here, little was known about annealing during HDR in animals or how the decision between annealing, dHJ formation, and TMEJ is regulated. My data provide *in vivo* evidence that Marcal1 mediates annealing during SDSA and SSA in *Drosophila*, and suggest that Marcal1 acts directly to anneal complementary strands, as abrogating Marcal1 translocation activity via Walker A mutation (*Marcal1*$^{K275M}$) recapitulates the null phenotype. The *Marcal1*$^{K275M}$ mutation reduces EJ as well as annealing during SDSA, which suggests that Marcal1$^{K275M}$ antagonizes EJ in contexts where EJ follows strand exchange, synthesis, and D-loop dissociation. Unlike *P*{*w*$^{a}$}, the *P*{*wIw*} assay for SSA did not reveal any differences between *Marcal1*$^{K275M}$ and null mutants which is likely due to differences in assay design (discussed in detail in Chapter 5).

The findings reported here provide evidence that Marcal1 mediates annealing in both SDSA and SSA. I have further shown that Marcal1 impacts EJ pathways (most likely TMEJ) during HDR, providing new information on the regulation of the anneal—EJ—strand re-invade decision point.

## Materials and methods

### *Drosophila* stocks

Fly stocks were maintained at 25° C on standard cornmeal medium. All *Marcal1* null assays were performed using heteroallelic null mutations *Marcal1*$^{del}$ and *Marcal1*$^{kh1}$. *Marcal1*$^{del}$ is a 679-bp deletion of part of the first exon and second intron generated via imprecise *P* element excision as described in (Baradaran-Heravi *et al.* 2012a). *Marcal1*$^{kh1}$

was generated using CRISPR/Cas9 technology (Gratz *et al.* 2013; Bassett and Liu 2014). Oligonucleotides (IDT) used for guide RNA were cloned into pU6 *Bbs*I chiRNA vector then injected into Bloomington stock #51323 ($y^1$ *M*{*vas::Cas9*}*ZH-2A* $w^{1118}$/*FM7c*) (BestGene). *Marcal1*$^{kh1}$ deletes 2L:4,955,554-4,956,729 (*Drosophila* annotated genome r6.13), which encompasses exon 1 through part of exon 2. The *Brca2*$^{43}$ null mutation was used *in trans* to the *Brca2*$^{47}$ null mutation in all assays. Both are large deletions produced via imprecise *P* element excision, described in (Thomas *et al.* 2013).

*Marcal1*$^{K275M}$ mutation was generated using CRISPR/Cas9. The gRNA vector was prepared as described for the *Marcal1*$^{kh1}$ allele. A repair template vector was generated by amplifying 1234 bp upstream and 643 bp downstream of the conserved lysine codon from BacPac genomic DNA clone library (ID BACR13M11) and inserted into the pSL1180 vector. QuickChange Site-Directed Mutagenesis Kit (Agilent Technologies) was used to introduce a mutation in the PAM recognition site as well as two single bp changes to alter the lysine codon to methionine (primer sequence: 5'- GAAATGGGCCTGGGCATGACTATCAGGCCTT GGCCGTAGCCG-3'). The repair vector was injected with the *Bbs*I chiRNA vector into the same stock used for generating the *Marcal1*$^{kh1}$ allele.

**Exposure assays**

Vials of five heterozygous *Marcal1*$^{del}$ females and three heterozygous *Marcal1*$^{kh1}$ males each were incubated for three days (brood 1) before being transferred to fresh vials of food for two additional days (brood 2), after which the adult flies were discarded. One day later, 250 µl of aqueous mutagenic solution was added directly to the food in brood 2 vials and the larvae were allowed to develop to adulthood (dosages listed in Table 3.1). For ionizing radiation experiments, larvae were exposed to Cesium-137 for the required time to reach the desired dosage. Surviving adults in both broods were quantified by genotype (heterozygous or heteroallelic null) and the ratio of heterozygous to heteroallelic was

calculated per vial. Exposed vials were normalized to unexposed paired brood 1 ratios. Paired *t*-tests were performed between unexposed and exposed ratios. Each round of biological replicates had 10-20 vials and each mutagen had two or more rounds.

| Mutagen | Dosage | Biological replicates | Unexposed progeny | Exposed progeny |
|---|---|---|---|---|
| Methyl methanesulfonate | 3.23 mM | 16 | 2864 | 1397 |
| Nitrogen mustard | 0.2 mM | 22 | 3828 | 3131 |
| Hydroxyurea | 100 mM | 22 | 3964 | 1841 |
| Etoposide | 10 mM | 9 | 1098 | 876 |
| Camptothecin | 0.05 mM | 26 | 3432 | 2233 |
| Ionizing radiation | 2000 rads (20 Gy) | 19 | 2196 | 1395 |

**Table 3.1. Dosage and sample sizes of mutagen exposure experiment.** *Marcal1* null mutants were treated with each mutagen in separate experiments as described in Materials and Methods. Biological replicates refers to individual vials assayed, each containing a single male (ratios of *wt*:*mutant* survival were calculated per vial). Progeny counts are the aggregated total number of flies scored for each mutagen.

**P{w$^a$} assays**

The *P*{*w*$^a$} assay was performed as previously described (Adams *et al.* 2003). Briefly, single males of the genotype *y w P*{*w*$^a$}; *Marcal1*$^{del}$/*Marcal1*$^{kh1}$; *Sb P*{Δ*2-3*, *ry*$^+$}/*TM6B* were crossed to four females homozygous for *y w P*{*w*$^a$} and *Sb*$^+$ female progeny were scored for red, yellow, or apricot eyes. Representative samples of red and yellow eyed females were collected and crossed to *FM7w* males to recover the repair product in subsequent males. DNA was extracted from a single adult male progeny with the repair product for PCR analysis. Multiple repair events were recovered per male, however, only repair events that could be confirmed unique were analyzed and reported. The same methods and transposase source were used for all genotypes.


| Description | Primer 1 | Primer 2 |
|---|---|---|
| 5 bp right side | CCGCGGCCGCGGACCACCTTATGTTATTT | GCCTTGCTTCTTCCACACAGCGTG |
| 0.9 Kb right side | CCCTCGCAGCGTACTATTGAT | AGATGGGTGTTTGCTGCCTCCG |
| 2.4 Kb right side | GAGCGAGATGGCCATATGGCTG | CGTTGTTTGCACGTCTCGCTCG |
| 4.6 Kb right side (into *copia*) | GGACTGGGCCCATAACCTGTTG | GAGCGACACATACCGGCG |
| 5 bp left side | CCGCGGCCGCGGACCACCTTATGTTATTT | ACCATTGCAAGCTACATAGCTGAC |
| 2 Kb left side | GACTGTGCGTTAGGTCCTGT | CGTTTCGTAGTTGCTCTTTCGC |
| 5.2 Kb left side (all *w* exons into *copia*) | TGCCAGAGAGCAAGTTCAGA | GAGGTCATCCTGCTGGACAT |

**Table 3.2 *P*{*w*$^{a}$} primers.** Diagram above table depicts PCR products. Sizes represent synthesis from break end, not PCR product size. The null *white* (*w*) gene in the *ywP*{*w*$^{a}$} genotype is a partial deletion of the 5' end of *w* leaving the 3' end intact. The left side of the construct above is identical to the 3' end of *w*; therefore, all PCRs of the left end must be anchored in the *P*-element ends or in *copia* to prevent amplification of the background copy of *w*.

Each vial of progeny from a single male was scored independently and a ratio of either red- or yellow-eyed progeny to total progeny was calculated per vial. Outliers were identified using the ROUT method and removed from the data set. No outliers were removed from the *Brca2* data set; one was removed from *Marcal1 Brca2*; and three were removed from *Marcal1*, wild type, and *Marcal1*$^{K275M}$ data sets. To determine and compare mean frequency of repair events, the red-eye (SDSA) ratios were compared between genotypes using parametric ANOVA and the mean ratios of each genotype were compared to the mean ratios of all other genotypes; the analysis was repeated for yellow-eye (EJ) ratios. Rate of lack of excision was calculated by subtracting the EJ rate of *Brca2* mutants from the total scored progeny as *Brca2* mutants are incapable of strand invasion. Rate of complete restoration of *P*{*w*$^{a}$} was calculated by summing the frequency of all repair events

in wild-type males and subtracting that rate from the EJ rate of *Brca2* mutants, using the assumption that all excisions were repaired by EJ in these mutants.

To assess synthesis capability, each repair event was analyzed with a series of seven PCRs (primers are listed in Table 3.2). Amplified products using one primer set were calculated as a percentage of total events analyzed and repeated for all primer sets (intervals). Percentage of events with positive PCRs were compared between genotypes using parametric ANOVA. When compared as individual PCRs, $P < 0.05$ was considered to be statistically significant; however, when asking how much difference exists between genotypes across all PCRs, *P*-values for each interval were multiplied by the number of intervals (7) to correct for multiple comparisons.

### *P{wIw}* assays

The *P*{*wIw*} assay was performed as previously described (Mukherjee *et al.* 2009). Briefly, four *MarcaI1*$^{del}$/CyO;*P*{*wIw*}/TM6B females were crossed to three *MarcaI1*$^{kh1}$/CyO; *Sb P*{70*I-Sce*I}/TM6B males for three days then the parents were discarded. One day later, the 1$^{st}$-instar larval progeny were heat-shocked at 37$^{o}$ for one hour. Heat shock was repeated on the following day to ensure all 1$^{st}$-instar larvae received treatment. Larvae were allowed to develop to adulthood. All *Sb*$^{+}$ progeny were scored for red or white eyes. All red-eyed flies were collected (up to a maximum of 10) from each vial; 10 white-eyed flies were collected per vial. DNA was extracted from each collected fly for analysis.

Red-eye events: The linker region was amplified (primer sets in Table 3.3) and subjected to digestion with *I-Sce*I. Events that failed to amplify or were not cut by *I-Sce*I were categorized as EJ events. Events that were successfully cut by *I-Sce*I could not be distinguished between EJ and uncut and were removed from the dataset.

White-eye events: The 5’ region of the upstream *mini-white* gene is 480 bp whereas the 5’ region of the downstream *mini-white* is 369 bp using the same primer set (Table S3). The presence of both products indicates SSA did not occur; these events were categorized as EJ events. A small number of events had only the 369-bp product, these were verified to be in the upstream location via primer anchored in the *P* element and categorized as SSA events. PCRs with no product were categorized as EJ events. The percentage of SSA events in the white class was calculated per vial. SSA and EJ events were then adjusted by this number. The adjusted percentages of SSA events per vial were compared via unpaired t-tests between control and mutant genotypes per experiment. *Marcal1*$^{K275M}$ heterozygotes and homozygotes were compared to each other, wild type, and *Marcal1* using parametric ANOVA.

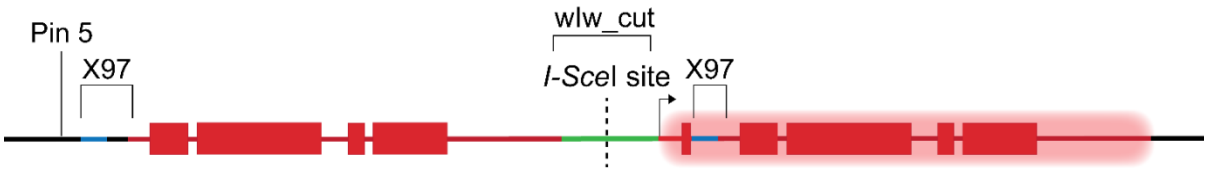


| Description | Primer 1 | Primer 2 |
|---|---|---|
| X97 | CGACGTGAACAGTGAGCTGT | GCTCATCTAACCCCGAACAA |
| wlw_cut | TGTGTGTTTGGCCGAAGTAT | CGCGATGTGTTCACTTTGCT |
| Pin 5 | GACTGTGCGTTAGGTCCTGT | |

**Table 3.3. *P{wlw}* primers.** Diagram above table depicts PCR products. The wlw_cut primer set was used to amplify the *I-Sce*I cut site in red-eyed repair events. The X97 primer set was used to assess annealing via SSA in white-eyed repair events. The upstream product is 480 bp whereas the downstream product is 369 bp. Presence of only the upstream product represents correct annealing via SSA; presence of both indicates EJ that abolishes *mini-white* function; the presence of only the downstream product was rare and verified to be in the upstream location using the Pin 5 and X97 primer 2 set. These events are interpreted as SSA with small deletions in the X97 region. Lack of amplification with the X97 primer set indicates EJ.

# CHAPTER 4: PRELIMINARY DATA REFINING THE ROLE OF *MARCAL1* IN DOUBLE STRAND BREAK REPAIR

As stated in Chapter 2, Human SMARCAL1 and its orthologs have been implicated in multiple repair pathways including replication-associated DNA damage repair and stability, gene expression in response to environmental stress (particularly heat stress), and non-homologous end joining. Most recently, I uncovered a role for the *Drosophila* ortholog, Marcal1, in homology-mediated repair of double strand breaks (DSBs) via synthesis-dependent strand annealing (SDSA). These data suggest that Marcal1 may be involved in other processes that rely on homology-directed repair (HDR), such as meiotic recombination. Additionally, Marcal1 does not have replication fork regression activity *in vitro* but this finding has not been corroborated *in vivo*. To refine the role of Marcal1 in HDR, I performed a series of experiments including meiotic nondisjunction assays, synthetic lethality assays, mutagen sensitivity/lethality experiments, and further SDSA assays. I did not find evidence for Marcal1 activity during meiosis or after annealing during SDSA; however, I did find complex genetic interactions with *Blm* helicase that provide insight into Blm activities during DNA damage repair.

## *Marcal1* null mutations do not affect meiotic chromosome segregation

Crossovers (CO) are necessary for proper segregation of chromosomes during meiosis. Formation of CO is tightly regulated to ensure the proper number and placement of CO. In *Drosophila*, more programmed DSBs are generated than are needed to achieve the proper distribution of one CO per chromosome arm; the remaining DSBs are repaired into non-crossovers (NCO) (Thacker and Keeney 2009). Meiotic NCOs have been shown to arise from SDSA in yeast (Allers and Lichten 2001) and I recently showed that *Marcal1* mutants were defective in annealing during mitotic SDSA (Chapter 3) which suggests Marcal1 may play a role in meiotic DSB repair by mediating the formation of NCO products.

A defect in NCO formation could result in persistent intermediates or the formation of unwanted double Holliday junctions (dHJ), both of which would result in mis-segregation of chromosomes called non-disjunction (NDJ). To determine if Marcal1 might be involved in NCO formation during meiosis, I tested *Marcal1* null mutants for NDJ and found the NDJ rate not significantly different from wild-type flies (Table 4.1). The previously published NDJ rate for *mei-9* mutants was used as a positive control (Kohl *et al.* 2012). Mei-9 is the dHJ resolvase responsible for the formation of CO during meiosis (Yildiz *et al*. 2002, Heyer *et al.* 2003).

| Genotype | Total progeny | Exceptional classes | NDJ rate | *P* value compared to wt |
|---|---|---|---|---|
| wild type | 1697 | 1 | 0.12% | N/A |
| *Marcal1*$^{del/kh1}$ | 620 | 3 | 0.96% | 0.136 |
| *Mei-9*$^{a/A2}$ | 1310 | 190 | 22.49% | < 0.0001 |

**Table 4.1 Comparison of *X* chromosome non-disjunction rates**. *Marcal1* null mutant females were crossed to NDJ marker males and all surviving progeny were scored. Exceptional class denotes an abnormal number of *X* chromosomes (XXY females or XO males). NDJ rates were calculated by multiplying the exceptional class by 2 to account for lethal NDJ and expressed as a percentage of total progeny. *P* values were calculated using the equations in (Zeng *et al.* 2010). Wild type and *Mei-9* data were previously published (Kohl *et al.* 2012).

Recent work from our lab has proposed that NCOs and COs arise from the same intermediate, an unligated dHJ, in *Drosophila* (Crown *et al.* 2014). In contrast, work in yeast suggests NCOs arise from a D-loop intermediate similar to mitotic SDSA (Hunter and Kleckner 2001). The intermediate predicted by Crown *et al.* is structurally distinct from D-loops (specifically in its lack of ssDNA) making it a poor substrate for Marcal1 since SMARCAL1 orthologs bind ssDNA:dsDNA junctions (Bétous *et al.* 2012). Likewise, it is currently unknown if annealing occurs concomitant with synthesis or D-loop disassembly during mitosis and it is similarly unknown how these steps are ordered during meiosis. If annealing occurs after intermediate disassembly, the ends could be joined via polymerase

theta (*Drosophila* mus308) mediated end joining (TMEJ) in *Marcal1* mutants, which would not affect disjunction. It is possible that a large defect in NCO formation could potentiate an increase in CO formation without increased NDJ, though it is likely to only be observable when multiple repair strategies are defective such as in *Marcal1*; *mus308* double mutants (which would affect both annealing and TMEJ). Séguéla-Arnaud *et al.* found that mutating *Blm* orthologs in conjunction with the *Fancm* ortholog (both are involved in promoting NCO during meiosis) in *Arabidopsis* resulted in significantly elevated COs without chromosome disjunction defects (Séguéla-Arnaud *et al.* 2015). However, mutations in *Blm* result in significantly elevated NDJ in *Drosophila* (McVey *et al.* 2007, Hatkevich and Kohl *et al.* 2017). It remains unclear if these differences are due to altered roles for Blm between orthologs or if there are key differences in meiotic disjunction mechanisms between organisms. Further studies of *Marcal1* genetic interactions with genes that antagonize recombination may help to clarify whether or not Marcal1 has a role in meiotic NCO formation.

## *Marcal1* genetically interacts with *Blm* helicase but not structure-specific endonucleases

Previous work has shown that structure-specific endonucleases are necessary in the absence of Blm helicase, specifically, the mus312-Slx1 complex (SLX4-SLX1 in humans), mus81, and Gen (GEN1 in humans, Yen1 in yeast). All three endonuclease orthologs have been shown to cleave Holliday junctions (HJs) (reviewed in Svendsen and Harper 2010) and are synthetically lethal with *Blm* mutations in flies (Johnson-Schlitz and Engels 2006; Trowbridge *et al.* 2007; Andersen *et al.* 2009, 2011). Work from our lab has shown that genetic interactions between endonucleases and *Blm* are partially rescued by mutations in *Spn-A* (the *Drosophila* ortholog of *Rad51),* suggesting that the synthetic lethality phenotype is predominantly due to the inability to process toxic intermediates during HDR.

In yeast, mutations in *MUS81* and *SLX4-SLX1* are synthetically lethal with mutations in *SGS1*, the yeast ortholog of *Blm*, whereas mutations in *YEN1* are not, though they do have increased sensitivity to DNA damaging agents (Fabre *et al.* 2002; Blanco *et al.* 2010). The synthetic lethality of *mus81*Δ *sgs1*Δ and *yen1*Δ *sgs1*Δ increased sensitivity are rescued by mutations in *RAD51,* as well*.* Interestingly*,* the same genetic interactions are also rescued by mutations in *RAD52*. *In vitro* assays of Rad52 and Rad51 strand exchange dynamics suggests that Rad52 is necessary for Rad51 loading (Benson *et al.* 1998; New *et al.* 1998; Song and Sung 2000); however genetic assays of HDR via ectopic gene conversion show additive effects of mutations in *RAD51* and *RAD52* suggesting that Rad52 may not be biologically necessary for strand exchange activity (Manthey *et al.* 2016).

Interestingly, Rad52 has also been implicated in 2$^{nd}$-end capture leading to dHJ formation during DSB repair (McIlwraith and West 2008; Wu *et al.* 2008; Nimonkar *et al.* 2009) as well as annealing during SSA in yeast and human cells (Ivanov *et al.* 1996; Storici *et al.* 2006; Wu *et al.* 2008; Bhargava *et al.* 2016). As previously mentioned, *Drosophila* do not have a known Rad52 ortholog and Marcal1 appears to be the major annealase during SSA in flies (see Chapter 3) raising the question of whether it may also mediate annealing in 2$^{nd}$-end capture. To test this hypothesis, I tested the viability of *mus81*, *Gen*, *mus312*, and *Blm* mutant combinations in a *Marcal1* null background (Table 4.2) with the prediction that *Marcal1* mutations would rescue synthetic lethality phenotypes in a similar manner to *Rad51* mutations by preventing the formation of dHJs.

| Gene(s) | Viability | *n* | Observed | Expected | *P* value | Viability with *Marcal1* | *n* | Observed | Expected | *P* value |
|---|---|---|---|---|---|---|---|---|---|---|
| *Marcal1* | + | 3381 | 1173 | 1127 | 0.094 | N/A | N/A | N/A | N/A | N/A |
| ENDONUCLEASES | | | | | | | | | | |
| *mus312* | + | 948 | 386 | 316 | $2.07 \times 10^{-6}$ | + | 406 | 58 | 45.1 | 0.05 |
| *mus81* | + | 2026 | 1081 | 1013 | 0.0025 | + | 609 | 216 | 203 | 0.266 |
| *Gen* | + | 745 | 292 | 248.3 | $8.09 \times 10^{-4}$ | + | 313 | 61 | 34.8 | $1.6 \times 10^{-5}$ |
| *mus312 Gen* | + | unk | unk | unk | unk | + | 410 | 37 | 45.6 | 0.166 |
| *Gen Blm* | - | unk | unk | unk | unk | - | 136 | 0 | 15.1 | $1.51 \times 10^{-8}$ |
| *mus312 Blm* | - | unk | unk | unk | unk | - | 57 | 0 | 6.3 | $2.48 \times 10^{-4}$ |
| HELICASES & POLYMERASES | | | | | | | | | | |
| *Fancm* | + | 1246 | 345 | 311.5 | 0.03 | + | 256 | 39 | 28.4 | 0.045 |
| *Blm* | + | 2568 | 1019 | 856 | $1.71 \times 10^{-11}$ | + | 154 | 20 | 17.1 | 0.469 |
| *mus308* | + | 1440 | 611 | 480 | $6.70 \times 10^{-13}$ | + | 348 | 42 | 38.7 | 0.574 |
| *Polα-180* / + | + | N/A | N/A | N/A | N/A | + | 710 | 292 | 236.7 | $1.5 \times 10^{-5}$ |

**Table 4.2 Viability in *Marcal1* double and triple mutants.** Combinations of null mutations were assayed for synthetic lethality or rescue of synthetic lethality by crossing heterozygous parents and scoring incidence of mutant progeny. Two-tailed *P* values were calculated by G-test for goodness of fit between observed and expected mutant progeny counts. *Fancm* single mutant data were from the control group in mutagen lethality assays reported in (Romero *et al.* 2016). *Mus308* and *mus312* single mutant data were generated by J. Carvajal Garcia (unpublished controls for mutagen lethality assays); *mus308* single mutant data are from $mus308^{118H}$ homozygotes whereas *Marcal1 mus308* double mutant data were generated with heteroallelic $mus308^{118H/2003}$. *Polα-180* mutations are homozygous lethal. *Gen* and *mus81* single mutant data were generated by S. Bellendir (controls for mutagen lethality assays, manuscript in review); *mus81 Marcal1* double mutant assay was performed using *mus81* homozygous mutants. “Unk” signifies that the assays were qualitative, not quantitative.

***The balancer effect***

I observed a statistically significant increase in homozygous progeny in all mutants tested, with the exclusion of *Marcal1*, compared to what is expected by Mendelian inheritance (Table 4.2). This phenomenon is likely due to the presence of balancer chromosomes in heterozygous genotypes.

Balancers are versions of a chromosome that have extensive inversions that prevent meiotic recombination from occurring between homologs, which is very useful for retaining recessive mutations in laboratory practices but can also lead to increased NDJ of that chromosome, slightly reducing fitness (Stocker and Gallant 2008). It is common to see slightly skewed progeny numbers in stocks that have a balancer and are homozygous viable.

**Marcal1 *does not have genetic interactions with structure-specific endonucleases***

The gene *mus81* is located on the *X* chromosome and the stock used in this assay has greatly improved fitness when homozygous for the mutant allele, $mus81^{nhel}$. Female flies have two *X* chromosomes while males have an *X* and a *Y* chromosome, making retention of a balancer increasingly difficult in stocks with a preference for homozygosity on the *X*. I therefore opted to test if *mus81* mutations affected *Marcal1* viability and found that *Marcal1* mutants were unaffected by *mus81* mutations suggesting that there is no significant genetic interaction between *mus81* and *Marcal1*.

I did not observe synthetic lethality when any gene was in a *Marcal1* mutant background. I also did not observe rescue of *Gen Blm* or *mus312 Blm* synthetic lethality phenotypes in a *Marcal1* null background. Synthetic lethality could be due to the inability to process dHJ joint molecules, as previously suggested, in which case I would expect rescue of the synthetic lethality if Marcal1 participated in formation of the dHJ via a role in $2^{nd}$-end capture. However, synthetic lethality could also be due to defects in DNA damage repair

during replication. Blm has been implicated in replication associated repair (Rao *et al.* 2005; Selak *et al.* 2008; Sidorova *et al.* 2013; Chaudhury *et al.* 2013; Manthei and Keck 2013) and all three endonucleases can cut other structures, including flaps and forks (Ehmsen and Heyer 2008; Ip *et al.* 2008; Rass *et al.* 2010; Wyatt *et al.* 2013). Mus81 has also been implicated in common fragile site expression via cleavage of under-replicated regions during mitosis (Naim *et al.* 2013; Ying *et al.* 2013). Additionally, SMARCAL1 has well-characterized roles in replication-associated repair and SMARCAL1 deficient cells have elevated mus81-dependent γH2AX staining (Bansbach *et al.* 2009; Bétous *et al.* 2013b; Couch *et al.* 2013). If the main source of synthetic lethality is accumulation of replication-associated damage, Marcal1 may fail to rescue the phenotype. Andersen *et al.* showed that mutations in *Spn-A* could partially rescue synthetic lethality by preventing strand exchange which suggests both potential causes (HDR joint molecule processing and replication-associated damage) contribute to the phenotype. It is possible that *Marcal1* mutations could have a modest effect on replication-associated repair resulting in partial rescue of synthetic lethality phenotypes, however, such incremental effects were not measured in this assay. It should be noted, however, that Marcal1 does not have fork regression activity *in vitro* (Kassavetis and Kadonaga 2014) nor have I observed increased lethality when *Marcal1* mutants are exposed to mutagens that have been proposed to be most lethal during replication such as MMS, HU, and ETS (Figure 3.1). Based on these data, it is unlikely that Marcal1 participates in 2$^{nd}$-end capture, however whether or not it has a role during replication remains unclear.

**Marcal1 *genetically interacts with* Blm**

While I did not observe lethality when any gene was in a *Marcal1* mutant background, I found that some genes, such as *Blm* and *mus308*, had significantly different genotype distributions in a *Marcal1* mutant background whereas other genes, such as *Fancm*, were less affected. To determine the cause of these differences, I scored each

balancer separately in two different crosses: *Marcal1 mus308* and *Marcal1 Blm* (Table 4.3). Both *mus308* and *Blm* single mutants were observed in a significantly higher amount than expected with *P* values of $6.70 \times 10^{-13}$ and $1.71 \times 10^{-11}$, respectively, whereas both *Marcal1 mus308* and *Marcal1 Blm* double mutants observed were not significantly different than expected with respective *P* values of 0.574 and 0.469. No change was observed for *Fancm*, another helicase implicated in D-loop dissociation suggesting *Marcal1* and *Fancm* do not genetically interact.

In *Marcal1 mus308* double mutants, I found that the number of double-balanced flies was slightly less than expected while the occurrence of Chr. *2* or Chr. *3* single-balanced progeny was roughly equal (89 and 86, respectively) and slightly more than expected (presumably as compensation). Despite these small variations, the overall distribution of genotypes in *Marcal1 mus308* double mutants was not significantly different than expected (*P* = 0.124).

| | *Marcal1 mus308* | | | *Marcal1 Blm* | | |
|---|---|---|---|---|---|---|
| Balancer combination | Expected | Observed | *P* value | Expected | Observed | *P* value |
| Chr. *2* only | 78 | 89 | 0.124 | 165.3 | 231 | $2.60 \times 10^{-9}$ |
| Chr. *3* only | 78 | 86 | | 165.3 | 182 | |
| Chr. *2* & Chr. *3* | 156 | 134 | | 330.7 | 260 | |
| Double mutant | 39 | 42 | | 82.7 | 71 | |
| | | *n* = 351 | | | *n* = 744 | |

**Table 4.3 Balancer chromosome distribution in viability assays.** Heterozygous flies for *Marcal1 mus308* or *Marcal1 Blm* double mutations were crossed and progeny were scored according to genotype. Observed counts were compared to expected counts based on genotype probability and a G-test for goodness of fit was used to calculate *P* values for each distribution.

In contrast, the occurrence of double-balanced flies in *Marcal1 Blm* double mutants was much less than expected (260 vs. 331 expected) and the single balanced flies were unevenly distributed (231 Chr. *2* and 182 Chr. *3* vs. 165 expected for both). These variations resulted in a significant deviation from the expected distribution.

| *Marcal1 mus308* | Expected | Observed | *P* value |
|---|---|---|---|
| Chr. *3* and double balanced | 234 | 220 | 0.116 |
| *mus308* mutant | 117 | 131 | |
| Chr. *2* and double balanced | 234 | 223 | 0.216 |
| *Marcal1* mutant | 117 | 128 | |

| *Marcal1 Blm* | Expected | Observed | *P* value |
|---|---|---|---|
| Chr. *3* and double balanced | 496 | 442 | $3.6 \times 10^{-5}$ |
| *Blm* mutant | 248 | 302 | |
| Chr. *2* and double balanced | 496 | 491 | 0.698 |
| *Marcal1* mutant | 248 | 253 | |

**Table 4.4 Analysis of single mutant distribution in two double mutants.** Data from Table 4.3 was used to calculate the occurrence of single mutants within double mutant backgrounds and a G-test for goodness of fit was used to calculate *P* values for distributions of single mutants.

I next asked if the distributions were due to additive effects of the single mutations. I analyzed the occurrence of each mutation singly within the double mutant class: for *Marcal1 mus308*, I combined the Chr. *2* balancer total with the double mutant total to get the total number of *mus308* mutant progeny; the remaining flies were *mus308* heterozygous and counted as balanced. This process was repeated for *Marcal1* in *Marcal1 mus308* double mutants and the entire method was repeated for the *Marcal1 Blm* double mutant data (Table 4.4). Interestingly, I found the distribution of *mus308* single mutants was not altered in a *Marcal1* mutant background whereas *Marcal1 Blm* mutant distributions were additive. These data suggest that *Marcal1* and *mus308* do not genetically interact whereas *Marcal1* and *Blm*

likely act in separate processes and/or at different times in the same pathway. These data further show that comparisons of double mutant and single mutant distributions are insufficient to determine genetic interactions, but balancer distribution in conjunction with single mutant distribution analysis in double mutant assays can uncover putative genetic interactions for further investigation.

**Marcal1 *mutant viability is increased in a* Polα-180/+ *background***

As previously mentioned, SMARCAL1 has known roles in replication-associated repair. Marcal1 does not exhibit regression activity on model replication fork structures *in vitro* (Kassavetis and Kadonaga 2014). SMARCAL1 has been shown to stabilize stalled replication forks during HU treatment (HU reduces the nucleotide pool, causing replication to stall) in cell culture assays (Yuan *et al.* 2009), however I found that *Marcal1* null mutants did not have increased lethality when exposed to HU. SMARCAL1 deficient cells are sensitive to CPT, which is proposed to cause DSBs during replication, and I did observe elevated lethality in mutants treated with CPT. These apparently conflicting data could be due to differences in mutagen stability, mechanism of action, or other cryptic variables. Lethality assays are performed by adding the agent in aqueous solution to the fly food and allowing larvae to consume it. It is possible that the difference in outcomes observed in HU- and CPT-treated groups is due to the stability of the agent in the food over time as well as how the agent is metabolically processed once consumed. Conversely, it is possible that CPT lesions are repaired via HDR (as I proposed in Chapter 3) and the elevated lethality is due to the role of Marcal1 in HDR rather than fork regression or stability functions. To assess replication specifically, I tested the ability of *Marcal1* mutants to survive in a *Polα-180* heterozygous background.

DNA polymerase alpha (Polα) is an essential gene that is required for both replication initiation and Okasaki fragment synthesis during eukaryotic replication (Pellegrini

2012). It is complexed with Primase and facilitates short DNA extension of RNA primers before processive extension by the replicative polymerases Pol δ and Pol ε. The *Polα-180* mutation is a premature stop codon in the catalytic subunit of Polα that results in loss of function (LaRocque *et al.* 2007). LaRocque *et al.* further showed that, while homozygous lethal, *Polα-180* heterozygotes had sufficiently reduced dosage to display proliferation defects in a checkpoint deficient background. *Polα-180* heterozygosity has been used to mimic partial replication blockage caused by low dosage aphidicolin treatment (a reversible Polα inhibitor) that can cause fork collapse resulting in DSBs (LaFave *et al.* 2014) and I hypothesized that *Marcal1* mutants would have reduced fitness in this background.

Surprisingly, I found a significant elevation in observed *Marcal1* mutants in a *Polα-180*/+ background compared to expected (Table 4.2), suggesting that Marcal1 may have a role in replication fork maintenance. It is possible that Marcal1 generates structures at the fork that are more likely to become DSBs during stalling/blockage. More studies are needed to verify this interaction is due to replication stalling and to explore this potential role.

### *Marcal1* and *Blm* have complex genetic interactions

Similar to SMARCAL1, BLM helicase (yeast Sgs1, *Drosophila* Blm) has been implicated in a variety of cellular processes from replication fork stability and repair to resection, D-loop dissociation, and dHJ processing during HDR (reviewed in Wu 2007; Mimitou and Symington 2009b; Manthei and Keck 2013). I observed the potential for an additive genetic interaction in *Marcal1 Blm* double mutants (Figure 4.4). To explore this relationship further and determine if Marcal1 and Blm have any overlapping functions, I performed a series of experiments with *Marcal1 Blm* single and double mutants.

**Marcal1 *mutants do not have elevated spontaneous mitotic crossovers***

Elevated sister chromatid exchange and increased wide-spectrum cancer predisposition are hallmarks of Bloom syndrome (BSyn), the disease caused by mutations in *BLM* (German 1993). Recent studies of Schimke immuno-osseous dysplasia (SIOD) patients have reported a chromosome breakage phenotype and increased incidence of specific cancers (Baradaran-Heravi *et al.* 2012b; Simon *et al.* 2014). The recombinational phenotype in BSyn patients is attributed to the role of Blm in dHJ processing (Ira *et al.* 2003; LaFave *et al.* 2014). I wanted to know if the chromosome breakage phenotype in SIOD patients could be attributed to similar mechanisms. To test this hypothesis, I performed a mitotic CO assay in the male germline of *Drosophil*a.

I crossed *Marcal1* mutant male flies heterozygous for the recessive markers *scarlet* (*st*), an eye color phenotype, and *ebony* (*e*), a body color phenotype, to females homozygous for *st e* and scored the progeny. Any progeny with both markers (*st e*) or no observable markers (wild type) did not have a CO whereas any progeny with only one marker (*st* $e^+$ or $st^+$ *e*) indicated a mitotic CO occurred in the father's germline (male *Drosophila* do not have meiotic recombination). I did not observe any COs in *Marcal1* null mutants which is not significantly different than wild type (Figure 4.1). In contrast, the mean CO rate in *Blm* mutants is 1.43% (LaFave *et al.* 2014). *Marcal1 Blm* double mutants had a mean CO rate of 1.57%, which was not significantly different from *Blm* single mutants. I next measured how many males had at least one progeny with a CO. 69% (61/88) of *Blm* mutant males assayed had progeny with a CO. The number of males with CO progeny significantly increased in *Marcal1 Blm* double mutants to 87% (27/31), with a *P* value of 0.02 (*G*-test and *t*-test with unequal variance).

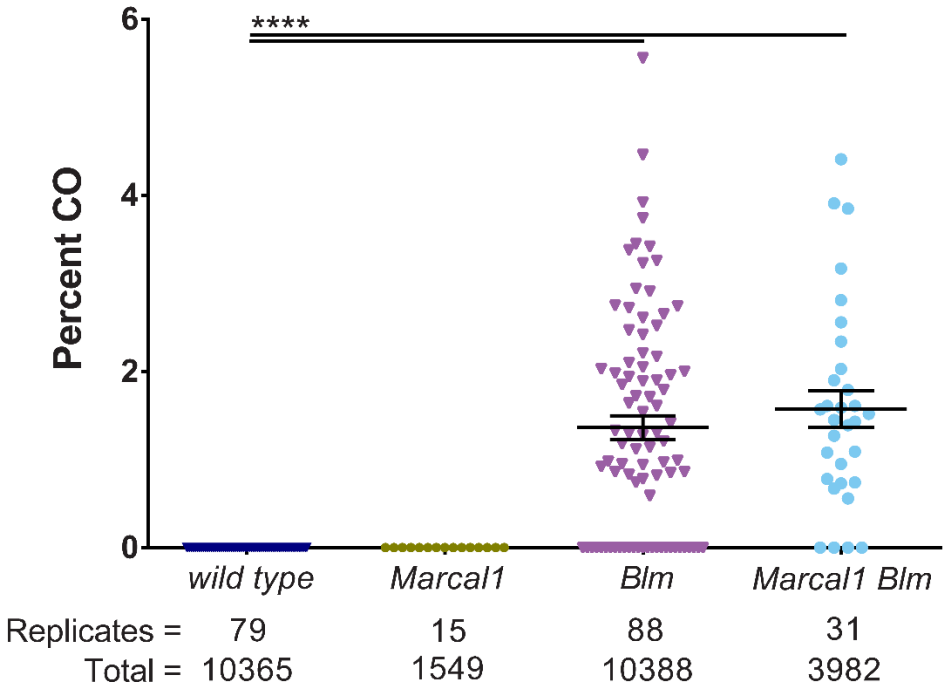


**Figure 4.1 *Marcal1* does not contribute to the formation of mitotic crossovers.** Males heterozygous for the recessive markers *scarlet* (*st*) and *ebony* (*e*) were crossed to females homozygous for *st e* and the progeny were scored for CO (*st* $e^+$ or $st^+$ *e*) or NCO (*st e* or $st^+$ $e^+$) repair events. Percent CO was calculated per male (replicate) as a percentage of total progeny scored. Parametric ANOVA was used to calculate significance between the mean percent CO of the different genotypes. **** $P < 0.0001$.

It is possible that DSBs are more likely to be repaired into a CO in a *Marcal1 Blm* mutant background, however, a more reasonable explanation is that *Marcal1* mutations contribute to the formation of DSBs that are repaired into a CO in a *Blm* mutant background. This hypothesis suggests that Marcal1 and Blm contribute to genome stability in similar, perhaps overlapping, pathways but do not directly interact.

### Marcal1 *and* Blm *have distinct functions* in vivo

*In vitro* studies of Marcal1 have shown that it cannot regress a model replication fork, however, a primary role of human SMARCAL1 is replication-associated repair via replication fork regression and restart (Bétous *et al.* 2012; Couch *et al.* 2013; Kassavetis and Kadonaga 2014). I observed increased survival of *Marcal1* mutants when replication speed

was reduced via *Polα-180* heterozygosity (Table 4.2) and *Marcal1* mutants are not sensitive to killing by hydroxyurea (HU) (Figure 3.1), a ribonucleotide reductase inhibitor that stalls replication forks (Table 4.5). These data suggest that Marcal1 has a role during replication that becomes detrimental during replication slowing/stalling, which is in contrast to human SMARCAL1 functions that protect and maintain forks during slowing/stalling.

Human BLM helicase has been implicated in fork maintenance and has fork regression and restart activity *in vitro* (Machwe *et al.* 2006, 2011; Sidorova *et al.* 2013). Additionally, BLM has been heavily implicated in replication progression and proper maintenance of under-replicated regions at the S- to M-phase transition (Chan *et al.* 2009; Naim and Rosselli 2009; Lukas *et al.* 2011; Sofueva *et al.* 2011; Naim *et al.* 2013; Ying *et al.* 2013). It is possible that both proteins play a role at the fork, however, this potential has yet to be explored. To test potential genetic interactions between *Marcal1* and *Blm*, I measured *Marcal1*, *Blm*, and *Marcal1 Blm* double mutant survival when exposed to an array of mutagens.

Previous studies in our lab have shown that *Blm* mutants have elevated lethality (sensitivity) when exposed to nitrogen mustard (HN2), methyl methanesulfonate (MMS), and ionizing radiation (IR), and these phenotypes are additive with *Fancm* mutations suggesting that multiple pathways are utilized in response to these agents (Kuo *et al.* 2014). I had previously tested *Marcal1* single mutants in a subset of mutagens (Figure 3.1) and found *Marcal1* mutants to be sensitive to fewer agents than previously reported for *Blm* mutants (Kuo *et al.* 2014). I therefore hypothesized that *Blm* single mutants would be more sensitive than *Marcal1* mutants to most of the agents tested (Table 4.5). I hypothesized that double mutant sensitivity would be additive for replication-associated agents and the remainder of double mutant phenotypes would not be significantly different from *Blm* single mutants, due

to the lack of sensitivity in *Marcal1* mutants to most agents and the epistatic role of *Blm* in HDR.

| Mutagen | | Lesion / mechanism | |
|---|---|---|---|
| Hydroxyurea | (HU) | Ribonucleotide reductase inhibitor—replication stalling | (Hammond *et al.* 2003) |
| Nitrogen mustard | (HN2) | Monoadducts & interstrand crosslinks (ICLs) | (Povirk and Shuker 1994) |
| Methyl methanesulfonate | (MMS) | DNA alkylation, DSBs? | (Ui *et al.* 2005; Lundin *et al.* 2005) |
| Ionizing radiation | (IR) | Double strand breaks (DSBs) | (Radford 1985) |
| Cisplatin | (CPL) | ICLs (different structure than HN2-induced) | (Sawant *et al.* 2017) |
| Formaldehyde | (HCHO) | DNA-protein crosslinks | (Grafstrom *et al.* 1984) |
| Camptothecin | (CPT) | Topoisomerase I inhibitor, repaired by HDR | (Pommier *et al.* 2010; Maede *et al.* 2014) |
| Etoposide | (ETS) | Topoisomerase II inhibitor, repaired by NHEJ | (Pommier *et al.* 2010; Maede *et al.* 2014) |

**Table 4.5 Mutagens tested in sensitivity assays.** Mutagens used for sensitivity assays; the abbreviation used in the text; the lesion created or mechanism of action, as applicable; reference for the lesion/mechanism.

I found that *Marcal1* mutants were not sensitive to IR at 1500 rads exposure ($P$=0.771), while the same exposure resulted in significantly reduced survival in *Blm* mutants ($P$<0.0001) (Figure 4.2A). The *Marcal1 Blm* double mutant mean survival was not significantly different from *Blm* single mutants (Figure 4.2A). Interestingly, the variability in survival was more similar to *Marcal1* mutants than *Blm* mutants suggesting that *Marcal1* mutations affect the *Blm* phenotype in the double mutant, both increasing and decreasing survival. I also observed that *Marcal1* mutants are sensitive to IR at 2000 rads (Figure 4.2B).

I observed a similar pattern when mutants were exposed to cisplatin (CPL) (Figure 4.2C). *Marcal1* mutants were not sensitive at 0.25 mM concentration whereas *Blm* mutants were not viable at the same dose. The potential contribution of *Marcal1* to the double mutant phenotype was unobservable, most likely due to the lethality of the dose in *Blm* mutants.

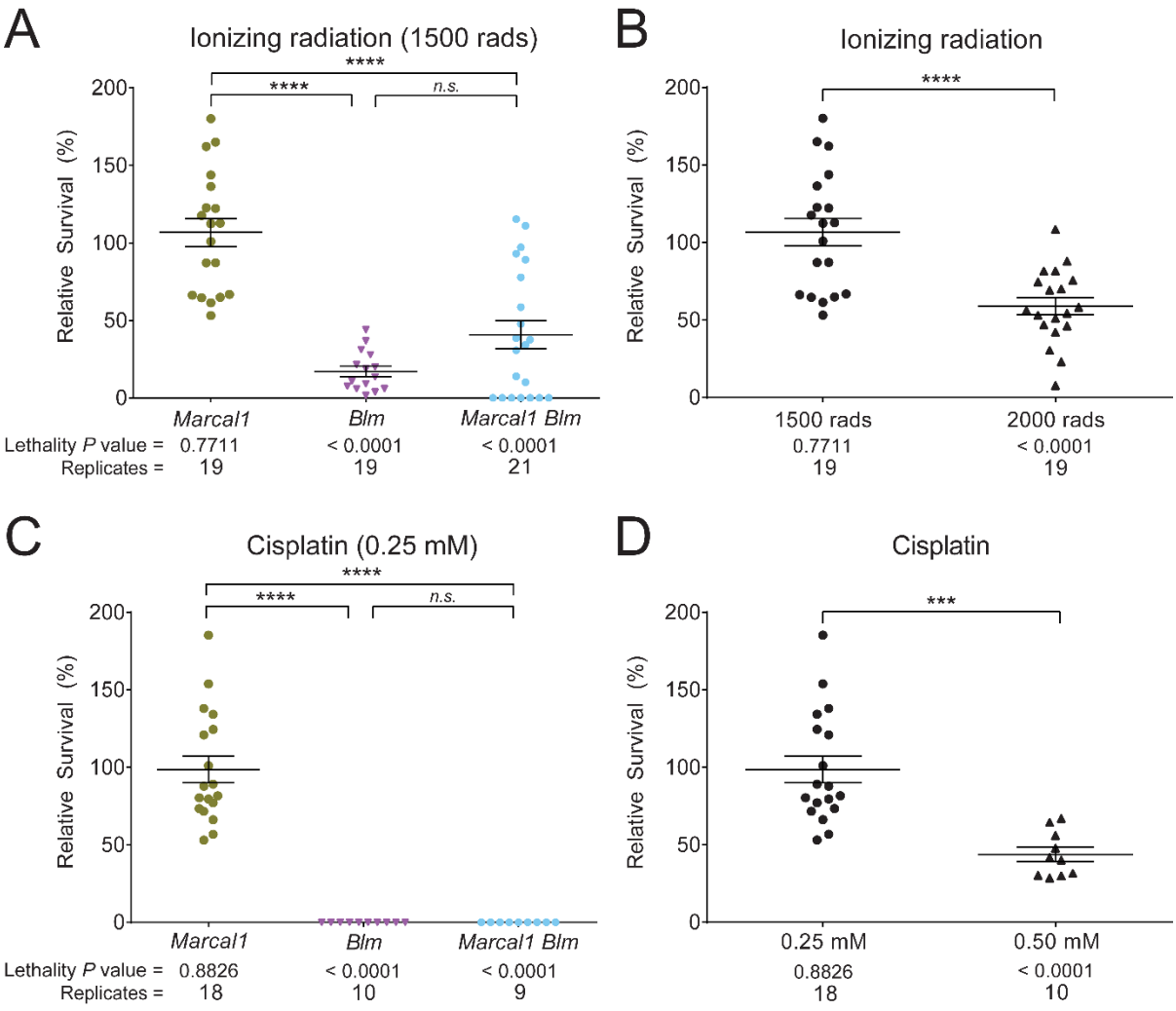


**Figure 4.2 *Marcal1* is more resistant to ionizing radiation and cisplatin than *Blm*.** (A) Flies heterozygous for null mutations in *Marcal1, Blm, or Marcal1 Blm* double mutations were mated in two broods of at least 10 vials, with each vial representing a biological replicate. Brood one was unexposed; brood two received a dose of ionizing radiation (IR) during larval feeding. Relative survival was calculated as the ratio of homozygous mutant to heterozygous control adults in treated vials, normalized to the same ratio in the corresponding unexposed vial. Lethality *P* value refers to the significance of relative survival in paired *t*-tests between unexposed and exposed vials and indicates sensitivity to killing when $P<0.05$. Parametric ANOVA was used to calculate significance between genotypes. *n.s.*: not significant; ****, $P<0.0001$. At 1500 rads, *Marcal1* mutants are not sensitive whereas *Blm* and *Marcal1 Blm* double mutants are similarly sensitive. (B) *Marcal1* flies were treated as described in (A) with 1500 rads or 2000 rads of IR. *Marcal1* mutants were significantly sensitive to 2000 rads of IR. (C) The same method was used to test sensitivity to cisplatin (CPL) by applying an aqueous solution of CPL to larval food and measuring survival to adulthood. *Marcal1* mutants were not sensitive at 0.25 mM concentration while *Blm* and *Marcal1 Blm* double mutants had no survival when exposed to the same treatment. (D) *Marcal1* mutants are significantly sensitive to CPL at 0.50 mM, $P=0.0001$.

In contrast to IR treatment, CPL-treated double mutants did not have any incidence of increased survival compared to *Blm* single mutants. Again, *Marcal1* mutants were sensitive to CPL at a higher dose than *Blm* mutants (Figure 4.2D).

The genetic relationship between *Marcal1* and *Blm* appears similar to IR and CPL when treated with MMS, HN2, and formaldehyde (HCHO) (Figure 4.A, C, E). *Marcal1* mutants were not sensitive to MMS or HN2, whereas *Blm* mutants were very sensitive. The double mutant had slightly increased sensitivity to MMS compared to *Blm* single mutants (Figure 4.3A). However, unlike IR and CPL treatment, *Marcal1* mutants were surprisingly insensitive to MMS, even at high dosages (Figure 4.3B), suggesting that few DSBs are generated when Blm is functional and supporting evidence from Lundin *et al* that DSBs do not form in cells treated with MMS (Lundin *et al.* 2005).

*Blm* mutants were significantly sensitive to HN2 treatment, whereas *Marcal1* mutants were not (Figure 4.3C). Similar to MMS, *Marcal1* mutants were insensitive to HN2 treatment independent of dose (Figure 4.3D). The double mutant was not tested for HN2 sensitivity, though I suspect it would behave in a similar manner to MMS. More studies are needed to test this hypothesis.

*Marcal1* mutants were not sensitive to HCHO treatment but *Blm* mutants were. Similar to the phenotype observed in IR-treated flies, the double mutant was not statistically different from the *Blm* single mutant, probably due to increased variation within the double mutant class (Figure 4.3E). Unlike IR, however, *Marcal1* mutants were insensitive to HCHO treatment at all dosages tested.

*Marcal1* mutants were sensitive to 70 mM HU (Figure 4.4A), however, this sensitivity was abolished by increasing the dose to 100 mM (Figure 4.4B) and it is likely that the sample size in the 70 mM treatment group lacks sufficient statistical power.

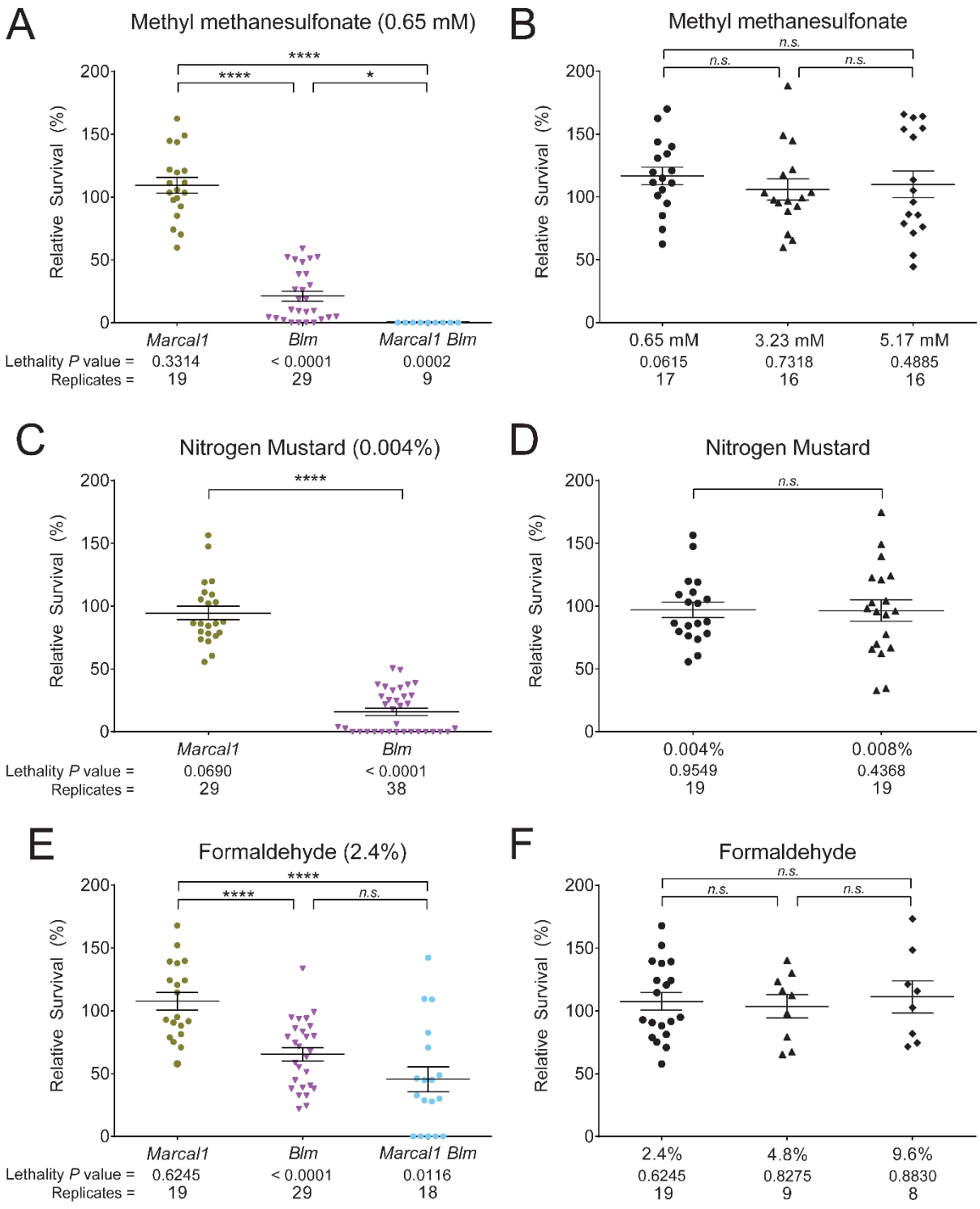
A
Methyl methanesulfonate (0.65 mM)
Relative Survival (%)
****
****
*
Marcal1
Blm
Marcal1 Blm
Lethality P value = 0.3314 < 0.0001 0.0002
Replicates = 19 29 9
B
Methyl methanesulfonate
n.s.
n.s.
n.s.
0.65 mM
3.23 mM
5.17 mM
0.0615 0.7318 0.4885
17 16 16
C
Nitrogen Mustard (0.004%)
****
Marcal1
Blm
Lethality P value = 0.0690 < 0.0001
Replicates = 29 38
D
Nitrogen Mustard
n.s.
0.004%
0.008%
0.9549 0.4368
19 19
E
Formaldehyde (2.4%)
****
****
n.s.
Marcal1
Blm
Marcal1 Blm
Lethality P value = 0.6245 < 0.0001 0.0116
Replicates = 19 29 18
F
Formaldehyde
n.s.
n.s.
n.s.
2.4%
4.8%
9.6%
0.6245 0.8275 0.8830
19 9 8

**Figure 4.3 *Blm* mutations can sensitize *Marcal1* mutants to damaging agents.** Flies were treated as described in Figure 4.2. Lethality *P* value refers to the significance of relative survival in paired *t*-tests between unexposed and exposed vials and indicates sensitivity to killing when $P<0.05$. Parametric ANOVA was used to calculate significance between genotypes. *n.s.*: not significant; *, $P<0.0424$; ****, $P<0.0001$. (A) *Marcal1* flies were not sensitive to 0.65 mM MMS, however *Blm* flies were significantly sensitive and *Marcal1 Blm* double mutants were more sensitive than *Blm*. (B) *Marcal1* flies were not sensitive to increasing concentrations of MMS. (C) *Marcal1* flies were not sensitive to 0.004% HN2 while *Blm* flies were very sensitive. No double mutants were tested. (D) *Marcal1* flies were not sensitive to increasing concentrations of HN2. (E) Marcal1 flies were not sensitive to 2.4% HCHO while Blm and Marcal1 Blm double mutants were similarly sensitive. (F) Marcal1 flies were not sensitive to increasing concentrations of HCHO.

Blm mutants were significantly sensitive to 70 mM HU (Figure 4.4A), supporting a role for Blm in maintaining stability at stalled replication forks. Interestingly, *Marcal1 Blm* double mutants were not significantly different from *Marcal1* mutants and had wide variation in survival (0 – 200% relative to unexposed siblings). HU was the only mutagen where the double mutant had a phenotype more similar to *Marcal1* than to *Blm*.

CPT treatment was the only mutagen that resulted in similar sensitivities in both *Marcal1* and *Blm* single mutants (Figure 4.4). Furthermore, these sensitivities are additive in the double mutant suggesting that at least two separate mechanisms facilitate repair of CPT-generated lesions. Marcal1 mutants are sensitive to CPT in a dose-dependent manner (Figure 4.4D), which is similar to human SMARCAL1 (Zhang *et al.* 2012).

Lastly, I tested mutant sensitivity to etoposide (ETS) and found that *Marcal1* mutants were not sensitive to 10 mM ETS whereas *Blm* mutants were significantly sensitive and double mutants were inviable at that dose (Figure 4.4E). This genetic interaction is similar to the one observed after MMS treatment (and possibly CPL) (Figure 4.3A, 4.2C) and suggests that *Blm* mutations sensitize *Marcal1* mutants to ETS.

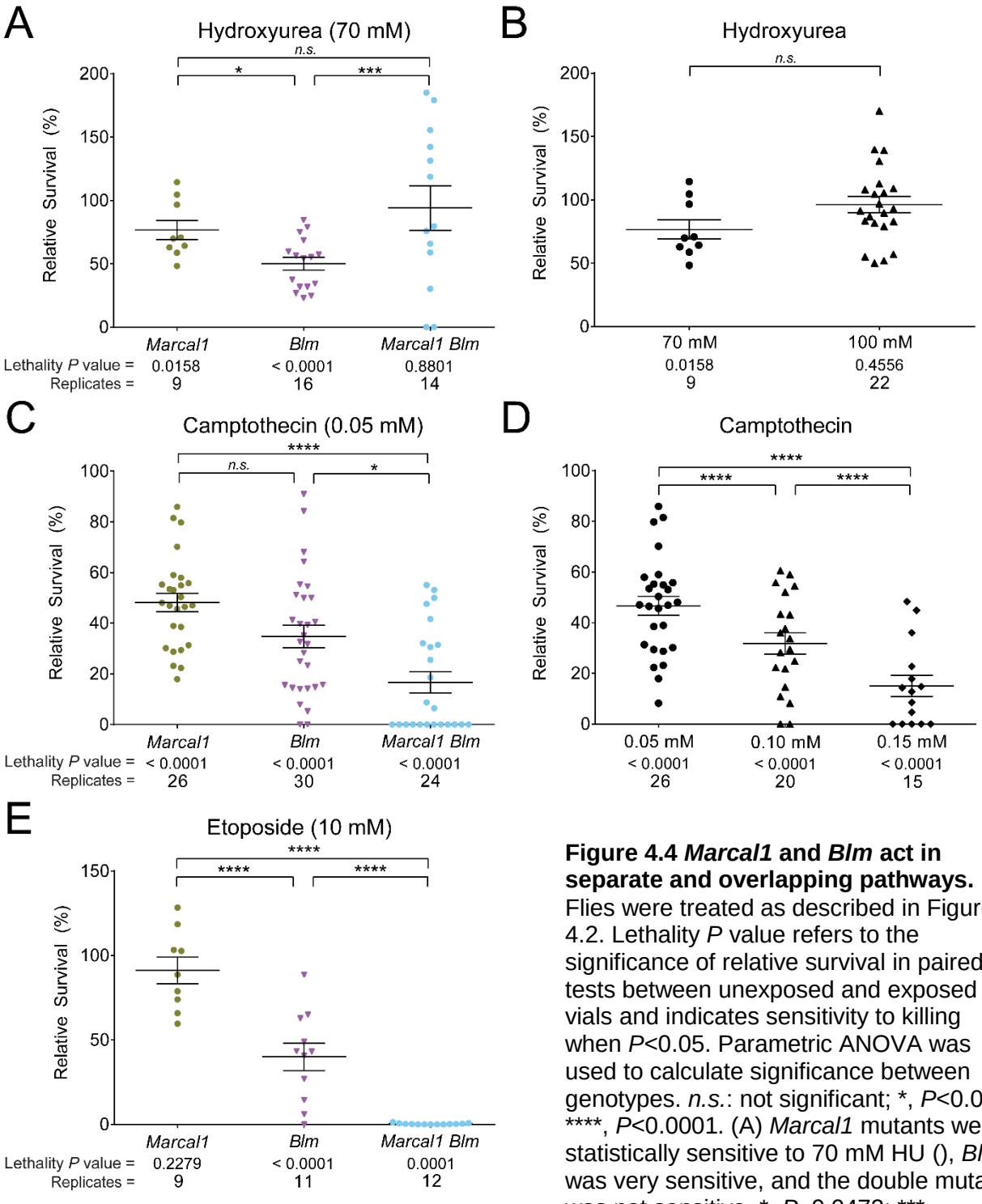


**Figure 4.4 *Marcal1* and *Blm* act in separate and overlapping pathways.** Flies were treated as described in Figure 4.2. Lethality *P* value refers to the significance of relative survival in paired *t*-tests between unexposed and exposed vials and indicates sensitivity to killing when $P<0.05$. Parametric ANOVA was used to calculate significance between genotypes. *n.s.*: not significant; *, $P<0.05$; ****, $P<0.0001$. (A) *Marcal1* mutants were statistically sensitive to 70 mM HU (), *Blm* was very sensitive, and the double mutant was not sensitive. *, $P=0.0472$; ***, $P=0.0004$. (B) *Marcal1* mutant sensitivity was abolished by increasing the dose of HU to 100mM. (C) *Marcal1* and *Blm* were similarly sensitive to CPT and this effect was additive in the double mutant. *, $P=0.0278$ (D) *Marcal1* mutants are sensitive to CPT in a dose-dependent manner. (E) *Marcal1* is not sensitive to ETS; *Blm* is significantly sensitive to ETS and the double mutant is more sensitive than *Blm* single mutants.

Altogether, these data show that Marcal1 and Blm do not have overlapping functions during DNA damage repair. *Blm* mutants were sensitive to every agent tested, which supports a role for Blm in a wide range of repair pathways (discussed in depth in Chapter 5). In contrast, *Marcal1* mutants were insensitive to most agents tested, suggesting it acts in aspecific damage repair pathway (most likely HDR). Interestingly, *Blm* mutations sensitized *Marcal1* mutants to an additional set of mutagens suggesting that these lesions become structures that are repaired via *Marcal1*-dependent pathways in the absence of Blm. Our lab has previously shown that mitotic CO are elevated in *Blm* mutants treated with MMS, HN2, and CPT but not HU, supporting my hypothesis that many of these structures are converted to DSBs that are then repaired via HDR in the absence of Blm (LaFave *et al.* 2014).

**Marcal1 *and* Blm *mutations are synergistic during gap repair***

I have shown that Marcal1 mediates annealing during SDSA in the *P*{$w^a$} assay (Chapter 3). Previous work from our lab established that Blm facilitated D-loop dissociation in the same assay (Adams *et al.* 2003). If these interpretations are correct, the *Marcal1 Blm* double mutant should have a phenotype similar to *Blm* single mutants. My data from sensitivity assays, however, suggest that *Marcal1* and *Blm* have both additive and synergistic relationships depending on the lesion, which I propose is due to Blm activity in a variety of repair pathways in addition to its established roles in HDR. To test this hypothesis, I performed the *P*{$w^a$} assay in the male germline of *Marcal1 Blm* double mutants (males do not undergo meiotic recombination).

The *P*{$w^a$} assay is described in detail in Chapter 3 (Figure 3.2). Briefly, the construct is a stably integrated *P* element that encodes a *white* (*w*) gene which is responsible for loading pigment into the eye. The gene is interrupted by a *copia* retrotransposon flanked by two 276-bp long terminal repeats (LTRs). The *copia* insertion causes a *w* splicing defect and results in an apricot-colored eye in hemizygous males or homozygous females. When

exposed to an inefficient source of *P* element transposase, the *P*{*w*$^{a}$} element is excised from one chromatid; the intact sister chromatid serves as an efficient template for HDR (the structure of the ends are poor substrates for end-joining via cNHEJ) (Symington and Gautier 2011). Repair events from single males are recovered in female progeny by crossing to females homozygous for *P*{*w*$^{a}$}.

For SDSA to occur, both sides of the break must be extended (via synthesis) beyond the first region of complementarity, the *copia* LTRs. If the LTRs are annealed correctly, SDSA is completed and these events are observable as red eyes in progeny inheriting this product. If EJ occurs either without synthesis or after incomplete synthesis, *w* function is completely lost, resulting in yellow-eyed progeny (due to the maternally-inherited full *P*{*w*$^{a}$} copy). Complete restoration of *P*{*w*$^{a}$} could occur via a dHJ intermediate or via SDSA or EJ that synthesizes sufficiently past the LTRs to retain a splicing defect. Apricot-eyed progeny are counted as part of total progeny scored but do not contribute to any repair class because they cannot be differentiated from a lack of excision. SDSA and EJ events are quantified as a percentage of total scorable progeny (daughters that do not inherit the transposase source) from each male.

I observed red-eyed progeny (SDSA events) from only one *Marcal1 Blm* double mutant male, which was removed from the data set after being categorized as an outlier by both ROUT and Grubbs tests (Figure 4.5A). These data were not statistically different than *Marcal1* or *Blm*, despite the increased occurrence of red-eyed progeny in both single mutants. Red-eyed progeny are sufficiently rare in these genotypes (0.95% in *Marcal1* mutants and 0.90% in *Blm* mutants) that the ability of parametric ANOVA to identify differences is limited when wild type frequency is included in the data set. While these data fail to show a statistically significant difference that could reveal an additive or synergistic

relationship, they do show that SDSA is severely compromised in a *Marcal1 Blm* double mutant.

I encountered the same statistical quandary when analyzing yellow-eyed progeny (EJ events) (Figure 4.5B). Wild-type and *Marcal1* EJ events were not statistically different, however both were significantly higher than *Blm* or *Marcal1 Blm* double mutants. In this data set, ROUT identified every EJ event as an outlier in the *Marcal1 Blm* double mutant class only though EJ events occurred at a higher frequency than SDSA events. Due to the increased incidence, I did not remove any EJ events in the *Marcal1 Blm* data set as outliers. From these data I conclude that EJ events, when they occur in *Marcal1 Blm* double mutants, are not significantly different from *Blm* mutants and EJ is compromised during SDSA in all *Blm* mutant backgrounds I tested.

I observed flanking deletions and significantly reduced synthesis in *Blm* single mutants, consistent with past observations (Chapter 3, Adams *et al.* 2003; McVey *et al.* 2004a). In contrast, *Marcal1* mutants have synthesis length that is not significantly different from wild type and I do not observe any flanking deletions in *Marcal1* mutants (Chapter 3). These data are consistent with past interpretations that Blm dissociates D-loops and Marcal1 mediates downstream annealing. To confirm these roles, I performed the standard series of PCRs to test synthesis length in *Marcal1 Blm* (Chapter 3, Materials and Methods). *Marcal1 Blm* double mutants were not statistically different from *Blm* single mutants (Figure 4.5C), supporting the model that Blm D-loop dissociation is epistatic to Marcal1 annealing during SDSA.

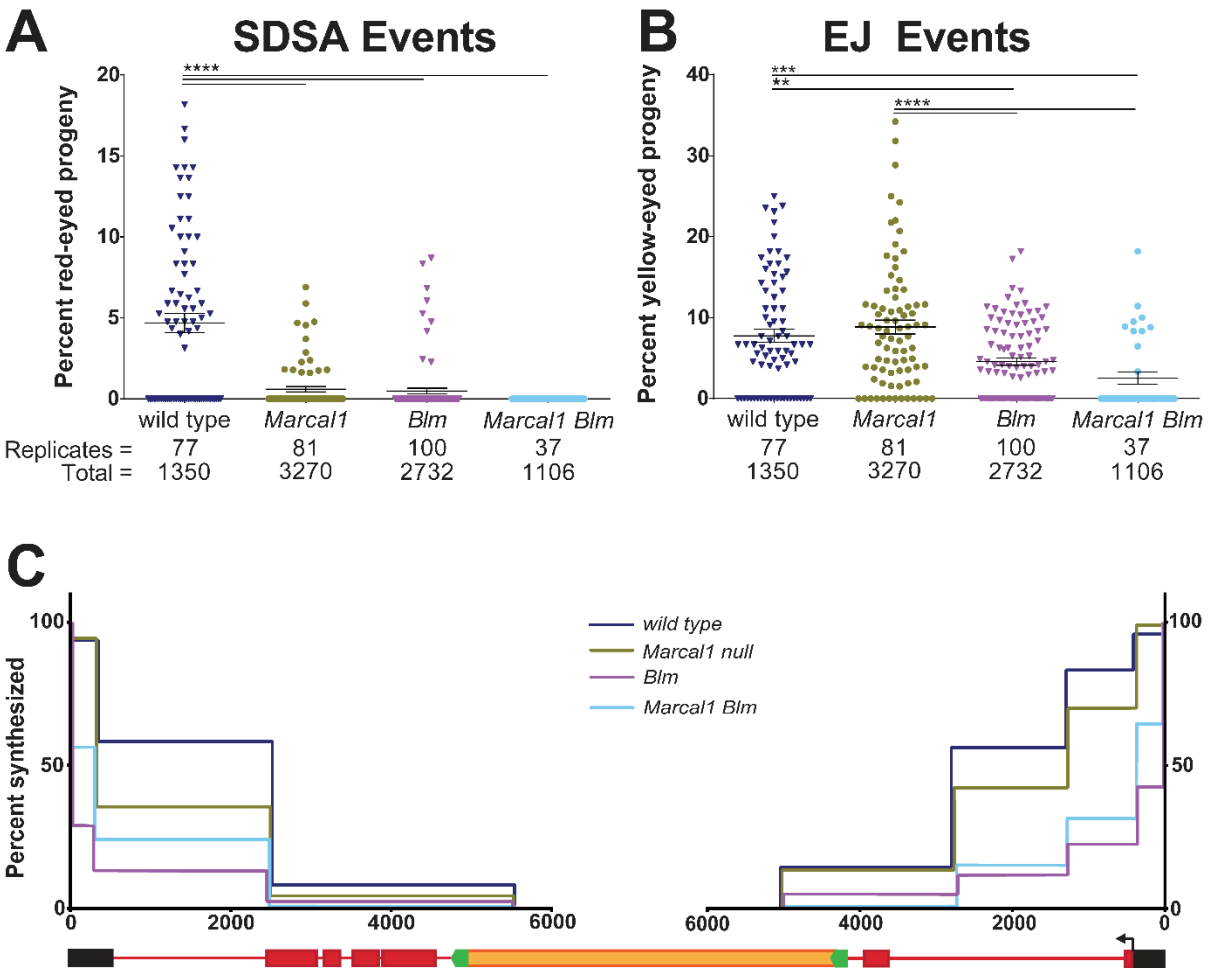


**Figure 4.5 *Marcal1* and *Blm* are additive during gap repair.** Wild type, *Marcal1*, and *Blm* data are from Chapter 3, Figure 3.3. (A) SDSA events are measured as the percentage of scored progeny with red eyes. Mean and SEM are indicated. *Marcal1* null mutant, *Blm* mutant, and *Marcal1 Blm* double mutant frequencies were all significantly reduced compared to wild type. The numbers of single males (biological replicates) and total progeny scored are listed below the graph. (B) EJ events were measured as the percentage of scored progeny with yellow eyes. *Blm* and *Marcal1 Blm* mutants had significantly reduced EJ compared to wild type and *Marcal1* single mutants. *P*-values: ****, $P < 0.0001$; ***, $P = 0.003$; **, $P = 0.0055$ based on parametric ANOVA. (C) Synthesis tracts in repair events recovered in yellow-eyed progeny were measured using a series of PCRs (Table 3.2). Each interval was measured independently and quantified as a percentage of total independent events analyzed. *X*-axis denotes distance (in nucleotides) from each end of the gap, on the same scale as the schematic of $P\{w^a\}$ below. *Y*-axis is percent of events analyzed that had a positive PCR and therefore synthesized at least as far as the most internal primer. *Marcal1* ($n = 90$) was not significantly different from wild type ($n = 48$) when corrected for multiple intervals (Chapter 3, Materials and Methods). *Blm* ($n = 75$) and *Marcal1 Blm* ($n = 26$) mutants were significantly different ($P < 0.0001$) from both wild type and *Marcal1*.

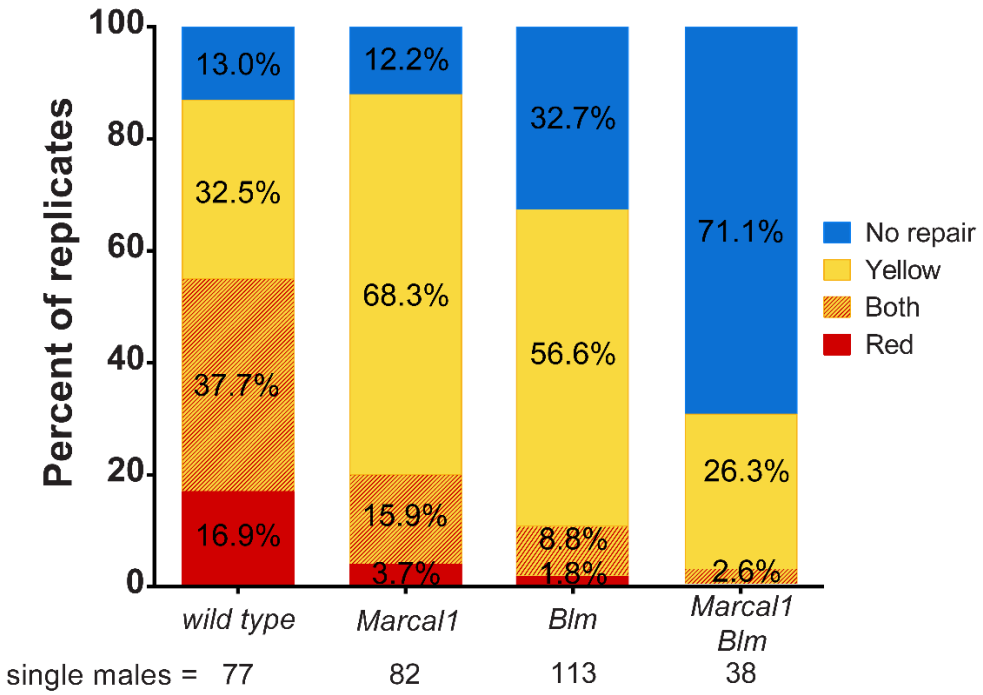


**Figure 4.6 The majority of repair events in the *P*{*w*$^a$} assay are unrecoverable in *Marcal1 Blm* double mutants.** Each male (replicate) from the *P*{*w*$^a$} assay was categorized according to the distribution of repair events observed in his progeny and the data are displayed as a percentage of all males assayed in each genotype. Red indicates red-eyed progeny were observed; yellow indicates yellow-eyed progeny; both indicates red- and yellow-eyed progeny; and no repair indicates no red or yellow-eyed progeny were observed. Apricot-eyed progeny were observed in the progeny of every male.

The ROUT data from *Marcal1 Blm* double mutants suggests that both SDSA and EJ are highly compromised to a greater extent than the single mutants. To test this hypothesis, I measured repair event distribution per male by counting the number of males in each genotype that had red-eyed progeny, yellow-eyed progeny, both eye colors in the progeny, or only apricot (no observable repair event) in the progeny (Figure 4.6). Surprisingly, the *Marcal1 Blm* phenotype was distinctly different from both *Marcal1* and *Blm* single mutants. Males with only apricot-eyed progeny represented the majority (71.1%) of *Marcal1 Blm* double mutants tested, whereas this class was only 32.7% of *Blm* single mutant males. The same class represented only 12.2% of *Marcal1* males, revealing synergism between *Marcal1* and *Blm* in the *P*{*w*$^a$} assay that results in a significant reduction in recoverable repair events.

## Discussion

The data presented here show that Marcal1 does not affect meiotic disjunction, which could be due to a variety of reasons. NCOs could be generated from SDSA-like structures but require meiosis-specific annealases, not Marcal1. NCOs could also be generated from alternate structures that do not resemble mitotic SDSA intermediates and are differentially regulated. It is also possible that meiotic chromosome segregation can tolerate reduced NCOs or a back-up mechanism like EJ is utilized in the absence of Marcal1 to facilitate NCO formation. More studies are needed to determine if Marcal1 has a role in meiosis.

Marcal1 also does not appear to genetically interact with any nucleases, including those responsible for replication fork collapse (mus81) and dHJ processing (Gen, mus312, mus81). I did observe potential interactions with genes involved in DSB repair such as *mus308* and *Blm*, though these interactions were very mild in the absence of exogenous DNA damage and require further studies to corroborate. Lastly, *Polα-180/+* increased *Marcal1* mutant survival, though the mechanism of this phenomenon remains unclear.

*Marcal1* mutants had a similar increase in survival to when exposed to HU and *Blm* mutations amplified this effect, suggesting that my observations of *Polα-180/+* were not due to cryptic variables in the assay. Interestingly, this phenotype was the only treatment where *Marcal1* was epistatic to *Blm*. Molecular experiments such as fiber combing may help to shed light on the mechanism behind this interaction.

Generally, *Marcal1 Blm* double mutants had a phenotype similar to *Blm* single mutants when exposed to mutagens, though I also observed that *Blm* mutations could sensitize *Marcal1* mutants to some mutagens (MMS, CPL). *Marcal1* mutants were generally less sensitive than *Blm* and the complex genetic interactions I observed between *Marcal1* and *Blm* is suggestive of multiple roles for Blm in DNA repair. Furthermore, some lesions

may be converted into DSBs in the absence of either Marcal1 or Blm, explaining the sensitization phenotype seen in *Marcal1 Blm* double mutants.

Finally, I found that *Marcal1 Blm* double mutants have severe gap repair defects indicative of a synergistic relationship between Marcal1 and Blm during HDR. *Marcal1 Blm* double mutants had no observable repair events in the majority of males assayed and the few repair events recovered revealed severe synthesis defects similar to those seen in *Blm* mutants. These data suggest that Blm has more roles in DNA repair than previously thought whereas Marcal1 activity is most likely specific to HDR.

## Materials and methods

### *Drosophila* stocks

Fly stocks were maintained at 25° C on standard cornmeal medium. All *Marcal1* null assays were performed using heteroallelic null mutations $Marcal1^{del}$ and $Marcal1^{kh1}$. $Marcal1^{K275M}$ assays were performed homozygous. Detailed descriptions of these alleles can be found in Chapter 3.

### Nondisjunction assay

Five heteroallelic *Marcal1* null females were crossed to three *y cv v f / $B^S$ Y $y^+$* males in a brood of six vials. Progeny were scored according to the number of *X* chromosomes and sex. Exceptional classes (*y cv v f* males or Bar-eyed females) indicated *X* chromosome nondisjunction. These totals were multiplied by 2 to account for inviable non-disjoined progeny and expressed as a percentage of total progeny. Confidence intervals and probability were calculated as described in (Zeng *et al.* 2010); *wild type* rates were previously published (Kohl *et al.* 2012).

**Synthetic lethality assays**

Five heterozygous females were crossed to three heterozygous males in a brood of five vials for each experiment. Progeny were scored and the number of homozygous flies observed was compared to the expected number (calculated by multiplying the total flies scored by the probability of observing the mutant class) using a G-test for goodness of fit.

**Crossover assay**

Single males of the genotype *Marcal1*$^{del}$/*Marcal1*$^{kh1}$ ; *st e*/+ were crossed to five homozygous *st e* females and progeny were scored. Mitotic crossovers derived from the male germline were measured as progeny with *st* + or *e* + phenotypes and expressed as a percentage of total progeny. Wild type and *Blm* single mutant data are from a previous publication but were performed by me in the same manner (*st e* on the same chromosome) (LaFave *et al.* 2014). Parametric ANOVA tests were performed for significance.

**Exposure assays**

All exposure assays were performed and analyzed as described in Chapter 3.

**P{w$^a$} assays**

All P{w$^a$} assays were performed and analyzed as described in Chapter 3.

# CHAPTER 5: CONCLUDING REMARKS

The variability of disease severity and penetrance in SIOD patients has resulted in a wide range of studies and interpretations of SMARCAL1 activity in the cell. SMARCAL1 has an established role in DNA damage repair during replication, however the level at which that impacts survival and symptoms is less clear. Early studies have implicated human SMARCAL1 in DNA double-strand break (DSB) repair but these roles were not fully explored until now.

The work discussed here establishes a role for the *Drosophila* ortholog of SMARCAL1, Marcal1, in DSB repair via synthesis-dependent strand annealing (SDSA). This role appears to be restricted to annealing of complementary sequences after synthesis and can affect downstream repair decisions including double Holliday junction (dHJ) formation and polymerase theta-mediated end joining (TMEJ). I failed to find direct evidence of Marcal1 fork regression activity that was similar to SMARCAL1, despite multiple approaches. Instead, I found evidence that supports a role for Blm in a similar capacity to SMARCAL1 during replication in *Drosophila*.

## Marcal1 in homology directed repair

DSB repair strategies can be thought of as a series of choices that are made by weighing a combination of complex factors, including availability of a repair template, cell cycle timing, nuclear architecture, and the chromatin context of the break itself (Figure 5.1).

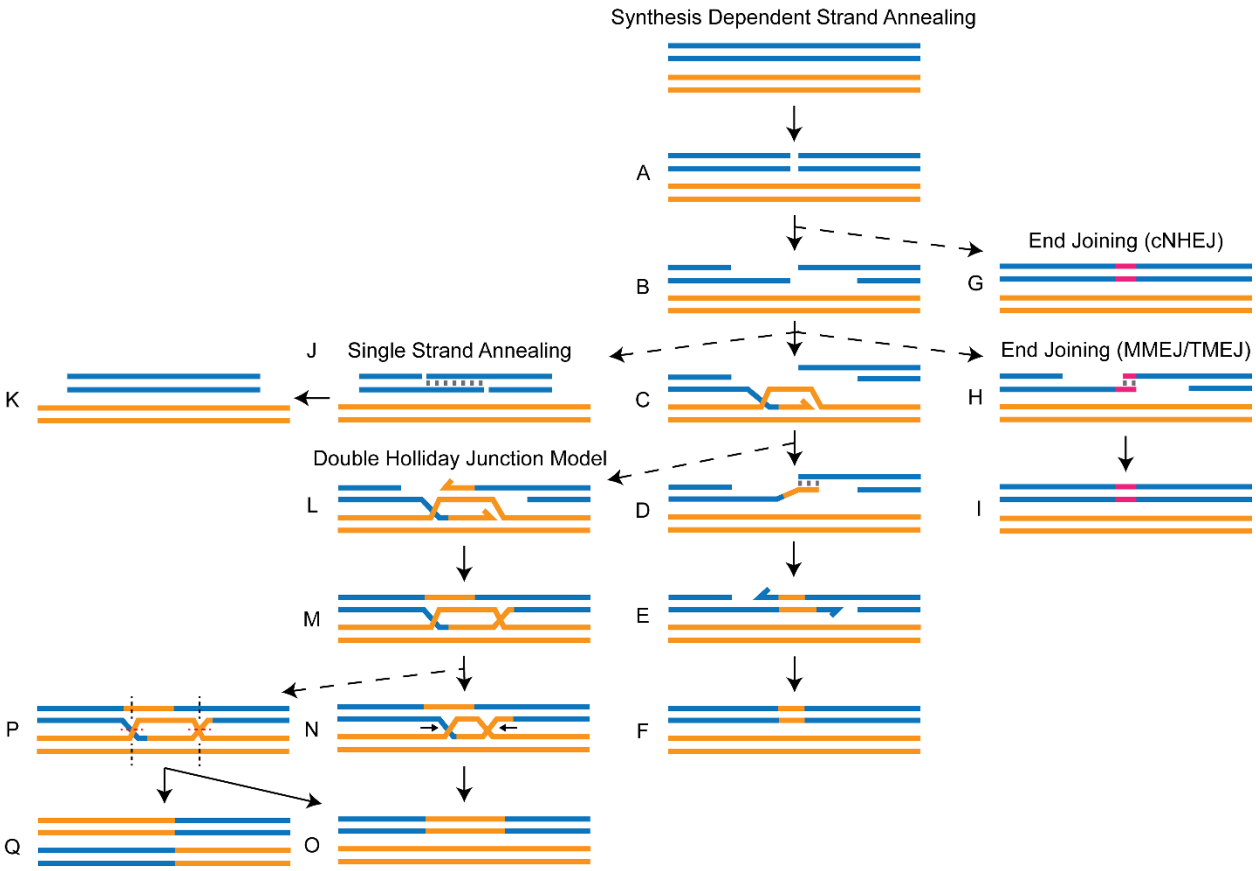


**Figure 5.1 DSB repair strategies.** Blue: dsDNA molecule; orange: dsDNA template (sister chromatid or homologous chromosome). (A) A DSB occurs in the blue DNA molecule. (B) 5' resection marks the first step of homology-directed repair and results in 3' ssDNA tails. (C) Rad51-coated ssDNA tail invades a template duplex, displacing one strand to creating a D-loop, and primes synthesis. (D) The D-loop is disassembled and a complementarity test between the opposing ends of the break occurs. (E) SDSA is defined by annealing between complementary sequences, followed by trimming and/or gap filling. (F) Ligation restores an intact duplex DNA molecule. *Alternative strategies* (dotted arrows). (G) Canonical non-homologous end joining can occur instead of resection, which directly ligates the ends and can generate small insertions and deletions (pink segment). (H) Microhomology-mediated end joining (catalyzed by DNA polymerase theta in metazoans) can occur prior to strand exchange or after failure to find or anneal at complementary sequences. (I) MMEJ/TMEJ can will usually generate a deletion or insertion (pink segment). (J) If the DSB occurs between two direct repeats, complementary sequences may be exposed during resection, and annealing can occur without synthesis, called single-strand annealing (SSA). (K) SSA results in deletion of one repeat. (L) $2^{nd}$-end capture (annealing of the opposing strand to the D-loop, allowing for extension of that strand) can occur during synthesis. (M) Ligation to the opposing 5' ends creates a double-Holliday junction (dHJ). (N) Dissolution of the dHJ involves migration of the junctions toward each other and decatenation via topoisomerase activity to (O) restore the DNA molecule. (P) Resolution involves endonucleolytic cleavage of the junctions which can be cut in either orientation, resulting in both (O) non-crossover (restoration of the DNA molecule) and (Q) crossover (recombinant) products.

The first key decision point is resection (Figure 5.1B), which dictates a commitment to HDR strategies (sequestering the ends of the break from resection results in direct ligation via cNHEJ (Figure 5.1G) (reviewed in Mimitou and Symington 2009)). Brca2 acts downstream of resection to facilitate strand exchange with the template and the phenotype of *Brca2 Marcal1* double mutants in the *P*{*w*$^{a}$} assay shows *Brca2* is epistatic to *Marcal1*, indicating that Marcal1 acts later in the HDR pathway and is unlikely to be involved in resection.

Resection almost invariably leads to strand exchange and synthesis. SSA is an exception (Figure 5.1J), but this can occur only when there are direct repeats flanking the break and perhaps primarily when there is no available template for HDR. It is unclear how much SSA is utilized outside of specialized assays such as *P*{*wIw*}, though Preston *et al*. found it was preferred over HDR when a similar construct was used that had a mutated *I-Sce*I site on the homologous chromosome (Preston *et al.* 2006b). It is possible that the preference for SSA in this context is due to the template being on the homolog and not the sister chromatid. Regardless, SSA is efficiently used in specific situations and the data presented here provide evidence that it shares a common annealing mediator, Marcal1, with other HDR strategies.

The second key decision point in HDR repair is disassembly of the D-loop, which dictates the choice between SDSA and the dHJ pathway (Figure 5.1C). Disassembly favors SDSA by promoting complementarity tests and annealing, whereas continued synthesis increases the likelihood of 2$^{nd}$-end capture and dHJ formation. In *Drosophila*, Blm helicase has been identified as a key mediator of D-loop disassembly (Adams *et al.* 2003; McVey *et al.* 2004b), and recent studies suggest Fancm may play a minor role in this step as well (Kuo *et al.* 2014; Romero *et al.* 2016), though studies in human cells do not show a role for FANCM in SDSA (Zapotoczny and Sekelsky 2017). I did not observe phenotypes indicative

of defects in D-loop dissociation in *Marcal1* mutants, suggesting that the role of Marcal1 is downstream of D-loop dissociation.

The third key decision point is annealing (Figure 5.1D), which I propose impacts the choice between SDSA (Figure 5.1, central model), EJ (primarily TMEJ) (Figure 5.1H-I), and re-invasion that can lead to dHJ formation (Figure 5.1L-Q). Prior to the studies reported here, little was known about annealing during HDR in animals or how the decision between these three options is regulated. My data provide *in vivo* evidence that Marcal1 mediates annealing during SDSA and SSA in *Drosophila*, and suggest that Marcal1 acts directly to anneal complementary strands, as abrogating Marcal1 translocation activity via Walker A mutation recapitulates the null phenotype. Furthermore, I did not observe genetic interactions with structure-specific endonucleases, indicating that Marcal1 activity is restricted to annealing of nascent DNA strands, not 2$^{nd}$ end capture or dHJ formation/processing.

The *Marcal1*$^{K275M}$ mutation reduces EJ as well as annealing during SDSA, which suggests that Marcal1$^{K275M}$ antagonizes EJ in contexts where EJ follows strand exchange, synthesis, and D-loop dissociation. EJ in *Marcal1* null mutants is unaffected, which further suggests the EJ phenotype in *Marcal1*$^{K275M}$ mutants is likely due to defective annealing activity leading to aberrant interactions with the DNA rather than a non-annealing protein-protein interaction. I propose the *Marcal1*$^{K275M}$ phenotype is a consequence of localization to the DNA without translocation activity, which may indicate Marcal1 precedes recruitment of EJ factors after D-loop dissociation. Further studies are needed to test this hypothesis.

An intriguing finding from my study is that synthesis tract length is not elevated in *Marcal1* mutants even though annealing is defective. Early studies of gap repair in *Drosophila* have shown that continuous synthesis averages 1379 bp and complete restoration decreases as template length increases (Gloor *et al.* 1991); additional studies

with the *P*{*w*$^{a}$} assay suggest that gap filling involves multiple cycles of strand exchange, synthesis, and D-loop dissociation (McVey *et al.* 2004b). These attributes appear unaffected in *Marcal1* mutants suggesting that the choice to strand re-invade or EJ during a given round is not solely dependent on the outcome of complementarity tests even though the reduction in EJ in *Marcal1*$^{K275M}$ mutants argues that Marcal1 is recruited to the nascent ends prior to recruitment of EJ factors. It is possible that rounds of strand invasion, synthesis, and D-loop disassembly are simply stochastic in nature, and after each a complementarity test is performed by Marcal1. When Marcal1 is present but defective, EJ factors may be excluded after D-loop dissociation, whereas when Marcal1 is completely absent EJ factors would have access to the DNA, but EJ would still be reliant on the synthesis machinery and unknown regulatory signals. These data support a model where complementarity tests are upstream of the EJ vs. strand re-invade decision.

I predicted *Blm* would be epistatic to *Marcal1* due to its role in D-loop dissociation, however, I found that *Marcal1* mutations were synergistic with *Blm* mutations in the *P*{*w*$^{a}$} assay. Repair events were significantly reduced in *Marcal1 Blm* double mutants and only one male had progeny with putative SDSA products; EJ events resembled *Blm* single mutants. Even though SDSA events represent less than 1% of total progeny in *Marcal1* and *Blm* single mutants, the number of males with red-eyed progeny represent 19.6% and 10.6%, respectively whereas only one male (2.6%) had progeny with red eyes. *Blm* mutations affect synthesis to the LTRs, resulting in a reduced number of repair events with the capacity for SDSA. However, if synthesis to the LTRs occurs and D-loop dissociation is achieved, perhaps through a back-up mechanism, Marcal1 can mediate annealing. This explains the residual red-eyed events in *Blm* mutants. Likewise, *Marcal1* mutations do not affect synthesis to the LTRs, resulting in a higher percentage of repair events with the capacity for SDSA. In this context, annealing is compromised but the higher number of

SDSA-proficient DNA ends results in residual red-eyed progeny, either through a back-up mechanism or through EJ that restores *w* splicing. The paucity of SDSA events in the double mutant suggests that the combination of D-loop dissociation defects and reduced annealing capacity are synergistic and all but abolish LTR annealing.

The extreme reduction in observable repair events in *Marcal1 Blm* double mutants compared to either single mutant suggests that either the majority of cells with *P* element excision were inviable or the majority of events synthesized into the *copia* element and resulted in apricot-eyed progeny. Considering that EJ events had significantly reduced synthesis compared to wild type and flanking deletions were observed, it is more likely that the majority of cells with an excision were inviable. Blm deficient cells cannot dissociate D-loops, resulting in cleavage of the structure and further resection (as proposed by Adams *et al.* 2003; McVey *et al.* 2004a) until a cryptic signal results in EJ of the ends. In *Marcal1 Blm* mutants, this process is further deregulated, suggesting both Blm and Marcal1 are part of the signaling process that activates EJ during gap repair. Further studies of genetic interactions between *Marcal1, Blm,* and EJ factors may help to clarify this interaction.

Unlike *P*{$w^a$}, the *P*{*wIw*} assay did not reveal any differences between *Marcal1*$^{K275M}$ and null mutants. *P*{$w^a$} requires multiple iterations of the anneal vs. EJ vs. re-invade decision (McVey *et al.* 2004b), providing increased opportunities to observe moderate defects in that decision among repair products. On the other hand, in the *P*{*wIw*} assay there is usually no intact homologous template for repair (in wild-type flies, <1% of the products were uncut or restored to the original sequence). While it is not possible to determine which repair strategy is initially favored at the break, the efficiency of *I-Sce*I cutting may ultimately select for HDR, since direct ligation would often restore the cut site, perhaps to be cut again. Once resected, annealing becomes the strongly favored strategy since long ssDNA tails are not ideal substrates for TMEJ or cNHEJ (Waters *et al.* 2014; Wyatt *et al.* 2016) and strand

invasion is not possible. SSA represents over 93% of all repair products in wild type and *Marcal1*$^{K275M}$ heterozygotes, supporting this interpretation. Because the anneal vs. EJ vs. strand re-invade decision point is highly altered and potentially de-regulated by the assay design, it is likely that EJ events in *P*{*wIw*} are facilitated through alternative pathways that are less influenced by Marcal1. My data support this interpretation as we see a large (>7-fold) increase in EJ events in both *Marcal1*$^{K275M}$ and null mutants. These EJ events are predominantly joined near the break site without large deletions, suggesting an alternative form of EJ is utilized on long resected ends when annealing is compromised. EJ was reported by Chan *et al*. in mutants defective in both cNHEJ and TMEJ (Chan *et al.* 2010), though the key mediator of this form of EJ remains unknown.

Interestingly, I observed that *Marcal1*$^{K275M}$ is completely recessive in the *P*{*wIw*} assay (Figure 3.7D). It is possible that Marcal1$^{K275M}$ mutant protein may bind DNA less tightly than the wild-type protein. While ATP-binding is not required for DNA binding by SMARCAL1, it can cause a conformational change that influences the DNA binding constant (Gupta *et al.* 2015). It is also possible that multiple Marcal1 molecules bind the nascent DNA and the presence of any wild-type protein is sufficient to rescue the *Marcal1*$^{K275M}$ phenotype. Recent work on the RPA-SMARCAL1 interface has shown that SMARCAL1 binds to the C-terminal region of RPA32 with 1:1 stoichiometry (Bhat *et al.* 2014; Xie *et al.* 2014) and it is likely that many molecules of Marcal1 bind the RPA-coated nascent DNA, allowing for multiple complementarity searches to occur simultaneously. Studies have revealed a similar mechanism for homology searching by Rad51-coated ssDNA (Wright and Heyer 2014; Qi and Greene 2016). Mutation of the Walker B motif to allow ATP binding (thus preserving DNA binding kinetics) but prevent ATP hydrolysis (translocation) as well as *in vitro* studies of Marcal1 interactions with long RPA-bound filaments may help to clarify the mechanistic basis of the *Marcal1*$^{K275M}$ phenotype.

The limitations of *P*{*wIw*} are predominantly due to extensive homology to either side of the break, which makes it difficult to definitively identify annealed events vs. MMEJ/TMEJ of approximately the same size. Molecular analysis revealed that 22% of white-eyed progeny in *Marcal1* mutants had this type of event (Figure 3.6) and it is highly probable that the true percentage is even higher but sequence similarity is an impediment to fine-scale amplification. Amplification of the entire construct followed by single-molecule sequencing, as done in the *S. cerevisiae* gap repair assay of Guo *et al.*, might allow sampling of a larger number of repair events from multiple tissues of a single individual and it could be further adapted to recover events in different progeny from a single male germline, as in my strategy (Guo *et al.* 2015). My work has highlighted the need for fine-scale assays capable of distinguishing true annealing events from microhomology-mediated events.

## Marcal1 mutations uncover roles for Blm at replication forks

*Marcal1* mutants had a phenotype consistent with a role in annealing during SDSA and SSA in every assay I performed. I did not find evidence of a role in replication, despite repeated approaches. In contrast, *Blm* mutants had elevated lethality when exposed to every mutagen tested indicating a role in a variety of DNA damage repair pathways. It is possible that Blm is part of a large genome surveillance complex called BASC consisting of BRCA1, BLM, resection proteins, ATM, and mismatch repair proteins, as proposed by Wang *et al*. (Wang *et al.* 2000). If such a complex exists in *Drosophila*, it is unclear which protein acts as the scaffold since the putative scaffold protein, BRCA1, does not have a known ortholog in flies. It is more likely that Blm has different roles depending on the context of the lesion and the type of repair required.

BLM is necessary for recruitment of Fanconi anemia (FA) proteins FANCM and FANCD2 to interstrand crosslinks (ICLs) (Hirano *et al.* 2005; Hemphill *et al.* 2009; Hoadley *et al.* 2012; Ling *et al.* 2016; Panneerselvam *et al.* 2016) and the high lethality I observed in

*Blm* mutants treated with nitrogen mustard (HN2) and cisplatin (CPL) support this role. Interestingly, Hirano *et al.* proposed that the interaction between Blm and FA proteins at ICLs was due to repair of the lesions via HDR mechanisms, however I was unable to corroborate this hypothesis since *Marcal1 Blm* double mutants did not survive CPL treatment nor were they assessed in HN2 treatment.

Blm and FA proteins have also been shown to interact during replication-associated repair. In human cells, BLM is recruited to replication forks stalled by aphidicolin treatment and this recruitment is FANCD2-dependent (Naim and Rosselli 2009; Chaudhury *et al.* 2013). FANCD2 also recruits HDR-associated proteins such as CtIP (resection) and BRCA2 (strand exchange) suggesting that replication fork maintenance is mediated via HDR mechanisms (Yeo *et al.* 2014; Raghunandan *et al.* 2015). Blm has been implicated in resection in both human cells and yeast (Nimonkar *et al.* 2011; Chen *et al.* 2013; Daley *et al.* 2014; Sturzenegger *et al.* 2014), which makes its role at stalled/blocked replication forks difficult to determine. Is it performing HDR roles or does it act on the fork itself to prevent recombinational repair?

My observations of mutants treated with methylmethansulfonate (MMS) suggest that Blm stabilizes blocked replication forks. I found that *Blm* mutants were sensitive to killing by MMS, but *Marcal1* mutants were not. The *Marcal1 Blm* double mutant was synergistically sensitive, consistent with a role for Blm in replication fork stability. In the absence of Blm, MMS-generated lesions are likely converted to DSBs at the fork (Ui *et al.* 2005). Blm also has roles in HDR, further sensitizing *Blm* mutants to MMS treatment. The residual repair in *Blm* mutants is likely due to single-strand annealing (SSA) mechanisms that bypass D-loop dissociation and are mediated by Marcal1. This hypothesis is supported by the complete lethality of *Marcal1 Blm* double mutants when exposed to MMS.

Interestingly, I observed a similar phenotype in response to etoposide (ETS) treatment. *Blm* mutants had elevated lethality when treated with ETS, *Marcal1* mutants were not sensitive, and *Marcal1 Blm* double mutants were inviable at the dose tested. ETS inhibits Topoisomerase II (TopII) which acts as a dimer and is responsible for relieving torsional stress during transcription and replication by cutting both DNA strands, rotating, and re-ligating them (reviewed in Yan *et al.* 2016). ETS can inhibit one or both dimers to generate nicks or DSBs. ETS is generally thought to affect viability through the creations of DSBs (ssDNA nicks can be converted to DSBs during replication). ETS lesions can be repaired by either cNHEJ or HDR in human and DT40 cells (de Campos-Nebel *et al.* 2010; Maede *et al.* 2014); however *Drosophila* lack the end processing machinery needed to remove covalently bound TopII from DNA ends so ETS lesions are most likely repaired via HDR in flies. It is possible that Blm helps prevent the formation of ETS-induced DSBs during replication, in a similar manner to its role in response to MMS treatment, and a subset of these can be repaired via Marcal1-mediated SSA. In the absence of both proteins, ETS lesions cause catastrophic fork collapse, resulting in total lethality in *Marcal1 Blm* double mutants.

*Blm* mutants were sensitive to ionizing radiation (IR) at lower doses than *Marcal1* mutants and the double mutant was not significantly different than *Blm* single mutants. The increased resilience of *Marcal1* mutants to IR compared to *Blm* mutants may be due to differences in specialization during HDR. Marcal1 mediates annealing later in the pathway (Chapter 3) whereas Blm has been implicated in multiple steps of HDR both before and after Marcal1 activity (Bachrati *et al.* 2006; Johnson-Schlitz and Engels 2006; Nimonkar *et al.* 2011). *Marcal1 Blm* double mutants had increased survival compared to MMS and ETS treated groups, suggesting IR does not impact replication to the same extent nor is it predominantly repaired via SSA as I hypothesized for MMS and ETS.

Interestingly, camptothecin (CPT) has a similar mechanism to ETS but did not result in synergistic lethality in *Marcal1 Blm* double mutants. CPT inhibits Topoisomerase I (TopI) after it nicks the DNA, resulting in a covalently-bound protein and a ssDNA break. *Marcal1* and *Blm* mutants had similarly elevated lethality when exposed to CPT and *Marcal1 Blm* double mutants had an additive phenotype at the same dose. Studies of the DNA damage response to CPT-induced lesions have shown that RPA2 is phosphorylated and both ATR and ATM are activated, suggesting a pleiotrpoic cellular response (reviewed in Pommier 2006). My data supports these findings and suggests that CPT lesions activate multiple separate pathways for repair that are additive when defective whereas ETS produces lesions that are repaired by fewer mechanisms that have catastrophic consequences when defective.

Formaldehyde (HCHO) causes protein/DNA crosslinks (Table 4.5), which can be converted to ssDNA breaks. These types of breaks are most detrimental when they escape ATM-mediated delay of entry into S-phase; if replication occurs across a ssDNA break, it can be converted into a one-ended DSB (Khoronenkova and Dianov 2015). It is possible that a replication-associated role for Blm confers sensitivity to *Blm* mutants, similar to my observations with MMS treatment. Unlike MMS, however, double mutants were not increasingly sensitive to HCHO compared to *Blm* single mutants, arguing against the formation of DSBs during replication. Previous studies in yeast indicate that acute, high doses of HCHO like the treatment used here are predominantly repaired via nucleotide excision repair (NER) pathways whereas low, chronic exposure is dependent on HDR for repair (de Graaf *et al.* 2009). Blm has not been shown to interact with proteins in the NER pathway outside of meiosis (Andersen *et al.* 2011; Hatkevich *et al.* 2016) nor has it been shown to have a role in repair of ssDNA gaps or protein-DNA crosslinks. More studies are needed to determine the mechanisms that contribute to HCHO sensitivity in *Blm* mutants.

*Marcal1* mutations significantly increased *Blm* mutant survival when exposed to the ribonucleotide reductase inhibitor hydroxyurea (HU), which depletes the nucleotide pool, causing replication fork stalling. Studies of HU-induced replication stress have shown that stalled forks are reset in a HDR-dependent manner (i.e. template switching) in human cells when exposure is <2 hours (Petermann *et al.* 2010). Petermann *et al.* further found that prolonged exposure (>12 hours) resulted in fork collapse (formation of DSBs). My data suggests that HU treatment during larval feeding more closely resembles short exposures since *Blm* mutants are sensitive, consistent with a role for Blm in replication fork maintenance, but *Marcal1* mutants are not.

The observation that *Marcal1* mutations enhance *Blm* mutant survival suggests that Marcal1 has a detrimental effect on stalled/slowed replication forks, which is consistent with the enhanced survival observed in *Marcal1* mutants n a *Polα-180*/+ heterozygous background. When Blm is present, Marcal1 is blocked from acting on stalled forks, though genome-wide replication slowing like that in *Polα-180*/+ heterozygotes may overwhelm the protection conferred by Blm and result in reduced viability in wild type compared to *Marcal1* mutants. In the absence of both proteins, Blm's function is no longer required and survival is enhanced. These data suggest that Blm's function at stalled forks is inherently different from its response to DNA lesions.

Extrapolating from this interpretation and the findings of Petermann *et al*., it is likely that the role of Blm at replication forks encountering DNA damage is restart through mechanisms that resemble HDR such as template switching, whereas its role at stalled forks is to exclude proteins that may erroneously identify the fork as an aberrant structure and attempt to process it into dsDNA. Studies of Blm during replication have focused on lesions that result in DSBs in the absence of Blm. My data have revealed a role for Blm at the fork

that protects forks from DSB formation by either lesion bypass (presumably via template switching) or by protecting a functional fork from aberrant processing by repair proteins.

The findings reported here provide evidence that Marcal1 mediates annealing in both SDSA and SSA. I have further shown that *Marcal1* and *Blm* genetically interact during gap repair. *Marcal1*$^{K275M}$ mutations as well as *Marcal1 Blm* double mutations impact EJ pathways (most likely TMEJ) during HDR, providing new information on the regulation of the anneal—EJ—strand re-invade decision point. Additionally, I uncovered evidence of fork maintenance roles for Blm during replication. Absence of Blm results in the conversion of some DNA lesions into damage that can be repaired by Marcal1, establishing a genetic interaction between *Blm* and *Marcal1* in contexts beyond gap repair. Understanding the interplay between Marcal1, Blm, and EJ mechanisms has broad implications for multiple applications including chemotherapeutics, genome editing technologies, and SIOD prognosis. Many cancer drugs generate DSBs as a primary mechanism; the role in DSB repair discovered here suggests SMARCAL1 is important for multiple repair mechanisms during S/G2, making it an attractive target for drug development, as has been proposed by Zhang, *et al.* (Zhang *et al.* 2012). Additionally, insertion of long fragments during CRISPR/Cas9 genome editing has been proposed to occur via SDSA (Byrne *et al.* 2015); understanding the regulation of SDSA will improve the efficiency of this technology. Lastly, understanding the interplay of multiple repair strategies as well as gaining insight into which strategies are used in different contexts enhances our understanding of both the basis of SIOD and its progression.

# REFERENCES


Adams M. D., McVey M., Sekelsky J. J., 2003 *Drosophila* BLM in double-strand break repair by synthesis-dependent strand annealing. Science 299: 265–7.

Allers T., Lichten M., 2001 Differential timing and control of noncrossover and crossover recombination during meiosis. Cell 106: 47–57.

Amunugama R., Groden J., Fishel R., 2013 The HsRAD51B-HsRAD51C stabilizes the HsRAD51 nucleoprotein filament. DNA Repair (Amst). 12: 723–732.

Andersen S. L., Bergstralh D. T., Kohl K. P., LaRocque J. R., Moore C. B., Sekelsky J., 2009 *Drosophila* MUS312 and the vertebrate ortholog BTBD12 interact with DNA structure-specific endonucleases in DNA repair and recombination. Mol. Cell 35: 128–135.

Andersen S. L., Sekelsky J., 2010 Meiotic versus mitotic recombination: Two different routes for double-strand break repair: The different functions of meiotic versus mitotic DSB repair are reflected in different pathway usage and different outcomes. BioEssays 32: 1058–1066.

Andersen S. L., Kuo H. K., Savukoski D., Brodsky M. H., Sekelsky J., 2011 Three structure-selective endonucleases are essential in the absence of BLM helicase in *Drosophila.* PLoS Genet. 7: e1002315.

Bachrati C. Z., Borts R. H., Hickson I. D., 2006 Mobile D-loops are a preferred substrate for the Bloom's syndrome helicase. Nucleic Acids Res. 34: 2269–2279.

Bakr A., Köcher S., Volquardsen J., Reimer R., Borgmann K., Dikomey E., Rothkamm K., Mansour W. Y., 2016 Functional crosstalk between DNA damage response proteins 53BP1 and BRCA1 regulates double strand break repair choice. Radiother. Oncol. 119: 276–281.

Bansbach C. E., Bétous R., Lovejoy C. A., Glick G. G., Cortez D., 2009 The annealing helicase SMARCAL1 maintains genome integrity at stalled replication forks. Genes Dev. 23: 2405–14.

Baradaran-Heravi A., Cho K. S., Tolhuis B., Sanyal M., Morozova O., Morimoto M., Elizondo L. I., Bridgewater D., Lubieniecka J., Beirnes K., *et al*., 2012a Penetrance of biallelic SMARCAL1 mutations is associated with environmental and genetic disturbances of gene expression. Hum. Mol. Genet. 21: 2572–2587.

Baradaran-Heravi A., Raams A., Lubieniecka J., Cho K. S., DeHaai K. A., Basiratnia M., Mari P.-O., Xue Y., Rauth M., Olney A. H., *et al*., 2012b SMARCAL1 deficiency predisposes to non-Hodgkin lymphoma and hypersensitivity to genotoxic agents *in vivo*. Am. J. Med. Genet. A 158A: 2204–13.

Barber L. J., Youds J. L., Ward J. D., Mcilwraith M. J., Neil N. J. O., Petalcorin M. I. R., Martin J. S., Collis S. J., Cantor S. B., Auclair M., *et al*., 2008 RTEL1 maintains genomic stability by suppressing homologous recombination. Cell 135: 261–271.

Basiratnia M., Baradaran-Heravi A., Yavarian M., Geramizadeh B., Karimi M., 2011 Non-Hodgkin lymphoma in a child with Schimke immuno-osseous dysplasia. Iran J. Med. Sci. 36: 222–225.

Bassett A. R., Liu J. L., 2014 CRISPR/Cas9 and genome editing in *Drosophila*. J. Genet. Genomics 41: 7–19.

Benson F. E., Baumann P., West S. C., 1998 Synergistic actions of Rad51 and Rad52 in recombination and DNA repair. Nature 391: 401–404.

Bétous R., Mason A. C., Rambo R. P., Bansbach C. E., Badu-Nkansah A., Sirbu B. M., Eichman B. F., Cortez D., 2012 SMARCAL1 catalyzes fork regression and Holliday junction migration to maintain genome stability during DNA replication. Genes Dev. 26: 151–62.

Bétous R., Glick G. G., Zhao R., Cortez D., 2013a Identification and characterization of SMARCAL1 protein complexes. PLoS One 8: e63149.

Bétous R., Couch F. B., Mason A. C., Eichman B. F., Manosas M., Cortez D., 2013b Substrate-selective repair and restart of replication forks by DNA translocases. Cell Rep. 3: 1958–1969.

Bhargava R., Onyango D. O., Stark J. M., 2016 Regulation of single-strand annealing and its role in genome maintenance. Trends Genet. 32: 566–575.

Bhat K. P., Betous R., Cortez D., 2014 High-affinity DNA binding domains of Replication Protein A (RPA) direct SMARCAL1-dependent replication fork remodeling. J. Biol. Chem. 290: 4110–4117.

Blanco M. G., Matos J., Rass U., Ip S. C. Y., West S. C., 2010 Functional overlap between the structure-specific nucleases Yen1 and Mus81-Mms4 for DNA-damage repair in *S. cerevisiae*. DNA Repair (Amst). 9: 394–402.

Bozas A., Beumer K. J., Trautman J. K., Carroll D., 2009 Genetic analysis of zinc-finger nuclease-induced gene targeting in *Drosophila*. Genetics 182: 641–651.

Brosh R. M., Li J. L., Kenny M. K., Karow J. K., Cooper M. P., Kureekattil R. P., Hickson I. D., Bohr V. A., 2000 Replication protein a physically interacts with the Bloom's syndrome protein and stimulates its helicase activity. J. Biol. Chem. 275: 23500–23508.

Brough R., Wei D., Leulier S., Lord C. J., Rong Y. S., Ashworth A., 2008 Functional analysis of *Drosophila melanogaster* BRCA2 in DNA repair. DNA Repair (Amst). 7: 10–19.

Byrne S. M., Ortiz L., Mali P., Aach J., Church G. M., 2015 Multi-kilobase homozygous targeted gene replacement in human induced pluripotent stem cells. Nucleic Acids Res. 43: e21.

Carroll C., Bansbach C. E., Zhao R., Jung S. Y., Qin J., Cortez D., 2014 Phosphorylation of a C-terminal auto-inhibitory domain increases SMARCAL1 activity. Nucleic Acids Res. 42: 918–25.

Carroll C., Hunley T. E., Guo Y., Cortez D., 2015 A novel splice site mutation in SMARCAL1 results in aberrant exon definition in a child with Schimke immuno-osseous dysplasia. Am. J. Med. Genet. Part A 167: 2260–2264.

Chalermrujinanant C., Michowski W., Sittithumcharee G., Esashi F., Jirawatnotai S., 2016 Cyclin D1 promotes BRCA2-Rad51 interaction by restricting cyclin A/B-dependent BRCA2 phosphorylation. Oncogene 35: 2815–2823.

Chan K. L., Palmai-Pallag T., Ying S., Hickson I. D., 2009 Replication stress induces sister-chromatid bridging at fragile site loci in mitosis. Nat. Cell Biol. 11: 753–60.

Chan S. H., Yu A. M., McVey M., 2010 Dual roles for DNA polymerase theta in alternative end-joining repair of double-strand breaks in *Drosophila*. PLoS Genet. 6: 1–16.

Chaudhury I., Sareen A., Raghunandan M., Sobeck A., 2013 FANCD2 regulates BLM complex functions independently of FANCI to promote replication fork recovery. Nucleic Acids Res. 41: 6444–59.

Chen S. H., Wu C.-H., Plank J. L., Hsieh T., 2012 Essential functions of C terminus of *Drosophila* Topoisomerase IIIα in double Holliday junction dissolution. J. Biol. Chem. 287: 19346–53.

Chen H., Lisby M., Symington L., 2013 RPA coordinates DNA end resection and prevents formation of DNA hairpins. Mol. Cell 50: 589–600.

Chiolo I., Minoda A., Colmenares S. U., Polyzos A., Costes S. V., Karpen G. H., 2011 Double-strand breaks in heterochromatin move outside of a dynamic HP1a domain to complete recombinational repair. Cell 144: 732–744.

Ciccia A., Bredemeyer A. L., Sowa M. E., Terret M.-E., Jallepalli P. V, Harper J. W., Elledge S. J., 2009 The SIOD disorder protein SMARCAL1 is an RPA-interacting protein involved in replication fork restart. Genes Dev. 23: 2415–25.

Ciccia A., Elledge S. J., 2010 The DNA Damage Response: Making it safe to play with knives. Mol. Cell 40: 179–204.

Clewing J. M., Fryssira H., Goodman D., Smithson S. F., Sloan E. A., Lou S., Huang Y., Choi K., Lücke T., Alpay H., *et al*., 2007 Schimke immuno-osseous dysplasia: Suggestions of genetic diversity. Hum. Mutat. 28: 273–283.

Coleman M. A., Eisen J. A., Mohrenweiser H. W., 2000 Cloning and characterization of HARP/SMARCAL1: a prokaryotic HepA-related SNF2 helicase protein from human and mouse. Genomics 65: 274–282.

Couch F. B., Bansbach C. E., Driscoll R., Luzwick J. W., Glick G. G., Bétous R., Carroll C. M., Jung S. Y., Qin J., Cimprich K. A., Cortez D., 2013 ATR phosphorylates SMARCAL1 to prevent replication fork collapse. Genes Dev. 27: 1610–23.

Crown K. N., McMahan S., Sekelsky J., 2014 Eliminating both canonical and short-patch mismatch repair in *Drosophila melanogaster* suggests a new meiotic recombination model. PLoS Genet. 10: e1004583.

Daley J. M., Chiba T., Xue X., Niu H., Sung P., 2014 Multifaceted role of the Topo IIIα-RMI1-RMI2 complex and DNA2 in the BLM-dependent pathway of DNA break end resection. Nucleic Acids Res. 42: 11083–11091.

Daley J. M., Niu H., Miller A. S., Sung P., 2015 Biochemical mechanism of DSB end resection and its regulation. DNA Repair (Amst). 32: 66–74.

de Campos-Nebel M., Larripa I., González-Cid M., 2010 Topoisomerase II-mediated DNA damage is differently repaired during the cell cycle by non-homologous end joining and homologous recombination. PLoS One 5: 1–13.

de Graaf B., Clore A., McCullough A. K., 2009 Cellular pathways for DNA repair and damage tolerance of formaldehyde-induced DNA-protein crosslinks. DNA Repair (Amst). 8: 1207–1214.

Deguchi K., Clewing J. M., Elizondo L. I., Hirano R., Huang C., Choi K., Sloan E. A., Lücke T., Marwedel K. M., Powell R. D., *et al*., 2008 Neurologic phenotype of Schimke immuno-osseous dysplasia and neurodevelopmental expression of SMARCAL1. J. Neuropathol. Exp. Neurol. 67: 565–577.

Dekanty A., Barrio L., Milán M., 2015 Contributions of DNA repair, cell cycle checkpoints and cell death to suppressing the DNA damage-induced tumorigenic behavior of *Drosophila* epithelial cells. Oncogene: 978–985.

Dekel B., Metsuyanim S., Goldstein N., Pode-Shakked N., Kovalski Y., Cohen Y., Davidovits M., Anikster Y., 2008 Schimke immuno-osseous dysplasia: Expression of SMARCAL1 in blood and kidney provides novel insight into disease phenotype. Pediatr. Res. 63: 398–403.

Ding H., Schertzer M., Wu X., Gertsenstein M., Selig S., Kammori M., Pourvali R., Poon S., Vulto I., Chavez E., Tam P. P. L., Nagy A., Lansdorp P. M., 2004 Regulation of murine telomere length by Rtel: An essential gene encoding a helicase-like protein. Cell 117: 873–886.

Do A. T., Brooks J. T., le Neveu M. K. , LaRocque J. R., 2013 Double-strand break repair assays determine pathway choice and structure of gene conversion events in *Drosophila melanogaster*. G3 4: 425–432.

Ehmsen K. T., Heyer W.-D., 2008 *Saccharomyces cerevisiae* Mus81-Mms4 is a catalytic, DNA structure-selective endonuclease. Nucleic Acids Res. 36: 2182–2195.

Fabre F., Chan A., Heyer W.-D., Gangloff S., 2002 Alternate pathways involving Sgs1/Top3, Mus81/ Mms4, and Srs2 prevent formation of toxic recombination intermediates from single-stranded gaps created by DNA replication. Proc. Natl. Acad. Sci. U. S. A. 99: 16887–92.

Fasching C. L., Cejka P., Kowalczykowski S. C., Heyer W. D., 2015 Top3-Rmi1 dissolve Rad51-mediated D loops by a topoisomerase-based mechanism. Mol. Cell 57: 595–606.

Feldkamp M. D., Mason A. C., Eichman B. F., Chazin W. J., 2014 Structural analysis of Replication Protein A recruitment of the DNA damage response protein SMARCAL1. Biochemistry: 3052–3061.

Forget A. L., Kowalczykowski S. C., 2012 Single-molecule imaging of DNA pairing by RecA reveals a three-dimensional homology search. Nature 482: 423–427.

Garcia A., Salomon R. N., Witsell A., Liepkalns J., Calder R. B., Lee M., Lundell M., Vijg J., McVey M., 2011 Loss of the Bloom syndrome helicase increases DNA ligase 4-independent genome rearrangements and tumorigenesis in aging *Drosophila*. Genome Biol. 12: R121.

German J., 1993 Bloom Syndrome: A Mendelian prototype of somatic mutational disease. Medicine (Baltimore). 76: 393–406.

Ghosal G., Yuan J., Chen J., 2011 The HARP domain dictates the annealing helicase activity of HARP/SMARCAL1. EMBO Rep. 12: 574–80.

Gloor G. B., Nassif N. a, Johnson-schlitz D. M., Preston C. R., Engels W. R., 1991 Targeted gene replacement in *Drosophila* via *P* element-induced gap repair. Science 253: 1110–1117.

Gorski M. M., Eeken J. C. J., de Jong A. W. M., Klink I., Loos M., Romeijn R. J., van Veen B. L., Mullenders L. H., Ferro W., Pastink A., 2003 The *Drosophila melanogaster* DNA Ligase IV gene plays a crucial role in the repair of radiation-induced DNA double-strand breaks and acts synergistically with Rad54. Genetics 165: 1929–1941.

Grafstrom R. C., Fornace A., Harris C. C., 1984 Repair of DNA damage caused by formaldehyde in human cells. Cancer Res.: 4323–4327.

Gratz S. J., Cummings A. M., Nguyen J. N., Hamm D. C., Donohue L. K., Harrison M. M., Wildonger J., O'Connor-Giles K. M., 2013 Genome engineering of *Drosophila* with the CRISPR RNA-guided Cas9 nuclease. Genetics 194: 1029–35.

Guo X., Lehner K., O'Connell K., Zhang J., Dave S. S., Jinks-Robertson S., 2015 SMRT sequencing for parallel analysis of multiple targets and accurate SNP phasing. G3 (Bethesda). 5: 2801–8.

Gupta M., Mazumder M., Dhatchinamoorthy K., Nongkhlaw M., Haokip D. T., Gourinath S., Komath S. S., Muthuswami R., 2015 Ligand-induced conformation changes drive ATP hydrolysis and function in SMARCAL1. FEBS J. 282: 3841–3859.

Hammond E. M., Green S. L., Giaccia A. J., 2003 Comparison of hypoxia-induced replication arrest with hydroxyurea and aphidicolin-induced arrest. Mutat. Res. - Fundam. Mol. Mech. Mutagen. 532: 205–213.

Haokip D. T., Goel I., Arya V., Sharma T., Kumari R., Priya R., Singh M., Muthuswami R., 2016 Transcriptional regulation of ATP-dependent chromatin remodeling factors: SMARCAL1 and BRG1 mutually co-regulate each other. Sci. Rep. 6: 20532.

Hatkevich T., Kohl K. P., McMahan S., Hartmann M. A., Williams A. M., Sekelsky J., 2016 Bloom syndrome helicase promotes meiotic crossover patterning and homolog disjunction. Curr. Biol. 27(1): 96-102.

Hawley R. S., 2002 Meiosis: How male flies do meiosis. Curr. Biol. 12: 660–662.

Hemphill A. W., Akkari Y., Newell A. H., Schultz R. A., Grompe M., North P. S., Hickson I. D., Jakobs P. M., Rennie S., Pauw D., *et al.*, 2009 Topo IIIα and BLM act within the Fanconi anemia pathway in response to DNA-crosslinking agents. Cytogenet. Genome Res. 125: 165–175.

Henikoff S., 1997 Nuclear organization and gene expression: homologous pairing and long-range interactions. Curr Opin Cell Biol 9: 388–395.

Heo K., Kim H., Choi S. H., Choi J., Kim K., Gu J., Lieber M. R., Yang A. S., An W., 2008 FACT-mediated exchange of histone variant H2AX regulated by phosphorylation of H2AX and ADP-ribosylation of SPT16. Mol. Cell 30: 86–97.

Heyer W. D., Ehmsen K. T., Solinger J. A., 2003 Holliday junctions in the eukaryotic nucleus: Resolution in sight? Trends Biochem. Sci. 28: 548–557.

Hirano S., Yamamoto K., Ishiai M., Yamazoe M., Seki M., Matsushita N., Ohzeki M., Yamashita Y. M., Arakawa H., Buerstedde J.-M., *et al.*, 2005 Functional relationships of FANCC to homologous recombination, translesion synthesis, and BLM. EMBO J. 24: 418–27.

Hoadley K. A., Xue Y., Ling C., Takata M., Wang W., Keck J. L., 2012 Defining the molecular interface that connects the Fanconi anemia protein FANCM to the Bloom syndrome dissolvasome. Proc. Natl. Acad. Sci. U. S. A. 109: 4437–42.

Hunter N., Kleckner N., 2001 The Single-End Invasion. Cell 106: 59–70.

Hunter K. B., Lücke T., Spranger J., Smithson S. F., Alpay H., André J. L., Asakura Y., Bogdanovic R., Bonneau D., Cairns R., *et al.*, 2010 Schimke immuno-osseous dysplasia: Defining skeletal features. Eur. J. Pediatr. 169: 801–811.

Ip S. C. Y., Rass U., Blanco M. G., Flynn H. R., Skehel J. M., West S. C., 2008 Identification of Holliday junction resolvases from humans and yeast. Nature 456: 357–361.

Ira G., Malkova A., Liberi G., Foiani M., Haber J. E., 2003 Srs2 and Sgs1 – Top3 Suppress crossovers during double-strand break repair in yeast. Cell 115: 401–411.

Ivanov E. L., Sugawara N., Fishman-Lobell J., Haber J. E., 1996 Genetic requirements for the single-strand annealing pathway of double-strand break repair in *Saccharomyces cerevisiae*. Genetics 142: 693–704.

Jasin M., Rothstein R., 2013 Repair of strand breaks by homologous recombination. Cold Spring Harb. Perspect. Biol. 5.

Jensen R. B., Carreira A., Kowalczykowski S. C., 2010 Purified human BRCA2 stimulates RAD51-mediated recombination. Nature 467: 678–683.

Jensen R. B., 2013 BRCA2: one small step for DNA repair, one giant protein purified. Yale J. Biol. Med. 86: 479–89.

Johnson-Schlitz D., Engels W. R., 2006 Template disruptions and failure of double Holliday junction dissolution during double-strand break repair in *Drosophila* BLM mutants. Proc. Natl. Acad. Sci. U. S. A. 103: 16840–5.

Kane D. P., Shusterman M., Rong Y., McVey M., 2012 Competition between replicative and translesion polymerases during homologous recombination repair in *Drosophila*. PLoS Genet. 8: e1002659.

Karpenshif Y., Bernstein K. A., 2012 From yeast to mammals: Recent advances in genetic control of homologous recombination. DNA Repair (Amst). 11: 781–788.

Kassavetis G. A., Kadonaga J. T., 2014 The annealing helicase and branch migration activities of *Drosophila* HARP. PLoS One 9: e98173.

Keka I. S., Mohiuddin, Maede Y., Rahman M. M., Sakuma T., Honma M., Yamamoto T., Takeda S., Sasanuma H., 2015 Smarcal1 promotes double-strand-break repair by nonhomologous end-joining. Nucleic Acids Res. 43: 6359–6372.

Khade N. V., Sugiyama T., 2016 Roles of C-terminal region of yeast and human rad52 in rad51-nucleoprotein filament formation and ssDNA annealing. PLoS One 11: 1–14.

Khoronenkova S. V, Dianov G. L., 2015 ATM prevents DSB formation by coordinating SSB repair and cell cycle progression. Proc. Natl. Acad. Sci. U. S. A. 112: 3997–4002.

Kilic S. S., Donmez O., Sloan E. A., Elizondo L. I., Huang C., André J. L., Bogdanovic R., Cockfield S., Cordeiro I., Deschenes G., *et al.*, 2005 Association of migraine-like headaches with Schimke immuno-osseous dysplasia. Am. J. Med. Genet. 135 A: 206–210.

Kim J. S., Krasieva T. B., Kurumizaka H., Chen D. J., Taylor A. M. R., Yokomori K., 2005 Independent and sequential recruitment of NHEJ and HR factors to DNA damage sites in mammalian cells. J. Cell Biol. 170: 341–347.

Kohl K. P., Jones C. D., Sekelsky J., 2012 Evolution of an MCM complex in flies that promotes meiotic crossovers by blocking BLM helicase. Science 338: 1363–5.

Kuo H. K., McMahan S., Rota C. M., Kohl K. P., Sekelsky J., 2014 *Drosophila* FANCM helicase prevents spontaneous mitotic crossovers generated by the MUS81 and SLX1 nucleases. Genetics 198: 935–945.

Kurkulos M., Weinberg J. M., Roy D., Mount S. M., 1994 *P* element-mediated *in vivo* deletion analysis of *white-apricot*: Deletions between direct repeats are strongly favored. Genetics 136: 1001–1011.

LaFave M. C., Andersen S. L., Stoffregen E. P., Holsclaw J. K., Kohl K. P., Overton L. J., Sekelsky J., 2014 Sources and structures of mitotic crossovers that arise when BLM helicase is absent in *Drosophila*. Genetics 196: 107–18.

LaRocque J. R., Dougherty D. L., Hussain S. K., Sekelsky J., 2007 Reducing DNA polymerase alpha in the absence of *Drosophila* ATR leads to P53-dependent apoptosis and developmental defects. Genetics 176: 1441–51.

Ling C., Huang J., Yan Z., Li Y., Ohzeki M., Ishiai M., Xu D., Takata M., Seidman M., Wang W., 2016 Bloom syndrome complex promotes FANCM recruitment to stalled replication forks and facilitates both repair and traverse of DNA interstrand crosslinks. Cell Discov. 2: 16047.

Lou S., Lamfers P., McGuire N., Boerkoel C. F., 2002 Longevity in Schimke immuno-osseous dysplasia. J. Med. Genet. 39: 922–925.

Lücke T., Billing H., Sloan E. A., Boerkoel C. F., Franke D., Zimmering M., Ehrich J. H. H., Das A. M., 2005 Schimke-Immuno-Osseous Dysplasia : New mutation with weak genotype – phenotype correlation in siblings. Am. J. Med. Genet. 135A: 202–205.

Lukas C., Savic V., Bekker-Jensen S., Doil C., Neumann B., Pedersen R. S., Grøfte M., Chan K. L., Hickson I. D., Bartek J., Lukas J., 2011 53BP1 nuclear bodies form around DNA lesions generated by mitotic transmission of chromosomes under replication stress. Nat. Cell Biol. 13: 243–53.

Lundin C., North M., Erixon K., Walters K., Jenssen D., Goldman A. S. H., Helleday T., 2005 Methyl methanesulfonate (MMS) produces heat-labile DNA damage but no detectable *in vivo* DNA double-strand breaks. Nucleic Acids Res. 33: 3799–811.

Machwe A., Xiao L., Groden J., Orren D. K., 2006 The Werner and Bloom syndrome proteins catalyze regression of a model replication fork. Biochemistry 45: 13939–46.

Machwe A., Karale R., Xu X., Lui Y.,Orrin D. K., 2011 The Werner and Bloom syndrome proteins help resolve replication blockage by converting (regressed) Holliday junctions to functional replication forks. Biochemistry 50: 6774–6788.

Madigan J. P., Chotkowski H. L., Glaser R. L., 2002 DNA double-strand break-induced phosphorylation of *Drosophila* histone variant H2Av helps prevent radiation-induced apoptosis. Nucleic Acids Res. 30: 3698–3705.

Maede Y., Shimizu H., Fukushima T., Kogame T., Nakamura T., Miki T., Takeda S., Pommier Y., Murai J., 2014 Differential and common DNA repair pathways for topoisomerase I- and II-targeted drugs in a genetic DT40 repair cell screen panel. Mol. Cancer Ther. 13: 214–20.

Mandemaker I. K., Vermeulen W., Marteijn J. A., 2014 Gearing up chromatin. Nucleus 5: 203–210.

Manthei K. A., Keck J. L., 2013 The BLM dissolvasome in DNA replication and repair. Cell. Mol. Life Sci. 70: 4067–84.

Manthey G. M., Clear A. D., Liddell L. C., Negritto M. C., Bailis A. M., 2016 Homologous recombination in budding yeast expressing the human RAD52 gene reveals a Rad51-independent mechanism of conservative double-strand break repair. Nucleic Acids Res. 52: 1–15.

Mason A. C., Rambo R. P., Greer B., Pritchett M., Tainer J. A., Cortez D., Eichman B. F., 2014 A structure-specific nucleic acid-binding domain conserved among DNA repair proteins. Proc. Natl. Acad. Sci. U. S. A. 111: 7618–23.

McIlwraith M. J., West S. C., 2008 DNA repair synthesis facilitates RAD52-mediated second-end capture during DSB repair. Mol. Cell 29: 510–516.

McVey M., Larocque J. R., Adams M. D., Sekelsky J. J., 2004a Formation of deletions during double-strand break repair in *Drosophila DmBlm* mutants occurs after strand invasion. Proc. Natl. Acad. Sci. U. S. A. 101: 15694–15699.

McVey M., Adams M., Staeva-Vieira E., Sekelsky J. J., 2004b Evidence for multiple cycles of strand invasion during repair of double-strand gaps in *Drosophila*. Genetics 167: 699–705.

McVey M., Andersen S. L., Broze Y., Sekelsky J., 2007 Multiple functions of *Drosophila* BLM helicase in maintenance of genome stability. Genetics 176: 1979–92.

McVey M., Khodaverdian V. Y., Meyer D., Cerqueira P. G., Heyer W.-D., 2016 Eukaryotic DNA polymerases in homologous recombination. Annu. Rev. Genet. 50: 393–421.

Mimitou E. P., Symington L. S., 2009a DNA end resection: Many nucleases make light work. DNA Repair (Amst). 8: 983–995.

Mimitou E. P., Symington L. S., 2009b Nucleases and helicases take center stage in homologous recombination. Trends Biochem. Sci. 34: 264–272.

Morimoto M., Yu Z., Stenzel P., Clewing J. M., Najafian B., Mayfield C., Hendson G., Weinkauf J. G., Gormley A. K., Parham D. M., Ponniah U., 2012 Reduced elastogenesis : a clue to the arteriosclerosis and emphysematous changes in Schimke immuno-osseous dysplasia Orphanet J. Rare Dis. 7(70): 1–17.

Mukherjee S., LaFave M. C., Sekelsky J., 2009 DNA damage responses in *Drosophila nbs* mutants with reduced or altered NBS function. DNA Repair (Amst). 8: 803–812.

Myler L. R., Gallardo I. F., Zhou Y., Gong F., Yang S.-H., Wold M. S., Miller K. M., Paull T. T., Finkelstein I. J., 2016 Single-molecule imaging reveals the mechanism of Exo1 regulation by single-stranded DNA binding proteins. Proc. Natl. Acad. Sci. U. S. A. 113: E1170-1179.

Naim V., Rosselli F., 2009 The FANC pathway and BLM collaborate during mitosis to prevent micro-nucleation and chromosome abnormalities. Nat. Cell Biol. 11: 761–8.

Naim V., Wilhelm T., Debatisse M., Rosselli F., 2013 ERCC1 and MUS81-EME1 promote sister chromatid separation by processing late replication intermediates at common fragile sites during mitosis. Nat. Cell Biol. 15: 1008–15.

Nassif N., Engels W., 1993 DNA homology requirements for mitotic gap repair in *Drosophila*. Proc. Natl. Acad. Sci. U. S. A. 90: 1262–1266.

Nassif N., Penney J., Pal S., Engels W. R., Gloor G. B., 1994 Efficient copying of nonhomologous sequences from ectopic sites via *P*-element-induced gap repair. Mol. Cell. Biol. 14: 1613–1625.

New J. H., Sugiyama T., Zaitseva E., Kowalczykowski S. C., 1998 Rad52 protein stimulates DNA strand exchange by Rad51 and replication protein A. Nature 391: 407–409.

Nimonkar A. V, Sica R. A., Kowalczykowski S. C., 2009 Rad52 promotes second-end DNA capture in double-stranded break repair to form complement-stabilized joint molecules. Proc. Natl. Acad. Sci. U. S. A. 106: 3077–3082.

Nimonkar A. V., Genschel J., Kinoshita E., Polaczek P., Campbell J. L., Wyman C., Modrich P., Kowalczykowski S. C., 2011 BLM, DNA2, RPA, MRN and EXO1, BLM, RPA, MRN constitute two DNA end resection machineries for human DNA break repair. Genes Dev. 25: 350–362.

Panneerselvam J., Wang H., Zhang J., Che R., Yu H., Fei P., 2016 BLM promotes the activation of Fanconi Anemia signaling pathway. Oncotarget 2: 1–11.

Pâques F., Leung W. Y., Haber J. E., 1998 Expansions and contractions in a tandem repeat induced by double-strand break repair. Mol. Cell. Biol. 18: 2045–2054.

Pellegrini L., 2012 The Pol α-Primase Complex. In: *The Eukaryotic Replisome: a Guide to Protein Structure and Function*, MacNeill S. (ed.) Springer Science and Media. Mainz, Germany

Petermann E., Orta M. L., Issaeva N., Schultz N., Helleday T., 2010 Hydroxyurea-stalled replication forks become progressively inactivated and require two different RAD51-mediated pathways for restart and repair. Mol. Cell 37: 492–502.

Pfeiffer P., Goedecke W., Obe G., 2000 Mechanisms of DNA double-strand break repair and their potential to induce chromosomal aberrations. Mutagenesis 15: 289–302.

Pipathsouk A., Belotserkovskii B. P., Hanawalt P. C., 2016 When transcription goes on Holliday: Double Holliday junctions block RNA polymerase II transcription *in vitro*. Biochim. Biophys. Acta 1860: 282–288.

Plank J. L., Wu J., Hsieh T.-S., 2006 Topoisomerase IIIalpha and Bloom's helicase can resolve a mobile double Holliday junction substrate through convergent branch migration. Proc. Natl. Acad. Sci. U. S. A. 103: 11118–11123.

Pommier Y., 2006 Topoisomerase I inhibitors: camptothecins and beyond. Nat. Rev. Cancer 6: 789–802.

Pommier Y., Leo E., Zhang H., Marchand C., 2010 DNA topoisomerases and their poisoning by anticancer and antibacterial drugs. Chem. Biol. 17: 421–433.

Postow L., Woo E. M., Chait B. T., Funabiki H., 2009 Identification of SMARCAL1 as a component of the DNA damage response. J. Biol. Chem. 284: 35951–61.

Povirk L. F., Shuker D. E., 1994 DNA damage and mutagenesis induced by nitrogen mustards. Mutat. Res. Genet. Toxicol. 318: 205–226.

Prakash R., Satory D., Dray E., Papusha A., Scheller J., Kramer W., Krejci L., Klein H., Haber J. E., Sung P., Ira G., 2009 Yeast Mphl helicase dissociates Rad51-made D-loops: Implications for crossover control in mitotic recombination. Genes Dev. 23: 67–79.

Preston C. R., Flores C., Engels W. R., 2006a Age-dependent usage of double-strand-break repair pathways. Curr. Biol. 16: 2009–2015.

Preston C. R., Flores C. C., Engels W. R., 2006b Differential usage of alternative pathways of double-strand break repair in *Drosophila*. Genetics 172: 1055–1068.

Prindle M. J., Loeb L. A., 2012 DNA polymerase delta in DNA replication and genome maintenance. Environ. Mol. Mutagen. 53: 666–82.

Qi Z., Redding S., Lee J. Y., Gibb B., Kwon Y., Niu H., Gaines W. A., Sung P., Greene E. C., 2015 DNA sequence alignment by microhomology sampling during homologous recombination. Cell 160: 856–869.

Qi Z., Greene E. C., 2016 Visualizing recombination intermediates with single-stranded DNA curtains. Methods 105: 62–74.

Radford I. R., 1985 The level of induced DNA double-strand breakage correlates with cell killing after x-irradiation. Int. J. Radiat. Biol. 48: 45–54.

Raghunandan M., Chaudhury I., Kelich S. L., Hanenberg H., Sobeck A., 2015 FANCD2, FANCJ and BRCA2 cooperate to promote replication fork recovery independently of the Fanconi Anemia core complex. Cell Cycle 14: 342–353.

Rao V. A., Fan A. M., Meng L., Doe C. F., North P. S., Hickson I. D., Pommier Y., North O. F., 2005 Phosphorylation of BLM, dissociation from topoisomerase IIIalpha, and colocalization with gamma-H2AX after topoisomerase I-induced replication damage. Mol. Cell. Biol. 25: 8925–37.

Rass U., Compton S. A., Matos J., Singleton M. R., Ip S. C. Y., Blanco M. G., Griffith J. D., West S. C., 2010 Mechanism of Holliday junction resolution by the human GEN1 protein. Genes Dev. 24: 1559–1569.

Reuter M., Zelensky A., Smal I., Meijering E., van Cappellen W. A. , de Gruiter H. M., van Belle G. J., van Royen M. E., Houtsmuller A. B., Essers J., Kanaar R., Wyman C., 2014 BRCA2 diffuses as oligomeric clusters with RAD51 and changes mobility after DNA damage in live cells. J. Cell Biol. 207: 599–613.

Rijkers T., van den Ouweland J., Morolli B., Rolink A. G., Baarends W. M., van Sloun P. P. H., Lohman P. H. M., Pastink A., 1998 Targeted inactivation of mouse *RAD52* reduces homologous recombination but not resistance to ionizing radiation. Mol. Cell. Biol. 18: 6423–6429.

Rodgers K., McVey M., 2016 Error-prone repair of DNA double-strand breaks. J. Cell. Physiol. 231: 15–24.

Romero N. E., Matson S. W., Sekelsky J., 2016 Biochemical activities and genetic functions of the *Drosophila melanogaster* Fancm helicase in DNA repair. Genetics 204: 531–541.

Rong Y. S., Golic K. G., 2003 The homologous chromosome is an effective template for the repair of mitotic DNA double-strand breaks in *Drosophila*. Genetics 165: 1831–1842.

Safder O., El-Desoky S. M., Bockenhauer D., Sabire N., Kari J. A., 2014 Steroid-resistant nephrotic syndrome in a child with dysmorphic features : Answers. Pediatr. Nephrol. 29: 839–840.

Sage E., Shikazono N., 2016 Radiation-induced clustered DNA lesions: repair and mutagenesis. Free Radic. Biol. Med. [epub ahea.

Saini N., Ramakrishnan S., Elango R., Ayyar S., Zhang Y., Deem A., Ira G., Haber J. E., Lobachev K. S., Malkova A., 2013 Migrating bubble during break-induced replication drives conservative DNA synthesis. Nature 502: 389–92.

Sarbajna S., Davies D., West S. C., 2014 Roles of SLX1-SLX4, MUS81-EME1, and GEN1 in avoiding genome instability and mitotic catastrophe. Genes Dev. 28: 1124–1136.

Sarin S., Javidan A., Boivin F., Alexopoulou I., Lukic D., Svajger B., Chu S., Baradaran-Heravi A., Boerkoel C. F., Rosenblum N. D., Bridgewater D., 2015 Insights into the renal pathogenesis in Schimke immuno-osseous dysplasia: A renal histological characterization and expression analysis. J. Histochem. Cytochem. 63: 32–44.

Sartori A. A., Lukas C., Coates J., Mistrik M., Fu S., Bartek J., Baer R., Lukas J., Jackson S. P., 2007 Human CtIP promotes DNA end resection. Nature 450: 509–514.

Sawant A., Floyd A. M., Dangeti M., Lei W., Sobol R. W., Patrick S. M., 2017 Differential role of base excision repair proteins in mediating cisplatin cytotoxicity. DNA Repair (Amst). 51: 46–59.

Selak N., Bachrati C. Z., Shevelev I., Dietschy T., van Loon B., Jacob A., Hübscher U., Hoheisel J. D., Hickson I. D., Stagljar I., 2008 The Bloom's syndrome helicase (BLM) interacts physically and functionally with p12, the smallest subunit of human DNA polymerase delta. Nucleic Acids Res. 36: 5166–79.

Sharma S., Hicks J. K., Chute C. L., Brennan J. R., Ahn J.-Y., Glover T. W., Canman C. E., 2012 REV1 and polymerase zeta facilitate homologous recombination repair. Nucleic Acids Res. 40: 682–691.

Sidorova J. M., Kehrli K., Mao F., Monnat R., 2013 Distinct functions of human RECQ helicases WRN and BLM in replication fork recovery and progression after hydroxyurea-induced stalling. DNA Repair (Amst). 12: 128–39.

Simon A. J., Lev A., Jeison M., Borochowitz Z. U., Korn D., 2014 Novel SMARCAL1 bi-allelic mutations associated with a chromosomal breakage phenotype in a severe SIOD patient. J. Clin. Immunol.: 76–83.

Sofueva S., Osman F., Lorenz A., Steinacher R., Castagnetti S., Ledesma J., Whitby M. C., 2011 Ultrafine anaphase bridges, broken DNA and illegitimate recombination induced by a replication fork barrier. Nucleic Acids Res. 39: 6568–84.

Song B. W., Sung P., 2000 Functional interactions among yeast Rad51 recombinase, Rad52 mediator, and replication protein A in DNA strand exchange. J. Biol. Chem. 275: 15895–15904.

Stocker H., Gallant P., 2008 *Drosophila* (C Dahmann, Ed.). Humana Press, Totowa, NJ.

Storici F., Snipe J. R., Chan G. K., Gordenin D. A., Resnick M. A., 2006 Conservative repair of a chromosomal double-strand break by single-strand DNA through two steps of annealing. Mol. Cell. Biol. 26: 7645–7657.

Sturzenegger A., Burdova K., Kanagaraj R., Levikova M., Pinto C., Cejka P., Janscak P., 2014 DNA2 cooperates with the WRN and BLM RecQ helicases to mediate long-range DNA end resection in human cells. J. Biol. Chem. 289: 27314–27326.

Svendsen J. M., Harper J. W., 2010 GEN1/Yen1 and the SLX4 complex: Solutions to the problem of Holliday junction resolution. Genes Dev. 24: 521–536.

Symington L. S., Gautier J., 2011 Double-Strand break end resection and repair pathway choice. Annu. Rev. Genet. 45: 247–271.

Szostak J. W., Orr-Weaver T. L., Rothstein R. J., Stahl F. W., 1983 The double-strand-break repair model for recombination. Cell 33: 25–35.

Thacker D., Keeney S., 2009 PCH'ing together an understanding of crossover control. PLoS Genet. 5: 2–3.

Thomas A. M., Hui C., South A., McVey M., 2013 Common variants of *Drosophila melanogaster* Cyp6d2 cause camptothecin sensitivity and synergize with loss of Brca2. G3 (Bethesda). 3: 91–9.

Trowbridge K., McKim K., Brill S. J., Sekelsky J., 2007 Synthetic lethality of *Drosophila* in the absence of the MUS81 endonuclease and the DmBlm helicase is associated with elevated apoptosis. Genetics 176: 1993–2001.

Tsai A. G., Lieber M. R., 2010 Mechanisms of chromosomal rearrangement in the human genome. BMC Genomics 11 Suppl 1: S1.

Ui A., Seki M., Ogiwara H., Onodera R., Fukushige S. I., Onoda F., Enomoto T., 2005 The ability of Sgs1 to interact with DNA topoisomerase III is essential for damage-induced recombination. DNA Repair (Amst). 4: 191–201.

Vilenchik M. M., Knudson A. G., 2003 Endogenous DNA double-strand breaks: production, fidelity of repair, and induction of cancer. Proc. Natl. Acad. Sci. 100: 12871–12876.

Wang Y., Cortez D., Yazdi P., Neff N., Elledge S. J., Qin J., 2000 BASC, a super complex of BRCA1-associated proteins involved in the recognition and repair of aberrant DNA structures. Genes Dev. 14: 927–939.

Waters C. A., Strande N. T., Wyatt D. W., Pryor J. M., Ramsden D. A., 2014 Nonhomologous end joining: A good solution for bad ends. DNA Repair (Amst). 17: 39–51.

Williams G. J., Hammel M., Radhakrishnan S. K., Ramsden D., Lees-Miller S. P., Tainer J. A., 2014 Structural insights into NHEJ: Building up an integrated picture of the dynamic DSB repair super complex, one component and interaction at a time. DNA Repair (Amst). 17: 110–120.

Wright W. D., Heyer W. D., 2014 Rad54 functions as a heteroduplex DNA pump modulated by its DNA substrates and Rad51 during D-Loop formation. Mol. Cell 53: 420–432.

Wu L., Bachrati C. Z., Ou J., Xu C., Yin J., Chang M., Wang W., Li L., Brown G. W., Hickson I. D., 2006 BLAP75/RMI1 promotes the BLM-dependent dissolution of homologous recombination intermediates. Proc. Natl. Acad. Sci. U. S. A. 103: 4068–4073.

Wu L., 2007 Role of the BLM helicase in replication fork management. DNA Repair (Amst). 6: 936–44.

Wu Y., Kantake N., Sugiyama T., Kowalczykowski S. C., 2008 Rad51 protein controls Rad52-mediated DNA annealing. J. Biol. Chem. 283: 14883–14892.

Wyatt H. D. M., Sarbajna S., Matos J., West S. C., 2013 Coordinated actions of SLX1-SLX4 and MUS81-EME1 for holliday junction resolution in human cells. Mol. Cell 52: 234–247.

Wyatt D. W., Feng W., Conlin M. P., Yousefzadeh M. J., Roberts S. A., Mieczkowski P., Wood R. D., Gupta G. P., Ramsden D. A., Alexandrov L. B., *et al*., 2016 Essential roles for polymerase θ-mediated end joining in the repair of chromosome breaks. Mol. Cell 63: 662–673.

Xie S., Lu Y., Jakoncic J., Sun H., Xia J., Qian C., 2014 Structure of RPA32 bound to the N-terminus of SMARCAL1 redefines the binding interface between RPA32 and its interacting proteins. FEBS J. 281: 3382–3396.

Yan H., Tammaro M., Liao S., 2016 Collision of trapped topoisomerase 2 with transcription and replication: Generation and repair of DNA double-strand breaks with 5' adducts. Genes (Basel). 7.

Yeo J. E., Lee E. H., Hendrickson E. A., Sobeck A., 2014 CtIP mediates replication fork recovery in a FANCD2-regulated manner. Hum. Mol. Genet. 23: 3695–3705.

Yildiz Ö., Majumder S., Kramer B. C., Sekelsky J., 2002 *Drosophila* MUS312 protein interacts physcially with the nucleotide excision repair endonuclease MEI-9 to generate meiotic crossovers. Mol. Cell 10:1503-1509.

Ying S., Minocherhomji S., Chan K. L., Palmai-Pallag T., Chu W. K., Wass T., Mankouri H. W., Liu Y., Hickson I. D., 2013 MUS81 promotes common fragile site expression. Nat. Cell Biol. 15: 1001–7.

Yu A. M., McVey M., 2010 Synthesis-dependent microhomology-mediated end joining accounts for multiple types of repair junctions. Nucleic Acids Res. 38: 5706–5717.

Yuan J., Ghosal G., Chen J., 2009 The annealing helicase HARP protects stalled replication forks. : 2394–2399.

Yuan J., Ghosal G., Chen J., 2012 The HARP-like domain-containing protein AH2/ZRANB3 binds to PCNA and participates in cellular response to replication stress. Mol. Cell 47: 410–421.

Yue Z., Xiong S., Sun L., Huang W., Mo Y., Huang L., Jiang X., Chen S., Hu B., Wang Y., 2010 Novel compound mutations of *SMARCAL1* associated with severe Schimke immuno-osseous dysplasia in a Chinese patient. Nephrol. Dial. Transplant. 25: 1697–1702.

Yusufzai T., Kadonaga J. T., 2008 HARP is an ATP-driven annealing helicase. Science 322: 748–750.

Yusufzai T., Kong X., Yokomori K., Kadonaga J. T., 2009 The annealing helicase HARP is recruited to DNA repair sites via an interaction with RPA. Genes Dev. 23: 2400–4.

Zapotoczny G., Sekelsky J., 2017 Human cell assays for synthesis-dependent strand annealing and crossing over during double-strand break repair. G3. doi: 10.1534/g3.116.037390 [epub ahead of print].

Zeng Y., Li H., Schweppe N. M., Hawley R. S., Gilliland W. D., 2010 Statistical analysis of nondisjunction assays in *Drosophila*. Genetics 186: 505–513.

Zhang L., Fan S., Liu H., Huang C., 2012 Targeting SMARCAL1 as a novel strategy for cancer therapy. Biochem. Biophys. Res. Commun. 427: 232–5.